Tesi di dottorato in Scienze e Ingegneria per l'Uomo e l'Ambiente/Science and Engineering for Humans and the Environment,
di Francesca Leone, discussa presso l'Università Campus Bio-Medico di Roma in data 26/07/2021.
La disseminazione e la riproduzione di questo documento sono consentite per scopi di didattica e ricerca,
a condizione che ne venga citata la fonte.

Francesca Leone

Università Campus Bio-Medico di Roma

PhD Course in Science and Engineering for humans and the environment

Pattern Recognition algorithms for upper-limb prosthetics control

PhD candidate: Francesca Leone

Coordinator:
Prof. Giulio Iannello

Supervisor:
Prof. Loredana Zollo
Co-Supervisor:
Ing. Francesca Cordella

Tesi di dottorato in Scienze e Ingegneria per l'Uomo e l'Ambiente/Science and Engineering for Humans and the Environment,
di Francesca Leone, discussa presso l'Università Campus Bio-Medico di Roma in data 26/07/2021.
La disseminazione e la riproduzione di questo documento sono consentite per scopi di didattica e ricerca,
a condizione che ne venga citata la fonte.

Academic Year 2017/2018

Tesi di dottorato in Scienze e Ingegneria per l'Uomo e l'Ambiente/Science and Engineering for Humans and the Environment, di Francesca Leone, discussa presso l'Università Campus Bio-Medico di Roma in data 26/07/2021.
La disseminazione e la riproduzione di questo documento sono consentite per scopi di didattica e ricerca, a condizione che ne venga citata la fonte.

Thesis advisor: Professor Loredana Zollo

Francesca Leone

Abstract

In the last 70 years, the evolution of technological and surgical techniques in the field of the upper limb prosthetic have leaded even more advanced solutions to address the future research towards the development of prostheses that are functional and able to mimic the lost upper limb behavior, replicating the performance of the human arm. To this purpose, nowadays, the surface electromyography (sEMG) signals represent a promising approach for decoding the motor intention of amputees with different amputation level. Several approaches based on proportional amplitude methods or simple thresholds on sEMG signals have been proposed, in literature, to control a single degree of freedom (DoF) at time, without the possibility of increasing the number of controllable multiple DoFs in a natural manner. To address this relevant issue, Pattern Recognition (PR) strategies have been proposed to reach a more natural and intuitive control of myoelectric prostheses, compared to the conventional myoelectric control methods. In detail, the major potentiality of the PR methods has been to add multiple DoFs by keeping low the number of electrodes and allowing the discrimination of different muscular patterns for each class of motion. However, the use of PR algorithms to simultaneously decode both gestures and forces has never been studied deeply.

Also the simultaneous control of a poliarticulated prostheses with several DoFs, related to the elbow, wrist, and hand joints, has to be yet investigated deeply to ensure greater dexterity than the conventional control strategies. This is considered a needed capability to restore upper limb functionality, especially for transhumeral and shoulder disarticulation amputees who have undergone Targeted Muscle Reinnervation (TMR) surgery. This surgical technique has been considered innovative and relevant for improving, together with PR strategies, prosthetic control by adding the number of controllable muscular sites. Indeed, the ultimate goal of the TMR is to obtain reinnervated areas that act as biological amplifiers of the motor control.

In this scenario, the potentiality of future clinical application of TMR and PR control strategies in the control of multifunctional prostheses was investigated to

Tesi di dottorato in Scienze e Ingegneria per l'Uomo e l'Ambiente/Science and Engineering for Humans and the Environment, di Francesca Leone, discussa presso l'Università Campus Bio-Medico di Roma in data 26/07/2021.
La disseminazione e la riproduzione di questo documento sono consentite per scopi di didattica e ricerca, a condizione che ne venga citata la fonte.

add value to the current knowledge in the field of upper-limb prosthetics. In detail, this thesis aims at providing promising PR-based strategies for (i) controlling simultaneously, with a hierarchical classification strategy, the hand/wrist gestures and exerted forces during grasping tasks; (ii) discriminating, with a parallel classification strategy, 27 motion classes related to the elbow, hand, and wrist joints. In detail, the parallel classification strategy uses three joint classifiers, one for each DoF. If only one of the three joints is involved in the desired movement, the parallel PR strategy will output a 1 DoF motion class; if instead, two or three joints are activated in a complex motion tasks, the parallel classification strategy will output a 2 or 3 DoFs motion class.

To reach the first objective, a hierarchical classification strategy was developed and validated on 31 healthy subjects and 15 transradial amputees, with the aim to discriminate seven hand/wrist gestures, as well as the desired three force levels to exert during grasping tasks. In detail, the results from healthy showed an average F1Score about equals to 96 % for the hand/wrist gestures and equals to 98 % for the force classifiers, with both the Non Linear Logistic Regression (NLR) and Linear Discriminant Analysis (LDA) classifiers.

To evaluate the robustness of the hierarchical PR system, both offline and in real-time, a prosthetic system composed of a hand (RoboLimb) and a wrist module (WristRotator) was employed by trans-radial amputees when they manage simultaneously the desired hand/wrist gestures and the three force levels. In detail, the results from transradial amputees reached an average F1Score values equals to 90 % for the hand/wrist gestures and equals to 96 % up to 98 % for the force classifiers, when considering the Logistic Regression (LR), NLR and LDA classifiers. Also considering the real-time performance metrics, the Mann-Whitney test (U-test) with Bonferroni correction points out no statistically significant difference between the three algorithms.

To the second purpose, a parallel classification strategy was developed and validated on 15 healthy subjects, to provide the simultaneous classification of 27 discrete and combined motion classes, by keeping the number of electrodes to a bare minimum and the classification error rates under 10 %. In detail, the discrete 1 DoF motion classes involved only one joint, while the combined 2 or 3 DoFs movements, provided the simultaneous activation of two or all the three joints. In detail, the mean F1Score values were above 90 % for all the joint classifiers, with both the LR and LDA algorithms. About the real-time results, the performance of the LR algorithm were statistically better than that obtained with the LDA, despite this last was considered the benchmark classifier for real-time employment. Then, also an analysis of the preliminary offline and real-time results, obtained

Tesi di dottorato in Scienze e Ingegneria per l'Uomo e l'Ambiente/Science and Engineering for Humans and the Environment, di Francesca Leone, discussa presso l'Università Campus Bio-Medico di Roma in data 26/07/2021.
La disseminazione e la riproduzione di questo documento sono consentite per scopi di didattica e ricerca, a condizione che ne venga citata la fonte.

Thesis advisor: Professor Loredana Zollo Francesca Leone

from a TMR subject, was carried out. In this case, the classification performance of the TMR patient reached lower mean F1Score values than that on healthy subjects, and they were about equals to 86 % for LR and LDA classifiers. From this preliminary results, there wasn't a statistical significance difference between the performance obtained with the LR and LDA algorithms.

In conclusion, this thesis aims to provide useful insights into the choice of the suitable classification strategies to discriminate simultaneously hand/wrist gestures and grasping forces and to classify complex tasks involving multiple joints. The outcomes of these objectives reveal that the use of non linear classification algorithm, as NLR, is as much suitable as the benchmark LDA classifier for implementing a hierarchical sEMG-based PR system, able both to decode hand/wrist gestures and to associate different performed force levels to grasping actions. This result is also more appreciable if we consider that we have tested this PR strategy in clinical practice, by employing a robotic hand and wrist module. Regarding the second purpose, the obtained results strongly encourage further investigation of the parallel classification strategy's performance for others TMR patients. In this way, an even more level of robustness and reliability of the proposed PR system can be reached to control simultaneously and in a natural way different joints of a complex multi-DoFs prosthetic device.

Tesi di dottorato in Scienze e Ingegneria per l'Uomo e l'Ambiente/Science and Engineering for Humans and the Environment, di Francesca Leone, discussa presso l'Università Campus Bio-Medico di Roma in data 26/07/2021.
La disseminazione e la riproduzione di questo documento sono consentite per scopi di didattica e ricerca, a condizione che ne venga citata la fonte.

Contents

Tesi di dottorato in Scienze e Ingegneria per l'Uomo e l'Ambiente/Science and Engineering for Humans and the Environment, di Francesca Leone, discussa presso l'Università Campus Bio-Medico di Roma in data 26/07/2021.
La disseminazione e la riproduzione di questo documento sono consentite per scopi di didattica e ricerca, a condizione che ne venga citata la fonte.

Listing of figures

Tesi di dottorato in Scienze e Ingegneria per l'Uomo e l'Ambiente/Science and Engineering for Humans and the Environment, di Francesca Leone, discussa presso l'Università Campus Bio-Medico di Roma in data 26/07/2021.
La disseminazione e la riproduzione di questo documento sono consentite per scopi di didattica e ricerca, a condizione che ne venga citata la fonte.

Tesi di dottorato in Scienze e Ingegneria per l'Uomo e l'Ambiente/Science and Engineering for Humans and the Environment, di Francesca Leone, discussa presso l'Università Campus Bio-Medico di Roma in data 26/07/2021.
La disseminazione e la riproduzione di questo documento sono consentite per scopi di didattica e ricerca, a condizione che ne venga citata la fonte.

Tesi di dottorato in Scienze e Ingegneria per l'Uomo e l'Ambiente/Science and Engineering for Humans and the Environment, di Francesca Leone, discussa presso l'Università Campus Bio-Medico di Roma in data 26/07/2021.
La disseminazione e la riproduzione di questo documento sono consentite per scopi di didattica e ricerca, a condizione che ne venga citata la fonte.

Tesi di dottorato in Scienze e Ingegneria per l'Uomo e l'Ambiente/Science and Engineering for Humans and the Environment, di Francesca Leone, discussa presso l'Università Campus Bio-Medico di Roma in data 26/07/2021.
La disseminazione e la riproduzione di questo documento sono consentite per scopi di didattica e ricerca, a condizione che ne venga citata la fonte.

Tesi di dottorato in Scienze e Ingegneria per l'Uomo e l'Ambiente/Science and Engineering for Humans and the Environment, di Francesca Leone, discussa presso l'Università Campus Bio-Medico di Roma in data 26/07/2021.
La disseminazione e la riproduzione di questo documento sono consentite per scopi di didattica e ricerca, a condizione che ne venga citata la fonte.

Tesi di dottorato in Scienze e Ingegneria per l'Uomo e l'Ambiente/Science and Engineering for Humans and the Environment, di Francesca Leone, discussa presso l'Università Campus Bio-Medico di Roma in data 26/07/2021.
La disseminazione e la riproduzione di questo documento sono consentite per scopi di didattica e ricerca, a condizione che ne venga citata la fonte.

Tesi di dottorato in Scienze e Ingegneria per l'Uomo e l'Ambiente/Science and Engineering for Humans and the Environment,
di Francesca Leone, discussa presso l'Università Campus Bio-Medico di Roma in data 26/07/2021.
La disseminazione e la riproduzione di questo documento sono consentite per scopi di didattica e ricerca,
a condizione che ne venga citata la fonte.

Alla mia famiglia,

Oramai fra di noi solo un passo
Io vorrei, non vorrei ma se vuoi
Come può uno scoglio
Arginare il mare
Anche se non voglio
Torno già a volare

Lucio Battisti

Tesi di dottorato in Scienze e Ingegneria per l'Uomo e l'Ambiente/Science and Engineering for Humans and the Environment, di Francesca Leone, discussa presso l'Università Campus Bio-Medico di Roma in data 26/07/2021.
La disseminazione e la riproduzione di questo documento sono consentite per scopi di didattica e ricerca, a condizione che ne venga citata la fonte.

Acknowledgments

E' arrivato il momento dei dovuti ringraziamenti, dopo questo impegnativo ma entusiasmante percorso di Dottorato, iniziato nel 2017 in un mondo del tutto diverso in cui si poteva sorridere spensierati e gioire tutti insieme appassionatamente e finito nel 2021 in cui tutti noi ci siamo ritrovati per lungo tempo a distanza e con la mascherina in viso, per sopravvivere all'aggressione di particelle virali di SARS-CoV-2, di appena 100 nm di diametro. E' proprio in questi momenti che ognuno di noi è chiamato a fermarsi per riflettere e rimettere le priorità al centro del villaggio. Tra queste vi era sicuramente il raggiungimento del Dottorato, nonostante tutto: perché la scienza e la ricerca non si fermano mai, e vanno sempre avanti verso nuovi progressi. La comunità mondiale ha sempre bisogno di loro. Quale miglior sprono, quindi, per non arrendersi?. Diventano, dunque, ancor più doverosi i ringraziamenti verso ogni singola persona del Laboratorio e dell'Università Campus Bio-Medico che mi hanno fatto sentire sempre parte di una grande famiglia e mi hanno permesso di crescere sia sotto il profilo professionale che umano. In primis, un dovuto ringraziamento va alla Prof.ssa Loredana Zollo ed il Prof. Eugenio Guglielmelli per avermi dato la possibilità in questi anni di lavorare ad importanti progetti di ricerca, il cui primario obiettivo era la riabilitazione di pazienti amputati, che sono diventati fin da subito persone speciali come Gessica e Roberto: entrambi li ho potuti seguire in prima persona in questo lungo percorso e li ringrazio sentitamente per ogni singolo giorno trascorso insieme. Un altro grande grazie è rivolto alle mie due guide di fiducia, Annalisa e Francesca, il cui supporto tecnico, morale e psicologico è stato fondamentale per acquisire nuove competenze ed autostima. Meriterebbero quasi la santità per la pazienza dimostrata ogni giorno nel superare insieme ansie e preoccupazioni. Un'altra forza motrice importante per il raggiungimento di questo obiettivo risiede nel supporto quotidiano di tutti i miei fantastici colleghi come Anna l'Abruzzese, Andrea er magggico, la santa Alessia, Christian l'imitatore, Cosimo il tutto fare, Federico il buono il brutto e il cattivo, il panettiere Francesco, Martina OI, Mat-

Tesi di dottorato in Scienze e Ingegneria per l'Uomo e l'Ambiente/Science and Engineering for Humans and the Environment, di Francesca Leone, discussa presso l'Università Campus Bio-Medico di Roma in data 26/07/2021.
La disseminazione e la riproduzione di questo documento sono consentite per scopi di didattica e ricerca, a condizione che ne venga citata la fonte.

tia il Calabrese, e tante altre persone speciali come Alessandro e Simone che mi hanno sempre sostenuto. Un altro doveroso ringraziamento è per le mie cavie fedeli e compagne di escursioni, Marianna e Marcella, che si sono sempre prestate ad ogni mio esperimento e per il Dott. Cancilleri, la mia guida fidata in ogni epica escursione. Un altro ringraziamento speciale va al settore sportivo del Campus Bio-Medico, organizzato da persone speciali come Antonio e Daniele e vissuto a pieno con le mie compagne e compagni speciali di tennis e calcio a 5, con cui ho intrapreso tornei sportivi con al centro i veri e sani valori dello sport. Ringrazio, poi, sentitamente tutti i miei professori che ho incontrato nella mia vita e che di anno in anno mi hanno permesso di raggiungere questo importante obiettivo. Continuo con il ringraziare assai coccolosamente il mio coccoloso, sempre al mio fianco, il mio tifoso numero 1, sempre pronto a credere in me, come tutta la sua famiglia Massimo, Marina e Francesco che mi hanno sempre sostenuto e supportato. Altro dovuto ringraziamento va a tutti i miei parenti, come zio Andrea, zia Euchery, Marta, Matteo, Zia Patrizia, Zio Massimiliano, la mia cara nonna Lisa e tanti altri che mi hanno sempre dimostrato tanto affetto e stima. Infine, un grazie speciale va ai miei genitori per avermi dato la possibilità di studiare e di imparare i valori fondamentali della vita, a mia sorella Giulia, sempre al mio fianco e complice dall'anno zero, e a mia sorella Cristina che mi ha saputo sempre infondere tanta allegria e spensieratezza. Insomma, grazie a tutti. Ad maiora

Tesi di dottorato in Scienze e Ingegneria per l'Uomo e l'Ambiente/Science and Engineering for Humans and the Environment,
di Francesca Leone, discussa presso l'Università Campus Bio-Medico di Roma in data 26/07/2021.
La disseminazione e la riproduzione di questo documento sono consentite per scopi di didattica e ricerca,
a condizione che ne venga citata la fonte.

1

Introduction

Upper limb amputation is a traumatic event that affects the quality of life by fully reducing the multifunctional hand capability during the activities of daily living (ADLs)[1]. Especially the hand function is the result of the evolution of the cortical mechanisms and sensory cortices in human beings[2]: the development of the neural pathways responsible for motor control and the importance of also sensory

Tesi di dottorato in Scienze e Ingegneria per l'Uomo e l'Ambiente/Science and Engineering for Humans and the Environment, di Francesca Leone, discussa presso l'Università Campus Bio-Medico di Roma in data 26/07/2021.
La disseminazione e la riproduzione di questo documento sono consentite per scopi di didattica e ricerca, a condizione che ne venga citata la fonte.

neuronal networks responsible for the sensory feedback have made the restoration of arm and hand function even more challenging. In this scenario, the evolution of technological and surgical techniques has made the restoring of the upper limb function possible[3]. However, the aim of obtaining an even more intuitive control of multiple joints using advanced prosthetic systems remains one of the principal challenges in the prosthetic field. Since 1948[4], the most common approach for translating the user's intention into arm and hand movements was based on surface electromyography (sEMG) signals. Over the years, it was employed for controlling, in a non invasive way, even more complex multifunctional prosthetic system with several degrees of freedom (DoFs)[5].

In literature, several solutions have been proposed to control from one DoF to multiple DoFs[6,7]. The conventional techniques[8] are based on the on/off strategy, typically used to control one DoF by setting a threshold based on the EMG amplitude of two residual antagonist muscles; the proportional control strategy which allowed to apply to the motor values of the voltage proportional to the contraction intensity of EMG signals. These conventional techniques are often associated with different methods for selecting the joint to be controlled, as the the co-contraction and the simultaneous method. However, the first method has the principal limit of controlling only one joint at a time. While the second allows the movement of more than one joint at the same time, but the number of controllable DoFs depends on the number of independent EMG control sites[1]. Moreover, these control methods, despite being extremely robust, require considerable cognitive effort and are less intuitive and unnatural than more complex techniques based

Tesi di dottorato in Scienze e Ingegneria per l'Uomo e l'Ambiente/Science and Engineering for Humans and the Environment, di Francesca Leone, discussa presso l'Università Campus Bio-Medico di Roma in data 26/07/2021.
La disseminazione e la riproduzione di questo documento sono consentite per scopi di didattica e ricerca, a condizione che ne venga citata la fonte.

on machine learning algorithms.

To overcome these limits, the Pattern Recognition (PR) strategies have been proposed to reach a more natural and intuitive control of myoelectric prostheses, compared to the conventional myoelectric control methods[9]. Indeed, the PR strategies have the advantage to not require independent muscle sites, but to consider muscular activation patterns of different muscle sites to classify several motion classes[1]. Different classification algorithms have been proposed in literature, including Euclidean Distance, Non Linear Logistic Regression, k-Nearest Neighbors (kNN), Hidden Markov Model (HMM), Artificial Neural Network (ANN), Support Vector Machine (SVM), Linear Discriminant Analysis (LDA)[10]. However, different arm positions[11], electrode shift[12], signal nonstationarity[13] and force variation[7] can affect the PR accuracy and robustness. In addition, physiological factors as motor unit (MU) recruitment, MU firing rate and contraction type (e.g. isometric, isotonic, concentric or eccentric) make difficult the extraction of sEMG-force relationship due to non-linear factors[14,15,16].

Although the presence of these confounding factors, the PR techniques have a key role in increasing the amputee's ability to control the prosthesis, in a more natural way, by increasing the number of controllable DoFs, by keeping low the number of employed electrodes[17]. However, the progresses made in this field based on EMG-PR approach are not yet enough to avoid the abandonment of the prosthetic device. In detail, many users imputed the major cause of the abandonment to the lack of robustness and unnaturalness of the control techniques[18].

In particular, requirements of prosthesis users are that control strategies must

Tesi di dottorato in Scienze e Ingegneria per l'Uomo e l'Ambiente/Science and Engineering for Humans and the Environment, di Francesca Leone, discussa presso l'Università Campus Bio-Medico di Roma in data 26/07/2021.
La disseminazione e la riproduzione di questo documento sono consentite per scopi di didattica e ricerca, a condizione che ne venga citata la fonte.

be simple, direct, and user-friendly[19].

The aforementioned limits are highlighted when it is necessary to control more degrees of freedom, as in the case of transhumeral amputations or shoulder disarticulation amputees.To overcome these issues, an invasive surgical intervention, as the Targeted Muscle Reinnervation (TMR), developed by Dr. Todd Kuiken and his team at the Rehabilitation Institute of Chicago[20], have reached major advancement in the field of upper-limb prosthetics, to control a multiple DoF prosthesis with a high level of dexterity. In detail, after TMR surgery, the residual nerves of the amputated limb are reinnervated to new target muscles that allow users to control the prosthesis more intuitively. In this way, the ADL can be performed in a more simply way, thanks to the neural information restored on the reinnervated muscle. The patient's intention can be translated into motions, through the amplified EMG signals of these targeted reinnervated muscles, used to control the prosthetic device.

However, it is worth noticing that the optimal control system depended also on the amputation level: bilateral shoulder disarticulation (BSD), shoulder disarticulation (SD), transhumeral (TH); transradial (TR). For each amputation level, the most appropriate control strategies that make myoelectric prostheses control easy, reliable, efficient, and therefore for lowering the users' cognitive burden, has yet to be assessed[21].

This thesis has the twofold purpose of developing and validating novel PR-based control strategies to (i) allow users, as the TR amputees, to control simultaneously both hand/wrist gestures and force levels by obtaining an intuitive and

Tesi di dottorato in Scienze e Ingegneria per l'Uomo e l'Ambiente/Science and Engineering for Humans and the Environment, di Francesca Leone, discussa presso l'Università Campus Bio-Medico di Roma in data 26/07/2021.
La disseminazione e la riproduzione di questo documento sono consentite per scopi di didattica e ricerca, a condizione che ne venga citata la fonte.

fluid multi-DoFs prosthetic control; (ii) to control simultaneously different prosthetic modules of hand, wrist and elbow, especially for amputee with BSD, SD, and TH. For the first purpose, the performance of the hierarchical classification approach that allowed to classify simultaneously the hand/wrist gestures and force levels, during grasping tasks, was evaluated, firstly on 31 healthy subjects and, then, on 15 transradial amputees. A statistical comparison, based on Wilcoxon Signed-Rank test, was applied among different supervised machine learning techniques, based on the Non-Linear Logistic Regression (NLR) and (LDA) classifiers. This serves to evaluate which classification algorithm is the most suitable for the hierarchical classification approach, when both hand/wrist gestures and three force levels were discriminated simultaneously. Then, this study was extended and adapted to allow 15 transradial amputees to manage simultaneously desired hand/wrist gestures and three force levels, with a prosthetic system composed of a hand (RoboLimb) and wrist module (WristRotator). In detail, the hierarchical classification system, based on a Finite State Machine, was validated by introducing both the offline and real-time performance. To improve the robustness of the introduced PR strategy, also the Logistic Regression algorithm (LR), besides the NLR, and the LDA algorithms, were compared in terms of performance with an without the features extraction (FE) step, by carrying out statistical analysis based on the Mann-Whitney test (U-test) with Bonferroni correction. For the second purpose, a novel PR-based parallel classification strategy was developed to recognize both discrete and combined elbow, wrist, and hand motions. This PR strategy was implemented by using two PR algorithms (LR and LDA) and

Tesi di dottorato in Scienze e Ingegneria per l'Uomo e l'Ambiente/Science and Engineering for Humans and the Environment, di Francesca Leone, discussa presso l'Università Campus Bio-Medico di Roma in data 26/07/2021.
La disseminazione e la riproduzione di questo documento sono consentite per scopi di didattica e ricerca, a condizione che ne venga citata la fonte.

both the offline and real-time performance metrics were evaluated on 15 healthy subjects and a statistical comparison among algorithms was made to assess the best solution for classifying simultaneously up to 3 DoFs motion classes. In detail, each DoF is related to the motion of each considered joint (as the elbow, wrist, and hand). If only one joint was involved in the desired movement, the parallel PR strategy classified a discrete 1 DoF motion. Instead, complex motions provided the simultaneous activation of 2 or 3 DoFs, according to the number of the joints employed in the motion tasks. The 27 discrete and complex elbow, hand and wrist motions were classified by keeping the number of electrodes to a bare minimum (six sEMG sensors) and the classification error rates under 10 %.

This thesis is structured as follows:

- In Chapter 2 an overview of PR approaches, developed for upper-limb prosthesis control, is reported, by focusing on the main strategies for gesture and force decoding and for the multi-DoFs prosthetic control.

- Chapter 3 reports the hierarchical classification PR-based approach validated on 31 healthy subjects and 15 transradial amputees with the aim to discriminate the desired hand/wrist gestures, as well as the desired force levels to exert during grasping tasks.

- In Chapter 4, we present the parallel classification system validated on 15 healthy subjects for the simultaneous multi-DoFs control of elbow, wrist, and hand joints. The system discriminates 26 motion classes and no-motion class. Then, also the preliminary results obtained on one TMR patient were

Tesi di dottorato in Scienze e Ingegneria per l'Uomo e l'Ambiente/Science and Engineering for Humans and the Environment,
di Francesca Leone, discussa presso l'Università Campus Bio-Medico di Roma in data 26/07/2021.
La disseminazione e la riproduzione di questo documento sono consentite per scopi di didattica e ricerca,
a condizione che ne venga citata la fonte.

analyzed.

- In chapter 5, conclusion and future works are drawn.

Tesi di dottorato in Scienze e Ingegneria per l'Uomo e l'Ambiente/Science and Engineering for Humans and the Environment,
di Francesca Leone, discussa presso l'Università Campus Bio-Medico di Roma in data 26/07/2021.
La disseminazione e la riproduzione di questo documento sono consentite per scopi di didattica e ricerca,
a condizione che ne venga citata la fonte.

2

Overview on PR-based control strategies

In this chapter, a literature analysis of PR approaches developed for upper-limb prosthesis control is reported. The main strategies for gesture and force decoding and for the multi-DoFs control of several prosthesis joints are pointed out.

Tesi di dottorato in Scienze e Ingegneria per l'Uomo e l'Ambiente/Science and Engineering for Humans and the Environment, di Francesca Leone, discussa presso l'Università Campus Bio-Medico di Roma in data 26/07/2021.
La disseminazione e la riproduzione di questo documento sono consentite per scopi di didattica e ricerca, a condizione che ne venga citata la fonte.

2.1 Introduction

Amputation of the upper limb causes a huge decrease in dexterity, with a significant reduction in patients' quality of life. People who have had an upper-limb amputation need a prosthesis that replaces the lost arm functionality. It is very difficult to find epidemiology data on amputations of the upper limb. Over the world, the population of amputees was estimated as 10 million, 30% of whom are upper limb amputees[22]. Focusing on European countries, in Italy, there were 2720 upper-limb amputations in 2018, equal to 18% of total amputations[23]; in 2003, in the UK, there were 5767 new amputations, 5% was upper limb amputees[24]. Between 2004 and 2013, only in the adult hand emergency clinic of the Nancy University Hospital (France), 2247 patients suffered an upper limb amputation (partial and pediatric amputation excluded) that was traumatic in 76.32% of cases[25]. Also in the USA, approximately 340,000 people have suffered the loss of a limb and every year there are 10,000 new upper limb amputations, as reported by the National Center for Health Statistics[26]. The relevance of the upper limb loss has pushed international research to seek new prosthetic solutions[1].

Prosthesis technology ranges from passive or cosmetic typologies on one end to active or functional types on the other (Figure 2.1).

Cosmetic prostheses are used to restore only the aesthetic aspect[27], while active ones are used to restore, as far as possible, the functionality of the lost arm. Active prostheses can be further classified into body powered, that exploit cables to control the device with the more proximal joints, and externally powered

Tesi di dottorato in Scienze e Ingegneria per l'Uomo e l'Ambiente/Science and Engineering for Humans and the Environment,
di Francesca Leone, discussa presso l'Università Campus Bio-Medico di Roma in data 26/07/2021.
La disseminazione e la riproduzione di questo documento sono consentite per scopi di didattica e ricerca,
a condizione che ne venga citata la fonte.

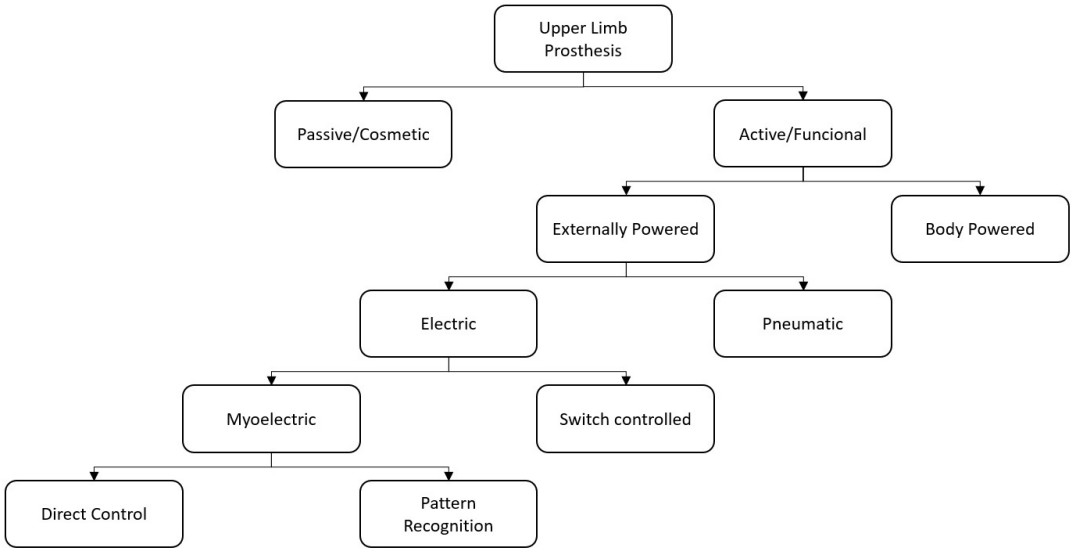

Figure 2.1: A Block diagram describing the types of Upper Limb Prostheses and control approaches.

(electric or pneumatic)[28], which allow the movement of the motors of the joints making up the prosthesis[29]. Externally powered prostheses require a control system in order to associate an input signal (generated by a sensor and/or a button) to an output action. One of the most used control systems is the myoelectric one, which exploits the electromyographic (EMG) signals of a specific muscle to provide discrete movement and of an antagonist muscle group to make complementary movements. EMG signals have been used to control prostheses since 1948[4] and, over the years, various control strategies have been identified: among these, the control strategies that directly associate a movement of the prosthetic limb to an EMG input signal are usually referred to as Direct Myoelectric Control or simply Direct Control (DC). The conventional techniques, to control from one Degree of Freedom (DoF) to multiple DoFs[8], are: the on/off strategy, typically

Tesi di dottorato in Scienze e Ingegneria per l'Uomo e l'Ambiente/Science and Engineering for Humans and the Environment, di Francesca Leone, discussa presso l'Università Campus Bio-Medico di Roma in data 26/07/2021.
La disseminazione e la riproduzione di questo documento sono consentite per scopi di didattica e ricerca, a condizione che ne venga citata la fonte.

used to control one DoF and allowing to perform two opposite movements based on the exceeding of a preset threshold by the EMG amplitude of two residual antagonist muscles; the proportional control strategy which considers, instead, the voltage applied to the motor proportional to the contraction level/intensity of EMG signals[7].

Such control strategies are generally associated with a method for selecting the joint to be controlled. The first one is the co-contraction method, which allows the patient to change from one joint to another by simultaneously contracting the muscles used to control the joint; however, the principal limit of this technique is that it is possible to control only one joint at a time. The second is the simultaneous method that is used to control multi-DoF prostheses, handling more than one joint at the same time. However, in this case, the number of controllable DoFs depends on the number of independent EMG control sites[1].

Thus, several control strategies were proposed in the literature for making myoelectric prostheses control easy, reliable, efficient, and therefore for lowering the users' cognitive burden. However, the optimal control system that allows users to control forces and gestures and multiple DoF prosthesis with dexterity, and by using intuitive interfaces between the user and the device, has not yet been developed[21]. In the following Sections (Sect. 1.2 and 1.3), the principal PR techniques that allowed to control, in a natural way, myoelectric prostheses will be presented.

Tesi di dottorato in Scienze e Ingegneria per l'Uomo e l'Ambiente/Science and Engineering for Humans and the Environment, di Francesca Leone, discussa presso l'Università Campus Bio-Medico di Roma in data 26/07/2021.
La disseminazione e la riproduzione di questo documento sono consentite per scopi di didattica e ricerca, a condizione che ne venga citata la fonte.

2.2 State of art of PR approach to decode gestures and forces

The use of surface electromyography (sEMG) allows the non-invasive extraction of pattern information useful to control active prosthetic hands. In the last 70 years, several solutions have been proposed to extract gestures information from sEMG[1,6]; the most simple were based on on-off[30], on Agonist/Antagonist[31] and Proportional Control[32].

Pattern recognition methods enabled performance improvements to reach an intuitive and coordinated control[9]. Moreover, these techniques allowed the increasing of the number of controllable Degree of Freedoms (DoFs)[1]. However, the use of PR techniques based on EMG signals that allowed amputees to restore simultaneously the hand/wrist gestures and force levels during grasping tasks, has not been studied deeply. Moreover, including also natural sensory feedback that allowing the prosthetic user to understand the force felt by the prosthetic hand remains challenging. The lack of prostheses to include sensory feedback information, make users unable to feel the prosthetic device connected to their hand and it is one of the main reasons for the high percentage of prosthesis abandonment (>30%)[33]. Thus, especially during grasping tasks that considered the interaction with objects, the muscle contraction forces have to be modulated to control the grasp force at different target force levels.

In literature, two main approaches, based on mathematical models and machine learning techniques, have been proposed to find a relationship between muscular activation and force. Regarding the mathematical models, the force estima-

Tesi di dottorato in Scienze e Ingegneria per l'Uomo e l'Ambiente/Science and Engineering for Humans and the Environment, di Francesca Leone, discussa presso l'Università Campus Bio-Medico di Roma in data 26/07/2021.
La disseminazione e la riproduzione di questo documento sono consentite per scopi di didattica e ricerca, a condizione che ne venga citata la fonte.

tion, based on surface electromyographic measurements, was determined through a sEMG-force mathematical relationship, by applying Nonlinear Wiener Hammerstein (NLWH) and Spectral Analysis Frequency Dependent Resolution (SPAFDR) models[34]. In Buchanan et al.[35], a computational neuro musculoskeletal model of the human arm was presented with the aim to estimate muscle forces, joint moments and joint kinematics from neural signals. Moreover, "crosstalk risk factors" (CRF), as the dependency of the relationship between the sEMG signals, muscle length and isometric contraction force, had to be quantified to understand the effectiveness of the muscular co-ordination in generating force[16]. Instead, about the machine learning techniques, the following studies have tried to address the problem of force estimation. In Srinivasan et al.[36], a method for estimating forces from surface electromyography (sEMG) signals was proposed by using an Artificial Neural Network (ANN). Wu et al.[37] presented a force estimation method employing a Regression Neural Network (GRNN) trained with sEMG and force signals. In the most recent study[38], force signals were divided in different grades from 0 N to 16 N, expressed as percentage of the Maximum Voluntary Contraction (MVC). They used SVM to establish nonlinear regression relationship between sEMG and force. Lv et al.[39] used Linear Discriminant Analysis (LDA) to classify five finger gestures at two different levels of force (i.e. 10% MVC and 50% MVC), by using EMG and accelerometer signals. Li et al.[9] proposed a method based on deep neural network to derive sEMG-force regression model for force prediction at eight different force levels. In order to investigate the performance of PR system in presence of variations in force, a LDA classifier with Time-Domain (TD) features

Tesi di dottorato in Scienze e Ingegneria per l'Uomo e l'Ambiente/Science and Engineering for Humans and the Environment, di Francesca Leone, discussa presso l'Università Campus Bio-Medico di Roma in data 26/07/2021.
La disseminazione e la riproduzione di questo documento sono consentite per scopi di didattica e ricerca, a condizione che ne venga citata la fonte.

extraction was evaluated[7], by using data of 10 classes performed at 20% and 80% of the strongest and reproducible contraction, except for the tenth class of no motion. The LDA classifier performed an error rate equals to 17% when trained and tested using data of 11 healthy subjects at all force levels. The error increased at $31-44\%$ when trained at one force level and tested with all force levels. Subsequently, the effect of contraction strength on pattern recognition based control was presented in Scheme et al.[40] by using a LDA classifier trained with dynamic ramp data of 10 healthy subjects, the classification error significantly improved ($11.16 \pm 0.54\%$).

Different strategies have been developed by combining the above techniques to make the control most fluid and intuitive for the user. Two proportional control algorithms were used to obtain a robust and proportional velocity commands that could improve the usability of PR (pattern recognition) based control[41]. In Fougner et al.[42], a novel pattern recognition system with mutex on-off control or proportional control of a commercial prosthetic hand and wrist was presented. In Young et al.[43], three classification strategies were introduced and compared in order to provide simultaneous DoFs control. The first classification approach used a single linear discriminant analysis (LDA) classifier to discriminate both discrete and combined motions. All the discrete and combined gestures were considered as separated classes. The second proposed approach was based on a hierarchical classification strategy and consisted of a hierarchy of LDA classifiers. The highest classifier in the hierarchy determined a motion class for a single DoF by using both discrete and combined motion data. The output of this classifier determined

Tesi di dottorato in Scienze e Ingegneria per l'Uomo e l'Ambiente/Science and Engineering for Humans and the Environment, di Francesca Leone, discussa presso l'Università Campus Bio-Medico di Roma in data 26/07/2021.
La disseminazione e la riproduzione di questo documento sono consentite per scopi di didattica e ricerca, a condizione che ne venga citata la fonte.

which classifier of the second level could be used for discriminating the motion class of a second DoF. Finally, the parallel classification strategy employed one LDA classifier for each DoF and the decision of the single classifier is independently defined. The parallel classification strategy was presented also to either allow the simultaneous control of three-digits of a monkey[44] or to control the elbow and hand/wrist movement of an active myoelectric transhumeral prosthesis[45].

A parallel classification strategy[46] was introduced for investigating the effect of force variation on sEMG-PR, by employing three parallel classifiers trained with data acquired at low, medium, and high force levels, respectively. The results were obtained on three able-bodied subjects by using four Trigno Wireless System for recording the no-movement (NM) and the following four motion classes, at three force levels: hand open (HO), hand close (HC), wrist extension (WE), and wrist flexion (WF), and the no-movement (NM). The force levels were set as follows: the high, medium and low force level was defined as 80 %, 50 % and 20 % of the MVC, respectively. For PR strategy, the mean value of MAV was compared with the predefined thresholds to select the target classifier related to each force level; then the selected classifier output the classification result. They demonstrated that the use of the LDA algorithm with TD features (MAV, WL, ZC, and SSC) increased the classification accuracy at different force levels with an average classification rate of 98.8%, with respect to the current method (91.9%).

In Castellini et al.[47], three trans-radial amputees were asked to perform six grasp postures, and also the force levels were recorded according to three modalities: teacher imitation that consisted of asking amputee to imitate with his stump

Tesi di dottorato in Scienze e Ingegneria per l'Uomo e l'Ambiente/Science and Engineering for Humans and the Environment, di Francesca Leone, discussa presso l'Università Campus Bio-Medico di Roma in data 26/07/2021.
La disseminazione e la riproduzione di questo documento sono consentite per scopi di didattica e ricerca, a condizione che ne venga citata la fonte.

the teacher's postures (healthy subject). The amputee had to reproduce the grasp with maximum strength, while the teacher mark the postures/grips by gripping the force sensor; regarding the bilateral action, the amputee had to grip the force sensor with his healthy hand and do the same thing with the phantom limb; the mirror-box is similar to the bilateral action but the mirror-box was added. The regression method, based on ε-SVR technique, was used to force estimation and the root mean-square error (RMSE), normalised with respect to the range of the force signal, was introduced as the performance index. The SVM classifiers approximated the force levels with an error of 7 %.

No hierarchical strategy has ever been proposed to simultaneously identify desired gestures and forces.

Regarding the possibility of embedding the force feedback within the prosthesis, for obtaining a closed-loop prosthesis control, the following studies have been investigated.

Generally, the vibrotactile stimulation is the most common choice to provide the force feedback[48,49]. In Chatterjee et al.[50], an haptic feedback system was employed to modulate, with a vibrotactile stimulus, the grasping force at three different force levels. In Meek et al.[51], a motor-driven pusher was able to measure the force against the skin by using a transducer placed on the final part of the pusher. However, few studies demonstrated how sensory information can be exploited to finely control a prosthetic hand. For instance, in Zollo et al.[52], electrical stimuli were employed to translate both force and slippage signals. In this way, the amputees were able to directly control the grasp stability and slippage infor-

Tesi di dottorato in Scienze e Ingegneria per l'Uomo e l'Ambiente/Science and Engineering for Humans and the Environment, di Francesca Leone, discussa presso l'Università Campus Bio-Medico di Roma in data 26/07/2021.
La disseminazione e la riproduzione di questo documento sono consentite per scopi di didattica e ricerca, a condizione che ne venga citata la fonte.

mation and to modulate the force level. Regarding the prosthesis control based on pattern recognition (PR) systems, it was demonstrated that force variations[53] can affect their performances, in terms of accuracy and robustness. There is little evidence about how grasping force variations affected the performance of gesture recognition when the force level changed. One reason for the degradation of the overall classification accuracy, is that the signal patterns associated to muscular contractions depended on force variations[54]. In literature, the following studies have faced how force level changes affect signals and recognition on healthy subjects.

In Scheme et al.[53], the effects of force level variation on the performance of PR-based EMG control were taken into account. Eleven healthy subjects performed nine motion classes related to hand and wrist joints: hand open, key grip, chuck grip, power grip, pinch grip, wrist flexion, wrist extension, wrist pronation, wrist supination. In detail, they were asked to vary the force level from 20% to 80% of the strongest contraction, felt as comfortable. The Linear Discriminant Analysis (LDA) classifier with time-domain (TD) features was trained at each force level and then tested with all force levels. The error rates were equals to 17 % when trained and tested the classifier at all force levels and increased at $31-44$ % when trained at one force level and tested with all force levels.

In Jiang et al.[55], the grasping force significantly affected the accuracy of the classification system based on a LDA classifier trained at a single force level and tested on eight different levels of force. Nine healthy subjects performed 16 grasp types: for each grasp, they were asked to perform the baseline force and eight

Tesi di dottorato in Scienze e Ingegneria per l'Uomo e l'Ambiente/Science and Engineering for Humans and the Environment, di Francesca Leone, discussa presso l'Università Campus Bio-Medico di Roma in data 26/07/2021.
La disseminazione e la riproduzione di questo documento sono consentite per scopi di didattica e ricerca, a condizione che ne venga citata la fonte.

different levels of forces normalized according to the baseline forces (i.e., 0, 0.25, 0.5, 0.75, 1, 1.5, 2, 3 times baseline force). The LDA classifier was trained with the the baseline level force grasps.Then, for the testing session, the predefined eight levels of force for each of the 16 grasps were taken into account. The accuracy of classification of the testing sessions increases from 71 % at 0 force level to about 86% at level 0.5, and then decreased after level 3. Thus, these results demonstrated that the 0.5 level of the natural force is the minimum grasping force that guarantee acceptable recognition performance without a significant degradation (i.e. with accuracy over 85 %).

In Samuel et al.[54], an LDA classifier was trained using the features extracted from the data for each force level and, then, was tested by using the features from data related to the remaining force levels. In details, three different force levels defined as follows were performed by five able-bodied subjects: low force level (20% of the maximum voluntary contraction (MVC)), medium force level (about 50% of the MVC), and high force level (around 80% of the MVC). The time-domain feature set that is invariant to force variation (invTDF), Huggins feature set (TD4), Fourth order autoregressive coefficient (AR4th), and a recently proposed two dimensional TD feature set denoted as NOV[56] was used with the LDA classifier to discriminate seven different classes: hand close (HC), hand open (HO), wrist extension (WE), wrist flexion (WF), wrist pronation (WP), wrist supination (WS) and no movement (NM). The classification error rate was much higher when training with data from the low or the high force level, due to the difficulty of naturally producing stable contractions. Instead, the medium force

Tesi di dottorato in Scienze e Ingegneria per l'Uomo e l'Ambiente/Science and Engineering for Humans and the Environment, di Francesca Leone, discussa presso l'Università Campus Bio-Medico di Roma in data 26/07/2021.
La disseminazione e la riproduzione di questo documento sono consentite per scopi di didattica e ricerca, a condizione che ne venga citata la fonte.

level obtained the least classification error when four different feature extraction methods were employed.

Regarding the impact of force level variations on the performance of the PR control strategies when enrolling trans-radial amputees, the following studies were reported.

In Al-Timemy et al.[57], the effect of changing the force levels on the PR system's performance was investigated on two trans-radial amputees. The performance of the LDA classifier with TD features was compared with respect to Auto Regression (AR) coefficients and Root Mean Square (RMS) features set. Six trials were recorded for the low force level for each gesture. The performance of the proposed classifier was tested according to different strategies: the first considered the classifier was trained and tested with a single force level; for the second strategy, the classifier was trained with single force level and tested with the unseen 2 force levels; finally, the classifier was trained with all 3 force levels and tested with a single force level at a time. The performance of the LDA classifier was better with TD features and when training it with all force levels while degraded up to 60% when the force level varied.

Also in another study[58], the same author reported that force level variations negatively affected the performance of PR system and caused the increase of the classification error rates. However, an increasing of $6-8\%$ in the classification performance can be reached by applying Time-Dependent Power Spectrum Descriptors (TD-PSD) features extraction to four classifiers (i.e. LDA, Random Forest (RF), Naive Bayes (NB), k-Nearest Neighbor (kNN)) and training with all

Tesi di dottorato in Scienze e Ingegneria per l'Uomo e l'Ambiente/Science and Engineering for Humans and the Environment, di Francesca Leone, discussa presso l'Università Campus Bio-Medico di Roma in data 26/07/2021.
La disseminazione e la riproduzione di questo documento sono consentite per scopi di didattica e ricerca, a condizione che ne venga citata la fonte.

forces across nine trans-radial amputees.

In[59], three different classifiers as the LDA, the Na¨ıve Bayes, and the multi-class SVM were tested to classify the six following hand gestures: spherical grip, index flexion, hook grip, thumb flexion, fine pinch, and tripod grip. In detail, nine different trans-radial amputees were asked to perform each gesture with three different force levels (low, medium, and high) and then two classification strategies were analyzed: the classification of only 6 motion classes without considering force levels; the classification of both the gesture and force level for an amount of 18 classes. The testing accuracies for the LDA, Na¨ıve Bayes, and the multi-class SVM classifiers, when considering 6 and 18 classes, were equals to 96.18% and 93.11 %, 78.65% and 76.86 % and 88.76% and 86.53 %, respectively.

In literature, also deep learning methods were investigated as possible solutions to solve the problem of force estimation when considering surface electromyography signals[60]. For instance in Shaoyang Hua et al.[61] the recurrent neural network (RNN) was employed to extract the temporal information and model the relation between sEMG signals and output forces. Another study of Shaoyang Hua et al. proposed the multi-task learning (MTL) method to learn multiple related tasks simultaneously for recognizing gestures and force levels synchronously. In particular, they extracted the frequency domain information with the convolutional neural network (CNN) and demonstrated that it is more suitable for gesture recognition with variable force levels. In Jabbari et al.[62], a Long Short-Term Memory (LSTM-based) neural network with the fusion of Time Domain Descriptors (fTDD) was employed to discriminate six grip gestures at three different force

Tesi di dottorato in Scienze e Ingegneria per l'Uomo e l'Ambiente/Science and Engineering for Humans and the Environment, di Francesca Leone, discussa presso l'Università Campus Bio-Medico di Roma in data 26/07/2021.
La disseminazione e la riproduzione di questo documento sono consentite per scopi di didattica e ricerca, a condizione che ne venga citata la fonte.

levels (low, medium, and high): 1-Thumb flexion, 2-Index flexion, 3-Fine pinch, 4-Tripod grip, 5-Hook grip, and 6-Spherical grip (power). The results obtained from nine trans-radial amputees showed that the LSTM with fTDD feature set reached the best average classification errors values, equals to 6.4 ± 3.3%, 8.6 ± 3.0 % and 9.2 ± 5.6 % for the low, medium and high force level testing, respectively. Thus, this proposed neural network can obtain high accuracy, with the classification errors that are contained within the errors presented in usable systems (< 10 %,[53]).

In this scenario, a new potential strategy will be introduced in Cap. 3 for mitigating the effect of different exerted forces within a given movement class. Indeed, the proposed method allowed to extract from EMG signals all the valuable information regarding not only muscle contractions related to hand/wrist motions but also the changes of muscle activation patterns depending on the influence of different force levels. To this purpose, a FSM has been introduced for the management of three classifiers (the "hand/wrist gestures classifier", the "Spherical force classifier", the "Tip force classifier"), that worked simultaneously in the hierarchical classification approach to discriminate both hand/wrist gestures and force levels, during grasping tasks. This control strategy avoids to face a more seven multi-class problem using a single classifier and make the system controllability less complex by activating the force classifiers only when the "hand/wrist gestures classifier" returns an output class belonging to a closure hand gesture. The results of this approach have been presented by considering both 31 healthy subjects (section 2.3.3, Cap.2) and 15 transradial amputees (section 2.4.2, Cap.2)

Tesi di dottorato in Scienze e Ingegneria per l'Uomo e l'Ambiente/Science and Engineering for Humans and the Environment, di Francesca Leone, discussa presso l'Università Campus Bio-Medico di Roma in data 26/07/2021.
La disseminazione e la riproduzione di questo documento sono consentite per scopi di didattica e ricerca, a condizione che ne venga citata la fonte.

and it has been introduced to improve the performance of the currently adopted prosthesis EMG control architectures when both desired gestures and force levels had managed in a more natural way. The ultimate goal will be to produce an intuitive controlled hand prosthesis integrating force regulation.

2.3 State of art on PR approaches to classify multi-DoFs motion classes

Over the years, the myoelectric control systems have been extensively used to make the prosthetic device able to restore the most movements in daily living activities[63].

In this field, the PR algorithms have become always more interesting to predict complex electromyography patterns involving more than 2 Degrees of Freedom (DoFs) movements[64]. The surface electromyographic signals (sEMG) are widely considered the best non-invasive representation of muscular activity[65] and a natural interface to control in a non-invasive way the prosthetic devices[7].

Generally, the PR strategies applied to the prosthetic control associated the several inputs based on sEMG signals of different movements to several outputs, as limb motions related to specific myoelectric patterns[66].

These PR algorithms consist of a first step based on feature extraction, in time and frequency domain[67], to enhance information about EMG contraction in selected time windows. Then, in the sequential control technique, a single classifier is trained based on linear or non-linear decision boundaries; instead, in the simultaneous control technique, multiple classifiers are trained to control multiple joints simultaneously or a single classifier is trained by considering discrete and

Tesi di dottorato in Scienze e Ingegneria per l'Uomo e l'Ambiente/Science and Engineering for Humans and the Environment,
di Francesca Leone, discussa presso l'Università Campus Bio-Medico di Roma in data 26/07/2021.
La disseminazione e la riproduzione di questo documento sono consentite per scopi di didattica e ricerca,
a condizione che ne venga citata la fonte.

combined movements as separate classes, as shown in Figure 2.2.

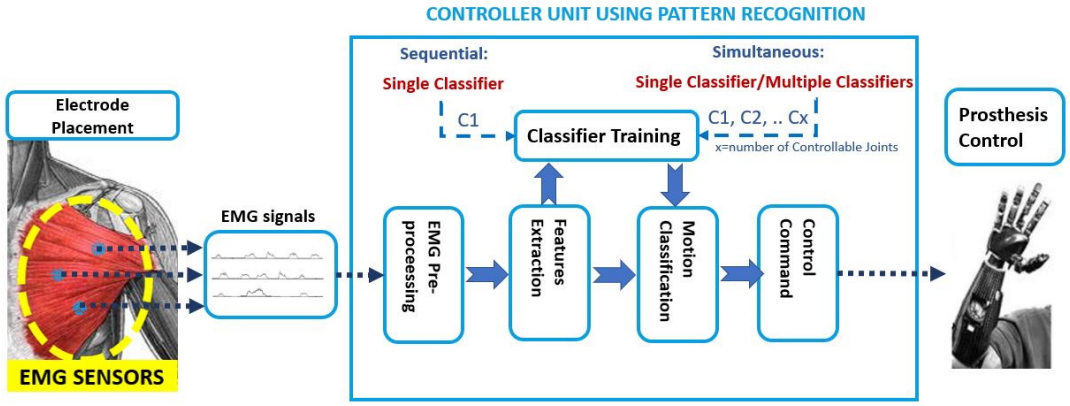

Figure 2.2: Pattern Recognition approach: the EMG signals are the input to the controller unit. Firstly the pre-processing step is done; then, in the features extraction step, the time and frequency domain features are used as input to train a single classifier or multiple classifiers. The classification output is the motion class to send as the command control to the prosthesis.

For instance, an extensive analysis can be found in the review study of Scheme et al.[7] and also in Bellingegni et al.[17], where a comparative analysis among Non-linear Logistic Regression (NLR), Multi-Layer Perceptron (MLP), Support Vector Machine (SVM) and Linear Discriminant Analysis (LDA) is proposed: the main difference between these algorithms is the linear and nonlinear shape of the decision boundary; straight line or plane for the LDA algorithm; curved line, or surface, for the NLR, MLP and SVM algorithms. Also the robustness and reliability of the proposed algorithms are a key factors for the online control of the prosthetic device and depend on their offline performance, complexity and computational time. In the case of trans-radial amputees, the LDA and NLR obtained statistically similar value in terms of F1 Score performance and computational burden[17] .

Tesi di dottorato in Scienze e Ingegneria per l'Uomo e l'Ambiente/Science and Engineering for Humans and the Environment,
di Francesca Leone, discussa presso l'Università Campus Bio-Medico di Roma in data 26/07/2021.
La disseminazione e la riproduzione di questo documento sono consentite per scopi di didattica e ricerca,
a condizione che ne venga citata la fonte.

The majority of the classification strategies, used for the prosthetic control, are based on single, hierarchical and parallel linear discriminant analysis (LDA) classifiers able to discriminate until 19 wrist/hand gestures (in the 3-DoFs case), considering both combined and discrete motions[68]. To sum up, these strategies used machine learning techniques (Figure 2.3) to increase the amputee's ability to control the prosthesis, in a more natural way, by adding the number of controllable DoFs, because they do not require independent EMG sites for classifying motion classes of different joints[69].

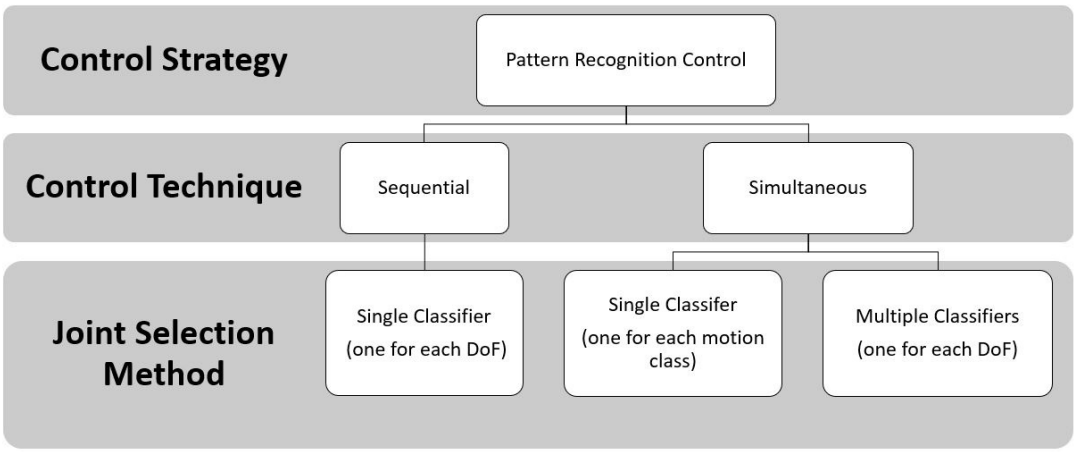

Figure 2.3: Schematic diagram of pattern recognition-based myoelectric control techniques and joint selection methods.

In the case of a poliarticulated prostheses with several DoFs, related to the elbow, wrist, and hand, the simultaneous control of combined movements of different joints (e.g. pouring water into a glass) ensure greater dexterity than the sequential one.

The simultaneous multi-DoFs control can be easier to implement and natural

Tesi di dottorato in Scienze e Ingegneria per l'Uomo e l'Ambiente/Science and Engineering for Humans and the Environment, di Francesca Leone, discussa presso l'Università Campus Bio-Medico di Roma in data 26/07/2021.
La disseminazione e la riproduzione di questo documento sono consentite per scopi di didattica e ricerca, a condizione che ne venga citata la fonte.

by using PR systems instead of conventional myoelectric control systems[70]. These last considered only the amplitude of the EMG signal for specific control sites[71,72].

The most employed PR algorithms for the classification of discrete and combined movements for two and three DoFs are: Linear Discriminant Analysis (LDA)[73], the Support Vector Machines (SVM)[74], Artificial Neural Networks (ANN)[75], Wavelet Neural Network (WNN)[76] and some deep learning methods based on the decoding of user's intention through sEMG signals[77], or the decoding of only the simultaneous multi-DoF Wrist movements[78]. In particular, regarding the deep learning algorithms, Zia ur Rehman et al.[79] proposed a deep networks, as the convolutional neural network (CNN) to classify six active motions and the rest, by using directly the EMG raw signals as inputs and the recordings of 15 consecutive days. The results of this study demonstrated that CNN significantly improved performance and increased robustness over time compared with standard LDA with features extraction. Another study of Du et al.[80] presented a benchmark database of HD-sEMG recordings that considered the hand gestures of 23 subjects and developed a multi-layer CNN based to enhance, with a deep domain adaptation framework, the sEMG-based inter-session gesture recognition. In Ulysse Côté-Allard et al.[79] aggregated data from different users were employed to evaluate the ability of deep learning algorithms to learn discriminant features from large datasets. The offline accuracy of the CWT-based ConvNet reached the 98.31 % for 7 gestures over 17 participants and 68.98 % for 18 gestures over 10 participants for the raw EMG-based ConvNet.

However, a limitation of the proposed pattern recognition and deep learning

Tesi di dottorato in Scienze e Ingegneria per l'Uomo e l'Ambiente/Science and Engineering for Humans and the Environment, di Francesca Leone, discussa presso l'Università Campus Bio-Medico di Roma in data 26/07/2021.
La disseminazione e la riproduzione di questo documento sono consentite per scopi di didattica e ricerca, a condizione che ne venga citata la fonte.

strategies is the sequential managing of one DoF at a time from the user, to control the prosthesis during complex multi-DoFs tasks. Such sequential control strategies have introduced cognitive burden in planning the intended movement because the user can not perform fluid, lifelike combined movements[43]. In particular, the simultaneous control of different joints is considered a needed capability to restore upper limb functionality, especially for patients as transhumeral and shoulder disarticulation amputees who have undergone TMR surgery[81].

There has been relatively little investigation into proposing novel PR strategies to simultaneously control multiple DoFs at different joints. From literature, Herberts et al.[82] employed 6 EMG channels to control three bidirectional movements simultaneously: 6 phantom wrist and hand movements (finger flexion (FF), finger extension (FE), pronation (P) and supination (S) of the stump, wrist flexion (WF) and wrist extension (WE)) were discriminated by separating classes with hyperplane computed with Lawrence method[83,84].

More recent studies have introduced PR-based simultaneous control systems up to the management of 2-3 DoFs[85,72,86]. In particular, three main approaches have been proposed in the literature to apply pattern recognition systems to both discrete and combined movements. The first approach trained a single LDA classifier by labeling as unique classes both discrete (1 DoF) and combined (2-DoFs) movements[87]; the second approach introduced three single LDA classifiers that predicted the simultaneous movement of three fingers in a non-human primate, by applying a parallel classification scheme[44]; the third one presented a control strategy for the classification of simultaneous movements of wrist and hand joints,

Tesi di dottorato in Scienze e Ingegneria per l'Uomo e l'Ambiente/Science and Engineering for Humans and the Environment, di Francesca Leone, discussa presso l'Università Campus Bio-Medico di Roma in data 26/07/2021.
La disseminazione e la riproduzione di questo documento sono consentite per scopi di didattica e ricerca, a condizione che ne venga citata la fonte.

(named "conditional parallel classification strategy") based on three parallel LDA classifiers that employed conditional probability to define the boundaries between similar classes of movement[88].

Another study of Young et al.[43] have employed a hierarchical and parallel classification strategies based on LDA classifiers in order to discriminate both discrete and combined motions as separated classes. The collected motions were: hand open/close (HO/HC), wrist extension/flexion (WE/WF), wrist supination/pronation (WS/WP), elbow extension/flexion (EE/EF), no motion (NM) and all 2-DoFs combined motions. The hierarchical strategy obtained the best performance from 6 healthy control subjects, by keeping below 15 % the classification errors.

To improve the classification performance when considering combined wrist/hand classification tasks, the use of intramuscular EMG was investigated on two PR methods[89]: the first was based on a single classifier that discriminated between 1 DoF and 2 DoFs motion classes; the second method employed a parallel set of three classifiers to predict up to 3 DoFs. The results showed that the classification error significantly decreased when using the intramuscular EMG compared to surface EMG for the parallel configuration ($p<0.01$), but not for the single classifier.

Moreover, most of the studies have considered only the offline accuracy and this may be a relevant limitation for the prosthetic control assessment, since many studies have shown that offline accuracy does not necessarily correspond to real-time performance[90,91].

Tesi di dottorato in Scienze e Ingegneria per l'Uomo e l'Ambiente/Science and Engineering for Humans and the Environment, di Francesca Leone, discussa presso l'Università Campus Bio-Medico di Roma in data 26/07/2021.
La disseminazione e la riproduzione di questo documento sono consentite per scopi di didattica e ricerca, a condizione che ne venga citata la fonte.

2.3.1 State of art of the multi-DoFs PR-based control techniques on TMR subjects

To improve the simultaneous control of multiple arm functions for many (ADLs), the TMR is considered very promising[92,93]. This surgical technique, combined with PR-based systems, represents an opportunity, especially for SD and TH amputees, to overcome the limited number of independent EMG sites available for controlling a multi-DoF prosthetic systems[94,95]. Indeed, the advanced EMG-based pattern recognition strategies have the potential to perform in a more natural way the simultaneous control of multiple DoFs with respect to the conventional myoelectric control methods[96], because they do not require independently control sites or mode-switching to activate multiple joints like elbow, wrist, and hand. The following 10 articles have been found in the literature in which pattern recognition algorithms have been employed in TMR patients:

In Mastinu et al.[97], the monitoring of TMR myoelectric signals of two TH amputee subjects, with TMR surgery and an e-OPRA, has been analyzed for 48 weeks after surgery to understand the potentiality compared to conventional surface electrodes. The TMR-radial and TMR-ulnar sites were used for hand opening and closure, respectively, while the triceps and biceps muscles for the flexion and extension of the elbow. The LDA classifier was used with four TD features: the summation of absolute value of EMG signals, defined as mean absolute value (MAV); the cumulative length of the EMG signal waveform defined as waveform length (WL); the zero crossing (ZC) that measures how many times two consecutive samples have different sign (when the EMG signal crosses zero) in

Tesi di dottorato in Scienze e Ingegneria per l'Uomo e l'Ambiente/Science and Engineering for Humans and the Environment, di Francesca Leone, discussa presso l'Università Campus Bio-Medico di Roma in data 26/07/2021.
La disseminazione e la riproduzione di questo documento sono consentite per scopi di didattica e ricerca, a condizione che ne venga citata la fonte.

order to detect the onset of movement during the procedure of data segmentation; and the slope sign changes (SSC) that represents the number of times the slope of EMG signal changes sign. Four discrete motions of elbow and hand were recorded with the Artificial Limb Controller, a prosthetic device designed for patients with e-OPRA implants[98].

In Kuiken et al.[94], five TMR patients with SD and TH amputations were able to perform, with a virtual prosthetic arm, 10 different motions related to different joints like elbow, wrist, and hand (elbow F/E, wrist F/E, wrist P/S, hand opening, 3 types of hand grasps -3 jaw chuck, fine pinch, tool grip, and no movement). For each subject, 12 self-adhesive bipolar EMG electrodes were placed over the reinnervated sites: in detail, four electrodes were placed according to clinical evaluation, while 8 additional sites were chosen by an electrode-placement optimization algorithm that allowed to select, from high density (HD) EMG recordings, a reduced number of electrodes necessary to preserve sufficient neural control information for accurate classification of user's intention[99]. The proposed PR algorithm was based on an LDA classifier with four TD features (MAV, ZC, WL, SSC). The LDA classifier was used to produce in real-time a new prediction every 100 ms. In details, the performance metrics as motion selection time (MST), motion completion time (MCT), and motion completion rate (MCR) were introduced for assessing the functionality, in real-time, of a virtual multifunction prosthesis.

In Smith et al.[100], the potentiality of PR myoelectric control was investigated when using wireless implantable devices. Five TMR subjects (three with SD and two with TH) were employed for evaluating the capability of performing nine mo-

Tesi di dottorato in Scienze e Ingegneria per l'Uomo e l'Ambiente/Science and Engineering for Humans and the Environment, di Francesca Leone, discussa presso l'Università Campus Bio-Medico di Roma in data 26/07/2021.
La disseminazione e la riproduzione di questo documento sono consentite per scopi di didattica e ricerca, a condizione che ne venga citata la fonte.

tion classes (rest state, elbow F/E, wrist P/S, F/E, hand O/C). However, two motion classes (hand open and wrist extension) were excluded for all subjects because two subjects (one with SD, one with TH) did not have a successful fine-wire insertion into sites. In particular, for two SD subjects, the number of reinnervated muscle sites was equal to three, while for one SD subject was equal to four. Both intramuscular EMG signals (imEMG) and sEMG signals were acquired by locating bipolar fine-wire electrodes and adhesive bipolar surface electrodes, respectively, on TMR sites. One subject with SD was excluded from pattern classification because he had the sEMG signals corrupted by a 60 Hz noise.

In Huang et al.[101], different spatial filters were tested to enhance the spatial selectivity of EMG recordings and the performance of EMG pattern classification by applying spatial filtering to high-density EMG recordings. Three subjects with TMR were recruited: the first one had a BSD amputation with four reinnervated muscle sites; the second one had a very short TH with four reinnervated muscle sites; the last TMR subject had a long TH amputation with two reinnervated muscle sites, and two natively innervated muscle sites. High-density surface EMG signals were recorded from the above mentioned muscle sites, that had been clinically selected. The following fifteen different movements were acquired: elbow F/E, wrist F/E, P/S, ulnar and radial deviation, two hand opening patterns (that included finger abduction and finger adduction), and five functional hand-closing patterns (power grip, prehensile (3-jaw chuck) grip, fine pinch grip, key grip, and trigger grip). The LDA classifier was used to classify the EMG signal with TD features (MAV, ZC, SSC, WL) and the surface EMG signals were processed by

Tesi di dottorato in Scienze e Ingegneria per l'Uomo e l'Ambiente/Science and Engineering for Humans and the Environment, di Francesca Leone, discussa presso l'Università Campus Bio-Medico di Roma in data 26/07/2021.
La disseminazione e la riproduzione di questo documento sono consentite per scopi di didattica e ricerca, a condizione che ne venga citata la fonte.

various high pass spatial filters including one-dimensional and two-dimensional filters.

In Zhou et al.[102], 16 movements of the arm, hand, and finger/thumb, with 8 degrees of freedom, were discriminated with an LDA classifier with the TD feature set, and a combination of AR coefficients and RMS (AR-RMS) of the signals. The recordings were made by using monopolar electrode configuration and three bipolar electrodes in three different directions: transversal, longitudinal, and diagonal. Four TMR subjects were recruited: the first one with a BSD with four reinnervated muscle sites, the second one with a very short TH and four reinnervated muscle sites, and two other subjects with long TH amputations with two reinnervated muscle sites and two natively innervated sites for elbow flexion/extension.

In Batzianoulis et al.[103], three different classification systems based on LDA, SVMs (with linear and non-linear kernel), and an Echo State Network (ESN) were evaluated by considering, for each proposed strategy, the classification performance on three phases of dynamic reach-to-grasp motions: acceleration (first phase), deceleration (second phase), and rest (third phase). Eight able-bodied control subjects and four TR amputees, two of which underwent TMR surgery for the neuroma pain, were enrolled. These TMR patients did not have additional muscle sites for improving myoelectric control. The EMG muscle activity was recorded with 12 sEMG sensors from seven muscles of the upper arm and five muscles of the forearm. For LDA and SVM, three features (i.e. average activation of each time window, waveform length, and number of slope changes) for each

Tesi di dottorato in Scienze e Ingegneria per l'Uomo e l'Ambiente/Science and Engineering for Humans and the Environment, di Francesca Leone, discussa presso l'Università Campus Bio-Medico di Roma in data 26/07/2021.
La disseminazione e la riproduzione di questo documento sono consentite per scopi di didattica e ricerca, a condizione che ne venga citata la fonte.

window of 150 ms have been extracted. Five grasp types (prismatic-2 fingers, precision disk, palm pinch, lateral, prismatic-4 fingers) were discriminated. In their most recent study[104], the same two TMR transradial amputees presented in[103] were employed to extend the previous results by addressing more insights on the LDA potentiality and introducing the use of the Hellinger distance to quantify the similarity between motion classes. In this case, the subjects were asked to perform a bimanual task by considering only three grasp types as the precision disk, lateral, and palm pinch motions. Different from[103], only the performance of an LDA classifier was evaluated in terms of classification accuracy when it was trained for each phase and over all motion phases. To train the classifier, the EMG signals of 5 muscles of the residual arm were recorded: Flexor Digitorum Superficialis, Extensor Digitorum Communis, Flexor Carpi Ulnaris, Extensor Carpi Ulnaris, Flexor Carpi Radialis.

In Xu et al.[105], the authors investigated how the rehabilitation training improved the separability of some channels of sEMG signals that remained still coupled over TMR. A TMR TH patient with 5 targeted muscles with coupled sEMG signals has been engaged. Five bipolar EMG electrodes have been placed on targeted muscles associated with the following movements: hand C/O, wrist P/S, elbow F/E. A new approach based on pattern recognition control with MAV-based threshold switches was introduced to improve the classification performance of an LDA classifier, based on Bayesian decision, with TD features (MAV, WL, ZC, SSC). Then, the obtained classification parameters have been used for allowing the patient to control a commercial prosthesis (Danyang Prostheses Co. Ltd,

Tesi di dottorato in Scienze e Ingegneria per l'Uomo e l'Ambiente/Science and Engineering for Humans and the Environment, di Francesca Leone, discussa presso l'Università Campus Bio-Medico di Roma in data 26/07/2021.
La disseminazione e la riproduzione di questo documento sono consentite per scopi di didattica e ricerca, a condizione che ne venga citata la fonte.

China): subset of the modified ARAT test was proposed to compare the online performance of the prosthetic operation.

The LDA classifier with TD-AR (time-domain and auto-regressive) features[106] was introduced for classifying elbow F/E, wrist S/P, hand O/C. A grid of stainless steel electrodes was placed over specific muscles. However, the exact sites of reinnervated muscles have been not described in detail. The outcome measures, obtained both with virtual reality and a physical prosthetic system, were introduced to evaluate the improvements in terms of offline classification errors. For obtaining physical outcomes all nine subjects used the following custom-fabricated prosthesis composed of: Boston Digital Elbow (Liberating Technologies Inc.), wrist Rotator (Motion Control Inc.), single DoF terminal device.

In Hargrove et al.[107], the outcome measures, obtained both with virtual reality and a physical prosthetic system, were introduced to evaluate the improvements in terms of offline classification errors of 9 transhumeral TMR subjects, when using prosthesis after a 6-week home trial. Three blocks of Target Achievement Control (TAC) test[108] were used to evaluate the performance of the LDA classifier with TD-AR (time-domain and auto-regressive) features[106]. For obtaining physical outcomes all nine subjects used the following custom-fabricated prosthesis composed of: Boston Digital Elbow (Liberating Technologies Inc.), wrist Rotator (Motion Control Inc.), single DoF terminal device.

In Tkach et al.[86] was demonstrated that a generic grid arrangement of electrodes performed equivalently or better than the control site (specific site for electrode placement). Four TMR amputee subjects were employed: two TH sub-

Tesi di dottorato in Scienze e Ingegneria per l'Uomo e l'Ambiente/Science and Engineering for Humans and the Environment, di Francesca Leone, discussa presso l'Università Campus Bio-Medico di Roma in data 26/07/2021.
La disseminazione e la riproduzione di questo documento sono consentite per scopi di didattica e ricerca, a condizione che ne venga citata la fonte.

jects had four reinnervated muscle sites; two SD subjects presented, instead, only two reinnervated muscles sites. EMG signals were acquired by using 15 bipolar pairs of EMG electrodes placed according to two conditions: in the "Control Site" condition, the electrodes were placed over muscle control sites, after clinical palpation; in the "Grid" condition, electrodes were positioned in a grid configuration, around the residual limb and the surface of the chest, for the TH and SD subjects, respectively. The LDA algorithm was used with the AR feature set including the six coefficients of a 6^{th} order autoregressive model.

To sum up, all the 10 studies presented in this sub-section take into account the pattern recognition strategy based on LDA classifier with different features set: TD features (MAV, WL, ZC, SSC)[105,102,101,100,94,97]; TD-AR features[106]; AR-RMS[102]; the AR feature set[86]; Hellinger distance[104]; the average activation of each time window, the waveform length, and the number of slope changes[103]. In Batzianoulis et al.[103] also the SVMs (with linear and non-linear kernel), and an Echo State Network (ESN) PR-based strategies were evaluated by considering, for each proposed strategy, the classification performance on five reach-to-grasp motions. The minimum number of discriminated classes was equals to 4 discrete motions related to the elbow and hand[97] or only the hand[103,104]. While, for the others 7 studies, always the elbow, wrist and hand joints were considered by including from 9 up to 29 motion classes[86] (for both discrete and simultaneous movements).

The following four studies presented also a comparison between direct control and pattern recognition based strategies, summarized in Tab. 2.2.

Tesi di dottorato in Scienze e Ingegneria per l'Uomo e l'Ambiente/Science and Engineering for Humans and the Environment, di Francesca Leone, discussa presso l'Università Campus Bio-Medico di Roma in data 26/07/2021.
La disseminazione e la riproduzione di questo documento sono consentite per scopi di didattica e ricerca, a condizione che ne venga citata la fonte.

Table 2.1: Summary of the reported analysis.

Study	No. of patients	Amp. Level	No. of reinnervated Sites / Control Sites	Prostheses/ Virtual Reality	DoF/ motion classes	Performance Evaluation methods
Mastinu et al.[97]	2	TH	2 reinnervated sites	PR without prosthesis	4 discrete hand and elbow motions	accuracy offline, classification error rate of LDA with 4 time domain features (MAV,WL,ZC,SSC)
Kuiken et al.[94]	5	SD, TH	4 reinnervated sites, 4 control sites	PR without prosthesis - VR	10 discrete elbow, hand and wrist motions	accuracy offline, motion selection time, motion completion time, and motion completion rate of LDA with TD features[102]
Smith et al.[100]	5	SD, TH	3-4 reinnervated sites (SD1,SD2), 2 reinnervated sites (TH)	PR without prosthesis	9 discrete elbow, hand and wrist motions	classification error rate of LDA with TD features[109]
Haung et al.[101]	3	BSD, TH	4 reinnervated sites (BSD), 4-2 reinnervated sites (STH,LTH)	PR without prosthesis	15 discrete elbow, hand and wrist motions	offline accuracy of LDA classifier with TD features (MAV, ZC,SSC,WL)
Zhou et al.[102]	4	BSD, STH, LTH	4 reinnervated sites (BSD), 4-2 reinnervated sites (STH,LTH)	PR without prosthesis	16 discrete movements of the arm, hand, and finger/thumb	offline accuracy of LDA classifier with TD feature set, and a combination of AR-RMS
Batzianoulis et al.[103]	2	TR	TMR surgery for the neuroma pain, not for control sites	PR without prosthesis	5 grasp types (prismatic-2 fingers, precision disk, palm pinch, lateral, prismatic-4 fingers)	offline accuracy, standard errors of LDA, two SVMs, and ESN Network
Batzianoulis et al.[104]	2	TR	TMR surgery for the neuroma pain, not for control sites	PR without prosthesis	3 grasp types (precision disk, lateral, and palm pinch)	offline accuracy of LDA classifier with TD feature
Xu et al.[105]	1	TH	3 reinnervated sites/ 5 control sites	Prosthesis - PR	6 discrete elbow, wrist and hand motions	offline accuracy, ARAT, LDA classifier with TD features (MAV, WL, ZC, SSC)
Hargrove et al.[107]	9	TH	not described	Prosthesis and VR - PR	6 discrete elbow, wrist and hand motions	SHAP, JTHFT, CRT, BBT, ACMC, the classification error rate, completion time, failure rate of LDA classifier with TDAR
Tkach et al.[86]	4	SD, TH	4 reinnervated sites (TH), 2 reinnervated sites (SD)	PR without prosthesis - VR	8 discrete and combined elbow, wrist and hand motions	offline accuracy of the LDA classifier with AR feature set
Hargrove et al.[110]	4	SD, TH	4-5 reinnervated control sites	Prosthesis - DC and PR	2 DoFs (sequentially PR system)	BBT, BST, CRT, classification error rates
Wurth et al.[111]	1	TH	4 control sites	PR and DC without prosthesis - VR	2 DoFs (sequentially and simultaneously PR systems)	FTAT, throughput (bits/second), path efficiency (%), completion rate (%)
Hargrove et al.[112]	8	TH	4 control sites	Prosthesis - DC and PR	2 DoFs	ACMC, SHAP, BBT, CRT
Young et al.[113]	3	SD, TH	2 reinnervated sites/ 4 control sites	Prosthesis - DC and PR	2 DoFs (sequentially and simultaneously PR systems)	TAC test (completion time, completion rate, length error), offline classification error

Acronyms of Table 2.1: BSD: Bilateral Shoulder Disarticulation; SD: Shoulder Disarticulation; TH: Transhumeral;LTH-STH: Long (L) - Short (S) Transhumeral; TR: Transradial; DC: Direct Control; PR: Pattern Recognition; VR: Virtual Reality; BBT: Box and Block Test CRT: Clothespin Relocation Test; WMFT: Wolf Motor Functions Tests; AMPS: Assessment of Motor and Process Skills; LDA: Linear Discriminant Analysis; MAV: Mean Absolute Value; WL: Waveform Length; ZC: Zero Crossing; SSC: Slope Sign Changes; TD: Time Domain ; AR-RMS: Auto Regressive-Root Mean Square; ESN: Echo State Network ;SVM:Support Vector Machine; TD-AR: Time Domain and Auto Regressive; ARAT: Action Research Arm Test; BST: Block stacking test; FTAT: Fitts' Target Acquisition Task; SHAP: Southampton Hand Assessment Procedure; JTHFT: Jebsen-Taylor test of Hand Function

Tesi di dottorato in Scienze e Ingegneria per l'Uomo e l'Ambiente/Science and Engineering for Humans and the Environment, di Francesca Leone, discussa presso l'Università Campus Bio-Medico di Roma in data 26/07/2021.
La disseminazione e la riproduzione di questo documento sono consentite per scopi di didattica e ricerca, a condizione che ne venga citata la fonte.

The first study that directly compared the performance of pattern recognition systems to direct control systems using a physical prosthesis with TMR patients is Hargrove et al.[110]. Four patients (one male with SD, two males and one female with TH amputation) had at least 4 reinnervated control sites (5 in one case) used for direct control of the elbow F/E and hand O/C joints. The P/S of the wrist joint was controlled and selected in different ways by the various patients, in a manner similar to that used with their old prostheses. For the PR-based control system, four pairs of bipolar electrodes have been added to the four pairs used for direct control. The PR control system was composed of a LDA classifier with TD features and AR coefficients. The velocity of the desired movement was computed using a simple proportional control algorithm. The performance achieved by all patients experts in the daily use of the myoelectric prosthesis with DC control and with experience in the laboratory use of the prosthesis controlled with PR, have been presented in Tab. 2.2. All subjects said they preferred PR-based control, because more intuitive. However, the authors pointed out that direct control allowed the simultaneous movement of two joints, while the PR-based control was limited to sequential control even when tasks required multiple DoFs.

In Wurth et al.[111], a real-time comparison between DC and PR-based control strategies was carried out to control a multi-DoF myoelectric prosthesis. Only one TH amputee among the enrolled subjects underwent the TMR procedure, with four independent control sites. The others were nine healthy control subjects and one TR amputee. For the DC control, the MAV EMG signals of the wrist flexors and extensors muscles were recorded from able bodied and TR subjects by using

Tesi di dottorato in Scienze e Ingegneria per l'Uomo e l'Ambiente/Science and Engineering for Humans and the Environment, di Francesca Leone, discussa presso l'Università Campus Bio-Medico di Roma in data 26/07/2021.
La disseminazione e la riproduzione di questo documento sono consentite per scopi di didattica e ricerca, a condizione che ne venga citata la fonte.

pre-gelled adhesive bipolar Ag-AgCl electrodes. Instead, for the TH amputee subject, four bipolar electrodes were placed on the flexor and extensor muscles, in order to control more than one DoF simultaneously. For the PR-control, the LDA classifier was used with four TD features (MAV, ZC, SSC, WL) and six AR coefficients. In particular, the able bodied and TH subjects were asked to perform hand O/C, wrist F/E, and no motion. Instead, for the TH subject, the elbow F/E was replaced by wrist F/E, because this DoF was considered more intuitive and relevant to be controlled for this level of amputation.

In Hargrove et al.[112], a clinical study was reported on 8 TH patients, with different levels of amputation and prosthetic solution composed of motorized Boston Digital Elbow (LTI), Motion Control Wrist Rotator (Motion Control Inc), and terminal device (7 hook from Greifer or EDT and 1 hand). All the subjects used prosthesis both in controlled (laboratory) and uncontrolled (home) environment. The eight patients were randomly divided into two groups of four subjects, each of which completed the home-trial using initially a prosthesis with a different control strategy, according to the group they belonged to. The two configurations were used for six weeks each. The electrode sites were identified with different methods depending on the different strategy adopted: when using direct control, the muscle sites were identified manually, using a combination of surgical notes when available, palpation, and myoelectric signal testing. As for the PR control, linear electrode locations were not targeted over specific muscles, rather a grid of electrodes was used. The algorithm used for PR-based control was the LDA described in[106]. For the DC control, dual-site differential DC system employed

Tesi di dottorato in Scienze e Ingegneria per l'Uomo e l'Ambiente/Science and Engineering for Humans and the Environment, di Francesca Leone, discussa presso l'Università Campus Bio-Medico di Roma in data 26/07/2021.
La disseminazione e la riproduzione di questo documento sono consentite per scopi di didattica e ricerca, a condizione che ne venga citata la fonte.

antagonistic muscle pair in order to control elbow F/E and terminal device O/C (hand or hook). In addition, mode switches were configured, for each subject, to control the wrist P/S DoF according to their previous device use.

In Young et al.[113], three different control strategies (direct control with proportional strategy, sequential PR control - one DoF at time, and simultaneous PR control - two DoFs at time) were analyzed in order to evaluate the ability of four amputees (2 TH and 2 SD), who underwent TMR surgery, to simultaneously control up to 2 DoFs with a virtual prosthesis. TH patients had two reinnervated muscle sites used for controlling hand O/C movements, and two natively innervated muscles (the biceps and triceps brachii) used for elbow F/E motions. The SD subjects had four reinnervated sites for controlling hand O/C and elbow F/E movements. Four pairs of self-adhesive Ag/AgCl bipolar surface electrodes were placed in the same muscle sites used for the conventional prostheses control. Other pairs of electrodes were placed near the primary sites where muscle activity could be palpated. The following 8 discrete and combined motions were acquired: elbow F/E, hand O/C, elbow F/E combined with hand O/C. The TMR amputees controlled discrete motions using their four independent muscle sites. For the PR-strategy, an LDA algorithm with four TD features (MAV, ZC, SSC, WL) and six AR coefficients of a sixth-order were used for the classification. As for the sequential control condition, the same methods introduced in[109] were used. Instead, for the simultaneous control strategy, the authors used the system tested on able-bodied subjects in[43].

To summarize, in all the articles of this section, a physical prosthetic device

Tesi di dottorato in Scienze e Ingegneria per l'Uomo e l'Ambiente/Science and Engineering for Humans and the Environment, di Francesca Leone, discussa presso l'Università Campus Bio-Medico di Roma in data 26/07/2021.
La disseminazione e la riproduzione di questo documento sono consentite per scopi di didattica e ricerca, a condizione che ne venga citata la fonte.

with two[111] or three DoFs[110,112] was employed, except for the[113], in which a virtual prosthesis was used instead of the physical one. As regards the direct control strategy, in all the studies, the simultaneous joint selection methods was employed. Only in Young et al.[113], the control technique was specified, i.e. the proportional control technique. As regards the reviewed papers on PR-based control, the LDA was always adopted with TD and AR features.

2.4 Conclusion

In this chapter, a review about PR control strategies of upper limb prosthesis to decode simultaneously gestures and forces and to discriminate multi-DoF motion classes has been presented. The main limitations of the current prosthetic systems is to be not very intuitive and unnatural[18], in spite of the progress made in this field based on EMG-PR[114]. To overcome these limitations, a hierarchical PR-based strategy have been presented in the Chapter 3, to allow amputees to restore simultaneously both the hand/wrist gestures and force levels during grasping tasks.

Tesi di dottorato in Scienze e Ingegneria per l'Uomo e l'Ambiente/Science and Engineering for Humans and the Environment, di Francesca Leone, discussa presso l'Università Campus Bio-Medico di Roma in data 26/07/2021.
La disseminazione e la riproduzione di questo documento sono consentite per scopi di didattica e ricerca, a condizione che ne venga citata la fonte.

Table 2.2: Evaluation of the performance obtained with the DC and PR systems.

Performance Evaluation Method	Metric Indicators	DC	PR		Study
BBT	Number of 1-inch blocks moved over a barrier in two min (average value on 4 TMR patients)	10.7±4.3	15±3		110
	Number of 1-inch blocks moved over a barrier in two min (average value on 8 TMR patients)	15.6± 2.7	13.4± 2.6		112
CRT	Time (s) to move three clothespins (average value on 4 TMR patients)	60±15	45±11		110
	Time (s) to move three clothespins (average value on 8 TMR patients)	137±60.2	90.2±39.6		112
ACMC	Test score (average value on 8 TMR patients)	44.4±3.4	47.3±3.9		112
SHAP	Index of function (average value on 8 TMR patients)	18±5	31±3		112
TAC	Completion Time (s) 1 DoF (average value on 4 TMR patients)	2.65±1.66	1.4 ± 0.3 (Seq)	2.03 ± 0.83 (Sim)	113
	Completion Time (s) 2 DoF (average value on 4 TMR patients)	3.55±1.66	3.6 ± 0.42 (Seq)	1.93 ± 0.82 (Sim)	
	Completion rate (%) 1 DoF (average value on 4 TMR patients)	86.25	100 (Seq)	93.75 (Sim)	
	Completion rate (%) 2 DoF (average value on 4 TMR patients)	81.25	92.5 (Seq)	98.75 (Sim)	
	Length error (%) 1 DoF (average value on 4 TMR patients)	97.4±81	13.96 ±4.65 (Seq)	32 ±29.52 (Sim)	
	Length error (%) 2 DoF (average value on 4 TMR patients)	86.65±52.77	67.88 ±11.8 (Seq)	21.88 ±25.08 (Sim)	
FTAT	Throughput (bit/s) (1 DoF)	2.64±0.24	3.67 ±0.23 (Seq)	2.11 ±0.18 (Sim)	111
	Throughput (bit/s) (2 DoF)	1.24±0.04	1.32 ±0.03 (Seq)	1.63 ±0.05 (Sim)	
	Path efficiency (%) (1 DoF)	90.1±0.23	97.00 ±0.96 (Seq)	96.3 ±1.12 (Sim)	
	Path efficiency (%) (2 DoF)	71.3±0.80	71.60 ±0.76 (Seq)	87.7 ±0.7 (Sim)	

Tesi di dottorato in Scienze e Ingegneria per l'Uomo e l'Ambiente/Science and Engineering for Humans and the Environment,
di Francesca Leone, discussa presso l'Università Campus Bio-Medico di Roma in data 26/07/2021.
La disseminazione e la riproduzione di questo documento sono consentite per scopi di didattica e ricerca,
a condizione che ne venga citata la fonte.

3

Simultaneous sEMG classification of hand/wrist gestures and forces

3.1 Introduction

After a careful study of the literature concerning the PR algorithms for the prosthetic control and the use of sEMG signals as a promising approach for decoding

Tesi di dottorato in Scienze e Ingegneria per l'Uomo e l'Ambiente/Science and Engineering for Humans and the Environment, di Francesca Leone, discussa presso l'Università Campus Bio-Medico di Roma in data 26/07/2021.
La disseminazione e la riproduzione di questo documento sono consentite per scopi di didattica e ricerca, a condizione che ne venga citata la fonte.

the motor intention of amputees in a non-invasive way, this chapter presents a hierarchical classification approach that aims at recognizing the desired hand/wrist gestures, as well as the desired force levels to exert during grasping tasks. In literature, two main approaches, based on mathematical models and machine learning techniques, have been analyzed to find a relationship between muscular activation and force. However, no hierarchical strategy, based on PR approach, has ever been proposed to simultaneously identify desired gestures and forces. Thus, in this chapter, firstly, the presented hierarchical PR approach has been described deeply (in section 3.3) to understand how it works. Then, it was tested and validated based on Non Linear Logistic Regression (NLR) and Linear Discriminant Analysis (LDA) algorithms, on 31 healthy subjects. A Finite State Machine was introduced to manage and coordinate three classifiers based on the NLR and LDA algorithms: the "hand/wrist gestures classifier" was introduced for the discrimination of 7 hand/wrist gestures (i.e. Rest, Spherical, Tip, Platform, Point, Wrist supination, and Wrist pronation), while the "Spherical" and "Tip" force classifiers were created for the identification of three force levels (i.e. Low, Medium, and High). This study reveals that the use of non-linear classification algorithm, as NLR, is as much suitable as the benchmark LDA classifier for implementing an EMG pattern recognition system, able both to decode hand/wrist gestures and to associate different performed force levels to grasping actions. Then, to investigate also the ability of trans-radial amputees to manage simultaneously desired hand/wrist gestures and three force levels, an extended analysis based on Logistic Regression (LR), NLR, and LDA algorithms has been carried out to assess the

Tesi di dottorato in Scienze e Ingegneria per l'Uomo e l'Ambiente/Science and Engineering for Humans and the Environment, di Francesca Leone, discussa presso l'Università Campus Bio-Medico di Roma in data 26/07/2021.
La disseminazione e la riproduzione di questo documento sono consentite per scopi di didattica e ricerca, a condizione che ne venga citata la fonte.

robustness of the hierarchical PR system. In this case, also the LR was evaluated to simplify the training step of the model (without the polynomial expansion) and to speed out the real time prediction (within 80 ms), without affecting the classification performance. The hierarchical PR system was tested and validated both offline and in real-time. For this purpose, the hand (RoboLimb) and a wrist module (WristRotator) were considered into the experimental protocol for real-time validation. Therefore, the real-time validation of the proposed method was evaluated in a real scenario, giving the trans-radial amputees the possibility of controlling a multi-DoF prosthetic system and exerting three different force levels. A statistical analysis based on the Mann-Whitney test (U-test) with Bonferroni correction ($p<0.016$) was carried out to assess the best solution when considering the performance of the three algorithms: the comparative analysis reports not statistically significant differences in terms of F1Score and misclassification errors between the LR, NLR and LDA classifiers. The best solution for controlling the prosthetic system in real-time by transradial amputees, seems to use simultaneously the LR algorithm with Time Domain (TD) features extraction (FE) for the "hand/wrist gestures classifier" and the NLR with TD-FE for the "Spherical" and "Tip" force classifiers.

Through these algorithms, the amputees obtained the lowest mean value of motion completion time (MCT) and the highest mean value of the motion completion rate (MCR).

Tesi di dottorato in Scienze e Ingegneria per l'Uomo e l'Ambiente/Science and Engineering for Humans and the Environment,
di Francesca Leone, discussa presso l'Università Campus Bio-Medico di Roma in data 26/07/2021.
La disseminazione e la riproduzione di questo documento sono consentite per scopi di didattica e ricerca,
a condizione che ne venga citata la fonte.

3.2 Experimental Setup and protocol on healthy subjects

Thirty-one healthy participants (age: 28 ± 7.6 years) were involved in the experiments. Six commercial active sEMG sensors (Ottobock $13E200 = 50$, 27 mm X 18 mm X 9.5 mm) were equidistantly fixed on an elastic adjustable bracelet and then were placed on the forearm of the able-bodied subjects in order to acquire sEMG signals (Fig.3.1). The study protocol complied with the Declaration of Helsinki and was approved by the local ethics committee (Comitato Etico Università Campus Biomedico di Roma, reference number: 15/16 PAR ComEt UCBM).
The bracelet was located about 5 cm below the subjects elbow, in line with the positioning of the electrodes, commonly used to control a prosthetic hand[115]. This type of electrodes outputs an enveloped signal of the "raw" signal (after amplification, filtering and rectification). The number of sEMG sensors was chosen equal to six because it is considered as the highest number that is possible to place into the socket[115]. Moreover, it allowed to reduce the data dimensionality and complexity[17]. The EMG sensors operated in the range $0-5V$ with a bandwidth of $90-450Hz$ and a common rejection ratio higher than $100dB$.

Five Force Sensitive Resistors (FSR), Model 402 by Interlink Electronics, were placed on a glove to verify the effective forces executed by the subjects. The relationship between the FSR voltage value V and the force value F was established with a statistical characterization as explained in[116]. The relation between voltage and force is described trough the following mathematical expression

$$F = p_1 V^5 + p_2 V^4 + p_3 V^3 + p_4 V^2 + p_5 V + p_6 \tag{3.1}$$

Tesi di dottorato in Scienze e Ingegneria per l'Uomo e l'Ambiente/Science and Engineering for Humans and the Environment, di Francesca Leone, discussa presso l'Università Campus Bio-Medico di Roma in data 26/07/2021.
La disseminazione e la riproduzione di questo documento sono consentite per scopi di didattica e ricerca, a condizione che ne venga citata la fonte.

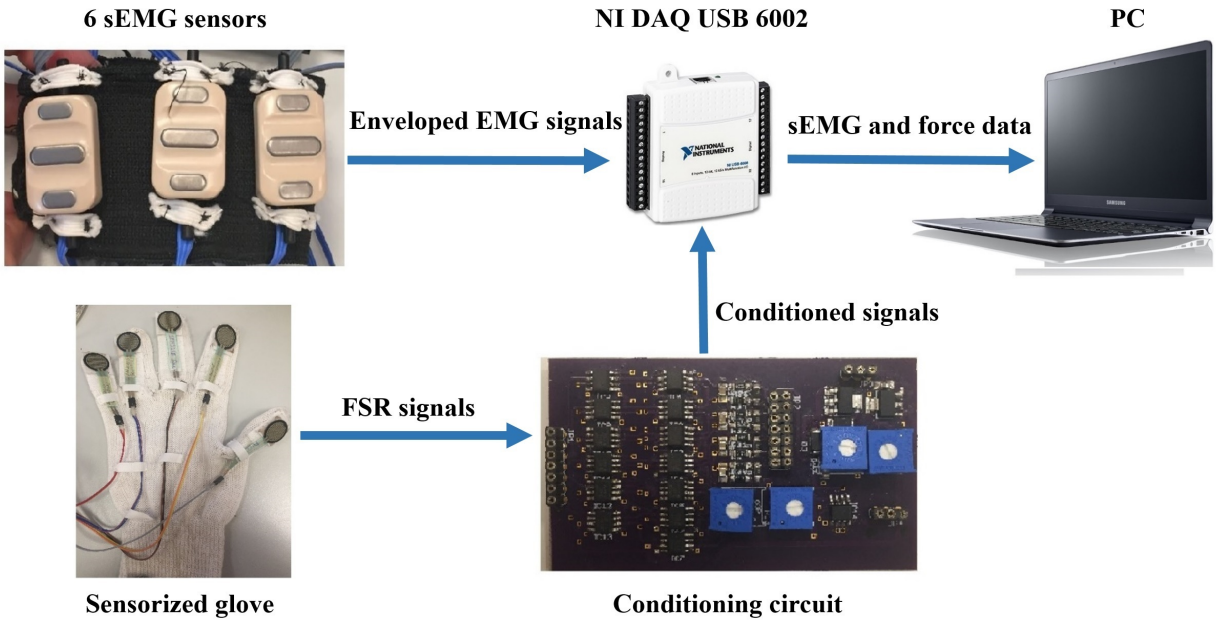

Figure 3.1: The experimental setup was composed by: (i) a sEMG elastic bracelet, (ii) NI DAQ USB 6002, (iii) a conditioning circuit and (iv) glove equipped with Force Sensitive Resistors (FSR), Model 402 by Interlink Electronics

obtained with the polynomial model

$$y = \sum_{i=1}^{n+1} p_i x^{(n+1-i)} \tag{3.2}$$

where $n+1$ represents the number of fitting coefficients, while n $(1 \leq n \leq 9)$ is the degree of the polynomial. The Anderson loop was used as signal conditioning circuit[117].

The EMG and force data were simultaneously acquired at 1 KHz, using a suitable software on Labview platform, by DAQ USB 6002 device. The PC (Samsung Intel(R) Core (TM) i7-4500U CPU @ 1.80 GHz) and DAQ communicated

Tesi di dottorato in Scienze e Ingegneria per l'Uomo e l'Ambiente/Science and Engineering for Humans and the Environment,
di Francesca Leone, discussa presso l'Università Campus Bio-Medico di Roma in data 26/07/2021.
La disseminazione e la riproduzione di questo documento sono consentite per scopi di didattica e ricerca,
a condizione che ne venga citata la fonte.

by means of an USB port.

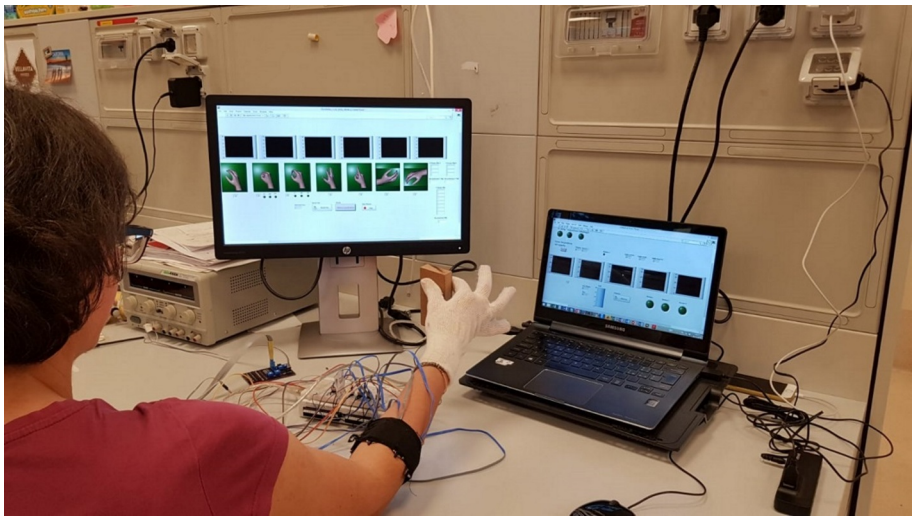

Figure 3.2: Subject positioning and data acquisition during experimental validation of the proposed approach. The subject was sitting in a comfortable chair in front of a PC monitor and was asked to perform six repetitions of each hand/wrist gesture. The subject performed "Spherical" and "Tip" gestures during the grasping of a rectangular object and executed three force levels. Written informed consent for the publication of this image was obtained.

The subject was sitting in front of a monitor (Fig.3.2) and was asked to perform the following seven hand gestures: Rest (hand relax), Spherical (hand with all fingers closed), Tip (hand with thumb and finger touching as if picking a small object), Platform (hand completely open and stretched), Point (hand with all fingers closed except for the index finger), Wrist supination and Wrist pronation. The participants were asked to produce each of these gestures for six times and hold it for 2 s with an interval of rest state about 2 s between each repetition. The tasks were performed in a single experimental session. The electrodes placement was the same over the repetition of each task. Demonstrations of each movement were displayed following a predefined list on a computer screen (Fig.3.2). For each

Tesi di dottorato in Scienze e Ingegneria per l'Uomo e l'Ambiente/Science and Engineering for Humans and the Environment,
di Francesca Leone, discussa presso l'Università Campus Bio-Medico di Roma in data 26/07/2021.
La disseminazione e la riproduzione di questo documento sono consentite per scopi di didattica e ricerca,
a condizione che ne venga citata la fonte.

Table 3.1: Measuring Performance: The Confusion Matrix

		ACTUAL	
		y=1	y=0
PREDICTED	h_θ=1	TP	FP
	h_θ=0	FN	TN

movement, the clinical operator instructed all participants to follow the demonstration of his motion and to perform it with a comfortable and consistent level of effort.

In a initial phase before the training, each subject was asked to produce maximum muscle contractions in order to perform the highest peak of force, while grasping a stiff object of rectangular shape (weight 66 g, dimensions $50 \times 100 \times 17mm$) with "Spherical" and "Tip" grasps. The object was used also during the training session.

The goodness of the classification was evaluated in terms of F1Score because it is considered more robust, in lieu of accuracy, to assess the performance[118].

In detail, if we considered an example of a simple confusion matrix (Tab.3.1), where true positive (TP) represents the number of the positive example that the model correctly classified as positive; true Negative (TN) is the number of negative examples that the model correctly classified as negative; false Positive (FP) represents the number of negative examples that the model incorrectly classified as positive; false Negative (FN) is the number of positive examples that the model incorrectly classified as negative; the F1Score can be evaluated as the harmonic mean of precision and recall taking both metrics into account in the following equation 3.5

Tesi di dottorato in Scienze e Ingegneria per l'Uomo e l'Ambiente/Science and Engineering for Humans and the Environment, di Francesca Leone, discussa presso l'Università Campus Bio-Medico di Roma in data 26/07/2021.
La disseminazione e la riproduzione di questo documento sono consentite per scopi di didattica e ricerca, a condizione che ne venga citata la fonte.

$$\begin{cases} Precision = \frac{TP}{TP+FP} \\ Recall = \frac{TP}{TP+FN} \\ F1Score = 2 * \frac{Precision*Recall}{Precision+Recall} \end{cases} \tag{3.3}$$

Three force thresholds were established at 30% (low), 60% (medium) and 90% (high) of the sum of all force contributions recorded from FSR sensors. Three force bands were defined as follows to reduce the difficult to perform a punctual value of force: the low level was fixed between the ±15% of the lowest threshold (i.e. 30%), the medium level was fixed as ±15% of the medium threshold (i.e. 60%), while the high level starts from −15% of the highest threshold (i.e. 90%) and continued until the maximum value. These bands were used to give a visual feedback to the subject during the recording of "Spherical" and "Tip" gestures.

In each subject's acquisition, the sEMG data were organized in a $84000 * 6$ dimensions matrix. Each column of the matrix was coupled with an EMG sensor.

Firstly, the enveloped EMG signal was acquired at 1 KHz to create 3 Datasets, used for both the NLR and LDA algorithms (Fig.3.3). The TrainingSet of the "hand/wrist gestures classifier" was composed by sEMG signals related to all the seven states of FSM. This TrainingSet included the recording of Spherical and Tip gestures performed at three different force levels in order to correctly classify gestures independently from muscular contraction changes due to force variations. The TrainingSets of "Spherical and Tip force classifiers" were composed only by sEMG data expressing different muscular contraction levels for these gestures.

For the NLR classifiers, the "raw" sEMG signals were used as input features in

Tesi di dottorato in Scienze e Ingegneria per l'Uomo e l'Ambiente/Science and Engineering for Humans and the Environment, di Francesca Leone, discussa presso l'Università Campus Bio-Medico di Roma in data 26/07/2021.
La disseminazione e la riproduzione di questo documento sono consentite per scopi di didattica e ricerca, a condizione che ne venga citata la fonte.

order to speed up the training and cross validation of the NLR algorithm (Fig.3.3 A). In detail, the use of only "raw" sEMG signals allowed a significant reduction of the classification time and of the response time without loss of system performance[119,120,121]. Moreover, the use of "raw" scaled sEMG signals as input features approximated the class evaluation time and system readiness to the sampling time[17]. Instead, for each of the three LDA classifiers, five time-domain (TD) features (Mean Absolute Value (MAV), Root Mean Square (RMS), Slope Sign Change (SSC), Waveform Length (WL) and Variance (σ^2)) were extracted from the corresponding channels of "raw" EMG data (Fig.3.3 B). In each analysis windows of 150 ms with an overlap of 100 ms were used[122].

3.3 Algorithm for hand/wrist gestures and force classification

In this section, the forces/gestures classification approach is explained deeply and it holds for each proposed classification algorithm because it works independently.

In detail, a hierarchical pattern recognition strategy was proposed for the classification of the desired hand/wrist gestures and force levels from muscular signals (Fig.3.4).

The FSM coordinated the hierarchical activation of the three classifiers. The highest classifier in the hierarchy was a single classifier able to discriminate seven discrete hand/wrist motion classes. The output of this classifier determined the desired hand/wrist gesture and, in case of "Spherical" or "Tip" class, the force classifier, lower in the hierarchy, to be activated. Thus, the force classifiers were activated for force levels recognition.

Tesi di dottorato in Scienze e Ingegneria per l'Uomo e l'Ambiente/Science and Engineering for Humans and the Environment,
di Francesca Leone, discussa presso l'Università Campus Bio-Medico di Roma in data 26/07/2021.
La disseminazione e la riproduzione di questo documento sono consentite per scopi di didattica e ricerca,
a condizione che ne venga citata la fonte.

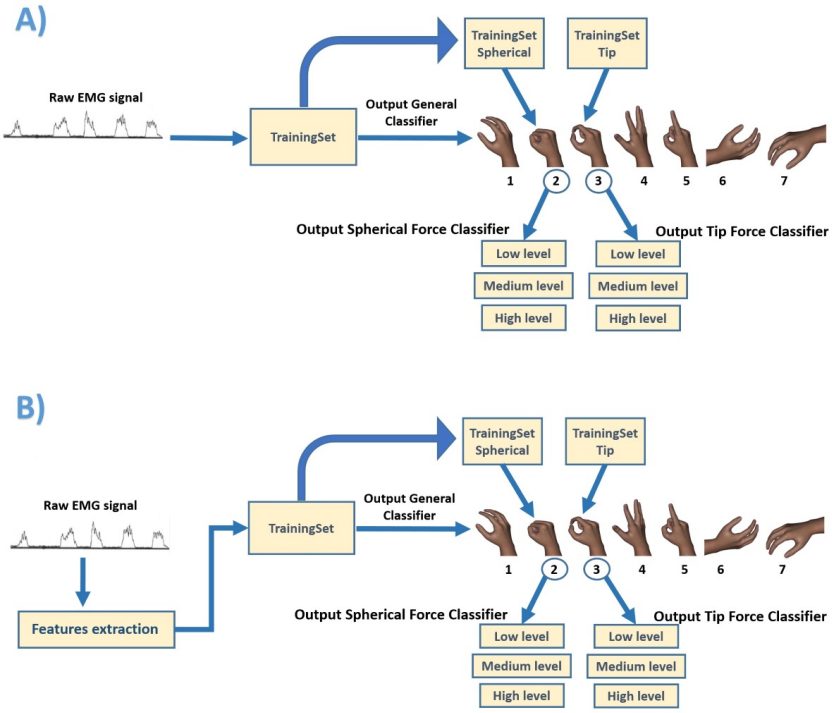

Figure 3.3: Block diagram of classification system for the creation of three different TrainingSet for obtaining the relative output classes. A) For the NLR classifiers, the raw sEMG signals are used as input features in order to speed up the training and cross validation of the NLR algorithm. B) For the LDA classifiers, five commonly used time domain features were extracted: Mean Absolute Value (MAV), Root Mean Square (RMS), Slope Sign Change (SSC), Waveform Length (WL) and Variance (σ^2).

The described hierarchy was implemented adopting NLR algorithm for both gesture and force classifiers. The same hierarchy was then reproduced using LDA algorithm in order to perform a comparative analysis. The Linear Discriminant Analysis (LDA), using time domain of the EMG signal, was frequently employed in literature because it was considered an efficient algorithm, simple to train and with an optimal compromise in terms of computational burden[81]. The Wilcoxon Signed-Rank test applied to the F1Score values was performed with significance

Tesi di dottorato in Scienze e Ingegneria per l'Uomo e l'Ambiente/Science and Engineering for Humans and the Environment,
di Francesca Leone, discussa presso l'Università Campus Bio-Medico di Roma in data 26/07/2021.
La disseminazione e la riproduzione di questo documento sono consentite per scopi di didattica e ricerca,
a condizione che ne venga citata la fonte.

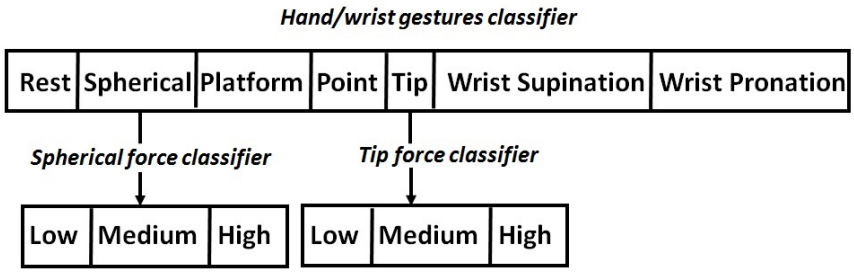

Figure 3.4: Hierarchical classification strategy."Hand/wrist gestures classifier" allowed the identification of the desired motion class among 7 different gestures. "Tip force classifier", lower in the hierarchy, allowed the classification of 3 force levels for "Tip" gesture. "Spherical force classifier", lower in the hierarchy, allowed the classification of 3 force levels for "Spherical" gesture.

threshold set to 0.05.

The FSM coordinated the three classifiers activation (i.e one for hand/wrist gestures and two for force levels).

The proposed classification system was characterized by three different classifiers (Fig.3.5):

- The "hand/wrist gestures classifier" was able to discriminate seven states, corresponding to seven hand and wrist gestures (blue circle states in Fig.3.5). This classifier was always active and it was the highest classifier in the hierarchy (Fig.3.5).

- The "Spherical force classifier" was able to discriminate three force levels (i.e. Low, Medium and High Level shown in Fig.3.5 in the red box). It was active if the "Spherical" gesture was identified and it was lowest in the hierarchy (Fig.3.5).

Tesi di dottorato in Scienze e Ingegneria per l'Uomo e l'Ambiente/Science and Engineering for Humans and the Environment,
di Francesca Leone, discussa presso l'Università Campus Bio-Medico di Roma in data 26/07/2021.
La disseminazione e la riproduzione di questo documento sono consentite per scopi di didattica e ricerca,
a condizione che ne venga citata la fonte.

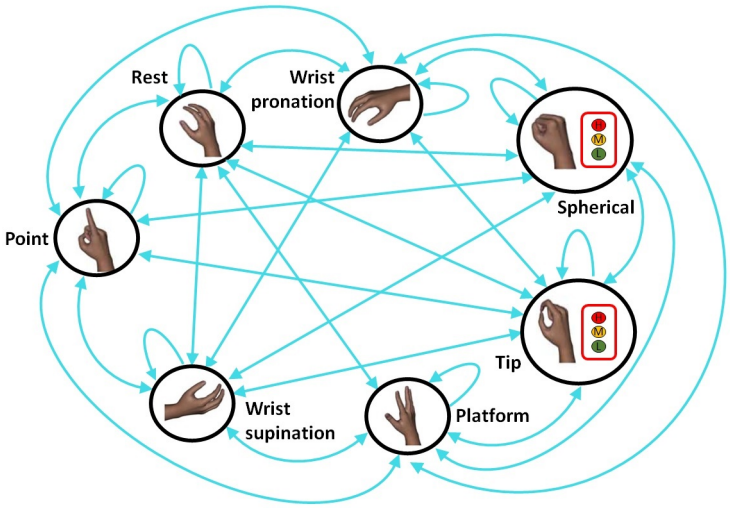

Figure 3.5: Finite State Machine (FSM) strategy for the classification of 7 different hand/wrist gestures and 3 force levels: the blue circle states indicated the hand gestures and wrist motions and they were all classified through the "hand/wrist gestures classifier". Three force levels (Low, Medium and High) can be classified through the "Spherical or Tip force classifier" if the "hand/wrist gestures classifier" discriminated the "Spherical" or "Tip" state, respectively. If the "Spherical" or "Tip" state was classified, the hierarchical classification strategy was adopted.

- The "Tip force classifier" was able to discriminate three force levels (i.e. Low, Medium and High Level shown in Fig.3.5 in the red box). It was active if the "Tip" gesture was identified and it was lowest in the hierarchy (Fig.3.5).

FSM determined the following different scenarios: until the FSM system remained in one of the two states (i.e. "Spherical" or "Tip"), the output of the FSM system provided hand/wrist gestures and the force levels information. The force classifier was conditioned on the decision of the first classifier of hand/wrist gesture. Thus, the classifiers of the second level of the hierarchy discriminated

Tesi di dottorato in Scienze e Ingegneria per l'Uomo e l'Ambiente/Science and Engineering for Humans and the Environment,
di Francesca Leone, discussa presso l'Università Campus Bio-Medico di Roma in data 26/07/2021.
La disseminazione e la riproduzione di questo documento sono consentite per scopi di didattica e ricerca,
a condizione che ne venga citata la fonte.

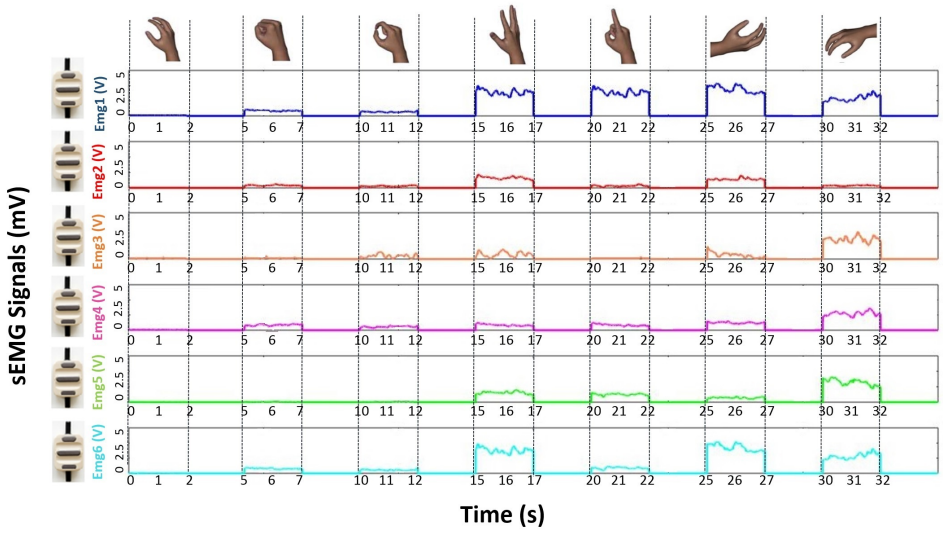

Figure 3.6: Plot of the raw sEMG recording for the six EMG channels, related to all the 7 performed movements of a single acquisition session from one of the subjects who was involved into the experiment. The plot of raw sEMG recording of "Spherical" and "Tip" classes are related to muscular activations performed at medium force level.

Differently from Young et al.,[43] the hierarchical classification system is used to discriminate simultaneously hand/wrist gestures and desired force levels.

The FSM use allowed the two classifiers of different grades of the hierarchy to work simultaneously. Until the "Spherical" or "Tip" state is classified by "hand/wrist gestures classifier", the "Spherical force classifier" or the "Tip force classifier" intervenes to discriminate force levels.

The raw sEMG recording for the six EMG channels, related to all the 7 per-

Tesi di dottorato in Scienze e Ingegneria per l'Uomo e l'Ambiente/Science and Engineering for Humans and the Environment, di Francesca Leone, discussa presso l'Università Campus Bio-Medico di Roma in data 26/07/2021.
La disseminazione e la riproduzione di questo documento sono consentite per scopi di didattica e ricerca, a condizione che ne venga citata la fonte.

formed movements of a single acquisition session, was reported in (Fig.3.6).

The NLR and LDA algorithms are employed for implementing the hierarchical classification approach, since both of them guaranteed statistically similar value for F1Score performance. Moreover they have also comparable computational burden, despite LDA has the fewest number of classification parameters[17]. In detail, several studies have been considered the LDA classifier with features extraction as ground truth[123,81] and it can be used for the online control of prosthetic devices[124] that is commercially available by COAPT (https://www.coaptengineering.com). Force information is provided only for the two grasping classes (i.e. "Spherical" and "Tip") in which an object interaction is expected. Seven hand/wrist gestures (i.e. Rest, Spherical, Tip, Platform, Point, Wrist supination and Wrist pronation) had been discriminated by using a Nonlinear Logistic Regression (NLR) algorithm. When the "Spherical" or the "Tip" class are identified, a second NLR-algorithm-based classifier, i.e., respectively, "Spherical force classifier" or "Tip force classifier" is activated simultaneously in order to discriminate three force levels (i.e. Low, Medium and High).

The same hierarchical pattern recognition strategy was implemented with three linear classifiers ("hand/wrist gestures classifier", "Spherical force classifier" and "Tip force classifier"), based on LDA with time domain features extraction. The performance of each algorithm (NLR and LDA) were measured by means of F1Score value and statistical analysis had been based on the Wilcoxon Signed-Rank test. A comparative analysis among NLR and LDA with feature extraction was implemented in order to define the most suitable classification algorithm for

Tesi di dottorato in Scienze e Ingegneria per l'Uomo e l'Ambiente/Science and Engineering for Humans and the Environment, di Francesca Leone, discussa presso l'Università Campus Bio-Medico di Roma in data 26/07/2021.
La disseminazione e la riproduzione di questo documento sono consentite per scopi di didattica e ricerca, a condizione che ne venga citata la fonte.

the realization of a gestures and forces classification architecture to control of a prosthetic device.

The performance of the proposed approach were evaluated during an experimental session involved 31 healthy subjects. The users are asked to perform 7 hand/wrist motions and to replicate three different force levels during the "Spherical" and "Tip" grasps. In order to provide a qualitative assessment of the ability to classify both gestures and force levels, only the offline results were reported for the healthy subjects. Then, an advanced experimental protocol that considered also the real-time performance was employed to translate results from laboratory to clinical practice, by using an upper-limb prostheses for transradial amputees.

3.3.1 LR and NLR classification algorithm and dataset organization

In this section, firstly the similarity and differences between LR and NLR algorithms are reported. In detail, the mathematical expressions, used for both LR and NLR algorithms, are introduced and the differences between them are explained. Then, the dataset organization is introduced by describing the data split approach employed. In this study the Logistic regression model used the following logistic function to evaluate the class membership probability Eq.3.4 for both LR and NLR classifiers

$$P(1 \mid x, \theta) = \begin{cases} g(\theta^T \cdot x) = \frac{1}{1+e^{-\theta^T \cdot x + \theta_0}} \\ 1 - P(y = 0 \mid x, \theta) \end{cases} \tag{3.4}$$

where θ and θ_0 are, respectively, the classification parameters vector and bias

Tesi di dottorato in Scienze e Ingegneria per l'Uomo e l'Ambiente/Science and Engineering for Humans and the Environment, di Francesca Leone, discussa presso l'Università Campus Bio-Medico di Roma in data 26/07/2021.
La disseminazione e la riproduzione di questo documento sono consentite per scopi di didattica e ricerca, a condizione che ne venga citata la fonte.

term, while $g(\cdot)$ is the logistic function. For the NLR classifiers, additional polynomial features (e.g. $x_1, x_2, x_1 * x_2, x_1^2, x_2^2$) were introduced to make non-linear this logistic regression model.

The following cross-entropy error cost function was introduced to train the supervised classification algorithm by minimizing a specific cross-entropy error cost function

$$J(\theta,\theta_0) = -\frac{1}{m}\left[\sum_{i=1}^{m} y^{(i)} \cdot \ln g\left(\theta^T \cdot x^{(i)} + \theta_0\right)\right] - \frac{1}{m}\left[\sum_{i=1}^{m}\left(1-y^{(i)}\right) \cdot \ln\left(1-g\left(\theta^T \cdot x^{(i)} + \theta_0\right)\right)\right] \tag{3.5}$$

where m is the number of samples of TrainingSet, $y^{(i)}$ is the known class membership of the i-th sample, θ and θ_0 are the classification parameters and $g(\cdot)$ is the logistic function. Resilient Backpropagation (RProp) was chosen as minimization algorithm in comparison to the Backpropagation, its faster of training and the rate of convergence tends to be less[125,17]. Each single classifier was iteratively trained with all possible configurations of its internal parameters that had an appropriate range of values[17].

For both the LR and NLR algorithms, the prediction of class labels h_θ was achieved by comparing the probability distribution $P(y|x)$ with a decision threshold (TH)

$$h_\theta = \begin{cases} P(1 \mid x,\theta) \geq TH \rightarrow 1 \\ P(1 \mid x,\theta) < TH \rightarrow 0 \end{cases} \tag{3.6}$$

Tesi di dottorato in Scienze e Ingegneria per l'Uomo e l'Ambiente/Science and Engineering for Humans and the Environment, di Francesca Leone, discussa presso l'Università Campus Bio-Medico di Roma in data 26/07/2021.
La disseminazione e la riproduzione di questo documento sono consentite per scopi di didattica e ricerca, a condizione che ne venga citata la fonte.

Both the LR and NLR algorithms guaranteed a prediction response within 100 ms, although the LR is able to make a prediction also within 80 ms and it is easier to use and simpler to interpret, due to the absence of the polynomial expansion. Indeed, the NLR with respect to LR consisted only in transforming the original features into higher degree polynomials before training the model. This has the advantage that can fit many more types of curves, but, on the other side, it can require more effort both to find the best fit and to interpret the role of the independent variables. Thus, the main advantage of using LR were: to simplify and speed out the training step of the model without affecting the classification performance.

To improve the robustness of the algorithms when considering sEMG data of transradial amputees (presented in Section 3.4.2), the regularization term was added to the cross-entropy error cost function to improve the generalization performance on unseen data

$$\begin{aligned} J(w) = \sum_{i=1}^{n} -y^{(i)} \cdot \ln g(\theta^T \cdot x^{(i)} + \theta_0) - (1 - y^{(i)}) \\ \cdot \ln\left(1 - g(\theta^T \cdot x^{(i)} + \theta_0)\right) + \frac{\lambda}{2}\|w\|^2 \end{aligned} \tag{3.7}$$

where λ is the regularization parameter that adds penalty on the cost function when the magnitudes of the fitting parameters increase. The gradient of the cost function is a vector where the $j^{(th)}$ element is defined as

$$\begin{cases} \frac{\partial J(\theta)}{\partial \theta_0} = \frac{1}{m} \sum_{i=1}^{m} (h_\theta(x^{(i)}) - y^{(i)}) x_j^{(i)} & \text{for j=0} \\ \frac{\partial J(\theta)}{\partial \theta_0} = \frac{1}{m} \sum_{i=1}^{m} (h_\theta(x^{(i)}) - y^{(i)}) x_j^{(i)} + \frac{\lambda}{m}\theta_j & \text{for j}\geq 0 \end{cases} \tag{3.8}$$

Tesi di dottorato in Scienze e Ingegneria per l'Uomo e l'Ambiente/Science and Engineering for Humans and the Environment, di Francesca Leone, discussa presso l'Università Campus Bio-Medico di Roma in data 26/07/2021.
La disseminazione e la riproduzione di questo documento sono consentite per scopi di didattica e ricerca, a condizione che ne venga citata la fonte.

Moreover, the first-order iterative optimization algorithm "Gradient descent" was used for finding a local minimum of the multivariate differentiable cost function, with a maximum number of iterations equals to 150[126]. In detail, the Polack-Ribiere flavour of conjugate gradients was used to compute search directions, and a line search with a quadratic and cubic polynomial approximations and the Wolfe-Powell stopping criteria was employed together with the slope ratio method for guessing initial step sizes[127].

Regarding the DataSet organization, three-way data split approach[128] was applied to the dataset ($84000 * 6$ sEMG data) and the Training Set (TR), the Cross Validation Set (CVS) and the Test Set (TS) were set to contain 60%, 20% and 20% of the data, respectively. A random shuffle was implemented for filling these subsets with a proper proportion of all classes samples distribution.

The unique operation done on sEMG data was the scaling: it consists of subtracting the mean value to each signal and dividing the result by the range, as done in[17].Then, downsampling (with a step=10, 100 Hz) was applied to reduce the data dimensions and training process.

The discarded data rising from the downsampling process (90% of initial data) composed a new set of data called Generalization Set (GS) used as a second test to obtain an estimation of the generalization capability of each classifier. The three way data split approach was applied on the data coming from downsampling process (10% of initial data): TR, CVS and TS were set to contain 6%, 2% and 2% of the data, respectively. The TR and CVS were used to train and cross validate the classifiers and the TS and GS were employed to test the performance

Tesi di dottorato in Scienze e Ingegneria per l'Uomo e l'Ambiente/Science and Engineering for Humans and the Environment,
di Francesca Leone, discussa presso l'Università Campus Bio-Medico di Roma in data 26/07/2021.
La disseminazione e la riproduzione di questo documento sono consentite per scopi di didattica e ricerca,
a condizione che ne venga citata la fonte.

of the classifiers.

Once the optimal classification model has been chosen, TS was used to evaluate the performance of classifier when new features were introduced as input. To avoid overfitting and explore the best model, the CVS was used to evaluate the performance of classifiers for each set of classification parameters[17].

3.3.2 LDA classification algorithm and dataset organization

In this section, firstly the time-domain (TD) features, used as input for the LDA algorithm, are described. Indeed, a proper features set that represent the sEMG signals[129], can improve the ability of a linear classifier to provide accurate movement classes and force level recognition. Then the mathematical expressions that defined the classifier and the dataset organization are presented. In our study, for each of the three LDA classifiers, five TD features (Mean Absolute Value (MAV), Root Mean Square (RMS), Slope Sign Change (SSC), Waveform Length (WL) and Variance (σ^2)) were extracted from the corresponding channels of "raw" EMG data. In each analysis windows of 150 ms with an overlap of 100 ms were used[122].

The MAV is defined as the summation of absolute value of EMG signals[17] and can be calculated as

$$MAV = \frac{1}{L}\sum_{i=1}^{L}|(x_i)| \tag{3.9}$$

where x_i is the ith time sample in a window and by L the total length of the window.

The WL represents the cumulative length of the EMG signal waveform and

Tesi di dottorato in Scienze e Ingegneria per l'Uomo e l'Ambiente/Science and Engineering for Humans and the Environment,
di Francesca Leone, discussa presso l'Università Campus Bio-Medico di Roma in data 26/07/2021.
La disseminazione e la riproduzione di questo documento sono consentite per scopi di didattica e ricerca,
a condizione che ne venga citata la fonte.

can be calculated as

$$WL = \sum_{i=2}^{L} |(x_i - x_{i-1})| \tag{3.10}$$

The Slope sign change represents the number of times the slope of EMG signal changes sign and it is defined as

$$\begin{aligned} SSC &= \tfrac{1}{L} \sum_{i=2}^{L-1} f[(x_i - x_{i-1}) \times (x_i - x_{i+1})] \\ f(x_i) &= \begin{cases} 1, & x \geq threshold \\ 0, & otherwise \end{cases} \end{aligned} \tag{3.11}$$

The Root Mean Square is the mean power of the signal and it is defined as

$$RMS = \sqrt{\frac{1}{L} \sum_{i=1}^{L} x_i^2} \tag{3.12}$$

The Variance represents a statistical measure of how signal varies from its average value and it is defined as

$$VAR = \frac{1}{L-1} \sum_{i=1}^{L} x_i^2 \tag{3.13}$$

Since the LDA classifiers do not require the setting of internal parameters[17], the training and test rely on a two ways data split approach[128]. Thus, the initial dataset was divided as follows: the TrainingSet (TR) contains 70% of the data and the test set contains the remaining 30% of the data. The training of the classifiers was performed by using the Eqs.(3.14,3.15). The subset were iteratively filled

Tesi di dottorato in Scienze e Ingegneria per l'Uomo e l'Ambiente/Science and Engineering for Humans and the Environment, di Francesca Leone, discussa presso l'Università Campus Bio-Medico di Roma in data 26/07/2021.
La disseminazione e la riproduzione di questo documento sono consentite per scopi di didattica e ricerca, a condizione che ne venga citata la fonte.

trough a random shuffle in order to obtain a configuration with proportionate class number[17]. The downsampling step was not necessary because the features extraction avoided the generation of large-scale-dataset and guaranteed a short time for the training of the classifiers. The Linear Discriminant Analysis (LDA) with features extraction is a binary supervised machine learning algorithm able to transform the features into a lower dimensional space, which maximizes the ratio of the between-class variance to the within-class variance. This guarantees the maximum class separability[130]. The training of the classifiers was performed by using the Eqs.(3.14,3.15). The following decision function is used to discriminate between only two different classes and to assign class label 1 or 2 to unknown data

$$h_{\beta}(x) = \begin{cases} (\beta^T \cdot x + \beta_0) \geq 0 \rightarrow 1 \\ (\beta^T \cdot x + \beta_0) < 0 \rightarrow 2 \end{cases} \tag{3.14}$$

where β and β_0 are, respectively, the classification parameters vector and the bias term. In details, the classification parameters can be evaluated as

$$\begin{cases} \beta = \Sigma^{-1} \cdot (\mu_1 - \mu_2) \\ \beta_0 = -\beta^T \cdot \left(\frac{\mu_1 + \mu_2}{2}\right) + \ln\left(\frac{\Pi_1}{\Pi_2}\right) \end{cases} \tag{3.15}$$

where Σ is the pooled covariance matrix, μ_1, μ_2, Π_1, Π_2 are the mean vectors and the prior probabilities of class 1 and class 2, respectively. Since LDA is a binary algorithm a one vs. all approach was implemented to solve the multi-class

Tesi di dottorato in Scienze e Ingegneria per l'Uomo e l'Ambiente/Science and Engineering for Humans and the Environment, di Francesca Leone, discussa presso l'Università Campus Bio-Medico di Roma in data 26/07/2021.
La disseminazione e la riproduzione di questo documento sono consentite per scopi di didattica e ricerca, a condizione che ne venga citata la fonte.

classification problem. The class label (c) is predicted as

$$h_\beta(x) = \max_c \left({}_c\beta^T \cdot x + {}_c\beta_0\right) and \begin{cases} {}_c\beta = \Sigma^{-1} \cdot (\mu_c) \\ {}_c\beta_0 = -{}_c\beta^T \cdot \left(\frac{\mu_c}{2}\right) + \ln(\Pi_c) \end{cases} \tag{3.16}$$

where ${}_c\beta$ and ${}_c\beta_0$ are the classification parameters vector and the bias term of c class, respectively. An ad hoc developed software was implemented in Matlab for the construction of the three LDA classifiers.

The LDA were trained and tested at 1KHz (without downsampling step) and for this reason the NLR model was evaluated considering the F1score on GS for the comparative analysis of the performance.

For the results obtained from amputees subjects (section 3.4.2), the EMAV and EWL were employed instead of the MAV and WL, respectively, because the combination of them with other EMG features have been considered valuable for performance enhancement in rehabilitation and clinical applications[131].

In detail, the EMAV is defined as the summation of absolute value of EMG signals[132] and can be calculated as

$$EMAV_i = \frac{1}{L}\sum_{i=1}^{L} |(x_i)^p| \qquad p = \begin{cases} 0.75, & if\, i \geq 0.2\,L \;\&\; i \leq 0.8\,L \\ 0.50, & otherwise \end{cases} \tag{3.17}$$

The EWL is an extension of WL that represents the cumulative length of the

Tesi di dottorato in Scienze e Ingegneria per l'Uomo e l'Ambiente/Science and Engineering for Humans and the Environment, di Francesca Leone, discussa presso l'Università Campus Bio-Medico di Roma in data 26/07/2021.
La disseminazione e la riproduzione di questo documento sono consentite per scopi di didattica e ricerca, a condizione che ne venga citata la fonte.

EMG signal waveform and can be calculated as

$$EWL = \sum_{i=2}^{L} |(x_i - x_{i-1})^p|$$
$$p = \begin{cases} 0.75, & if\, i \geq 0.2\, L \,\&\, i \leq 0.8\, L \\ 0.50, otherwise \end{cases} \tag{3.18}$$

where, in both the Eqs.3.17, 3.18, the parameter p is used to enhance the information content at the middle region of the time window[131].

3.4 Experimental results on healthy subjects

The results of the "hand/wrist gestures classifier" are reported in Tab.3.2 in terms of the average accuracy and F1Score for NLR and LDA algorithms.

The results of LDA classifiers with time domain features extraction were obtained with data sampled at 1 KHz (without downsampling). Thus, for the comparative analysis, we reported the results of NLR classifiers tested on "GS" because they represent the behaviour of the classifiers when data sampled at 1 KHz are provided as input[17]. Average classification accuracy for the NLR "hand/wrist gestures classifier", the NLR "Spherical force classifiers" and "Tip force classifiers" are respectively equals to 98.78%, 98.80%, 96.09%. The LDA "hand/wrist gestures classifier" reaches an average classification accuracy equals to 95.41%, while the LDA "Spherical force classifiers" and "Tip force classifiers" show an average classification value of 98.74% and 97.60%, respectively.

The results of the two force classifiers, "Spherical force classifier" and "Tip force classifier" are shown, respectively, in Tab. 3.3 and Tab.3.4, in terms of

Tesi di dottorato in Scienze e Ingegneria per l'Uomo e l'Ambiente/Science and Engineering for Humans and the Environment, di Francesca Leone, discussa presso l'Università Campus Bio-Medico di Roma in data 26/07/2021.
La disseminazione e la riproduzione di questo documento sono consentite per scopi di didattica e ricerca, a condizione che ne venga citata la fonte.

Table 3.2: Mean value and standard deviation of F1Score and Accuracy of the "hand/wrist gestures classifier" calculated for 31 healthy subjects with NLR and LDA algorithms.

Hand/Wrist gestures Classifier								
	NLR Classifier				LDA classifier			
	F1_Score		Accuracy		F1_Score		Accuracy	
Classes	Mean (%)	Dev_std	Mean (%)	Dev_std	Mean (%)	Dev_std	Mean (%)	Dev_std
Rest	98,25	4,05	99,50	1,24	97,62	4,31	99,05	3,55
Spherical	95,63	6,22	98,71	1,94	94,28	7,58	93,89	7,76
Tip	95,56	4,93	98,69	1,55	94,25	6,14	93,68	7,56
Platform	95,97	6,58	98,86	1,84	94,60	6,32	95,96	5,25
Point	92,69	9,25	97,63	3,58	93,52	6,02	92,38	7,67
Wrist supination	95,70	6,70	98,64	2,26	95,57	6,18	95,27	7,36
Wrist pronation	98,20	4,93	99,41	1,7	98	3,53	97,66	4,41

Table 3.3: Mean value and standard deviation of F1Score and Accuracy of the "Spherical force classifier" calculated for 31 healthy subjects with NLR and LDA algorithms. The classification performance for the NLR classifiers are evaluated on "GS", while LDA classifiers are tested on "TS" with data sampled at 1 KHz (without downsampling).

Spherical Force Classifier								
	NLR Classifier				LDA Classifier			
Classes	F1_Score		Accuracy		F1_Score		Accuracy	
	Mean (%)	Dev_std	Mean (%)	Dev_std	Mean (%)	Dev_std	Mean (%)	Dev_std
Low	97,49	4,84	98,35	3,13	98,49	2,62	98,7	2,76
Medium	97,43	4,21	98,25	2,86	98,43	2,46	98,05	3,35
High	99.69	1,2	99,80	0,78	99,47	1,33	99,48	1,81

Table 3.4: Mean value and standard deviation of F1Score and Accuracy of the "Tip force classifier" calculated for 31 healthy subjects with NLR and LDA algorithms.

Tip Force Classifier								
	NLR Classifier				LDA Classifier			
Classes	F1_Score		Accuracy		F1_Score		Accuracy	
	Mean (%)	Dev_std	Mean (%)	Dev_std	Mean (%)	Dev_std	Mean (%)	Dev_std
Low	91,54	8,61	94,46	5,42	97,11	3,46	97,79	4,34
Medium	91,56	8,24	94,36	5,14	96,31	4,17	96,36	5,46
High	99,03	1,96	99,26	1,31	99,16	2,03	98,66	3,77

the average F1Score and accuracy for the NLR and LDA classifiers. The average classification accuracy of the NLR "Spherical force classifier" is 98.35% for the low force level, 98.25% for the medium force level and 99.80% for the high force level. The LDA "Spherical force classifier" shows an average classification accuracy of

Tesi di dottorato in Scienze e Ingegneria per l'Uomo e l'Ambiente/Science and Engineering for Humans and the Environment, di Francesca Leone, discussa presso l'Università Campus Bio-Medico di Roma in data 26/07/2021.
La disseminazione e la riproduzione di questo documento sono consentite per scopi di didattica e ricerca, a condizione che ne venga citata la fonte.

98.7% for the low force level, 98.05% for the medium force level and 99.48% for the high force level. The average classification accuracy of the NLR "Tip force classifier" is 94.36% for the low force level, 94.46% for the medium force level and 99.26% for the high force level. The LDA "Tip force classifier" shows an average classification accuracy of 97.79% for the low force level, 96.36% for the medium force level and 98.66% for the high force level.

Fig.3.7 shows the average confusion matrix when testing the NLR and LDA "hand/wrist gestures classifier" on "GS" and "TS", respectively.

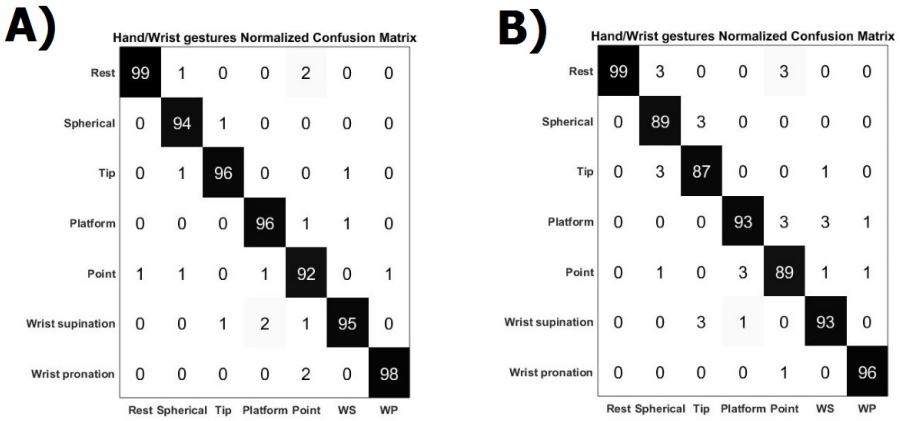

Figure 3.7: Normalized confusion matrix of the "hand/wrist gestures classifier" obtained with NLR algorithm (A) and LDA algorithm (B). On the main diagonal the cardinality of the correct classifications is reported; in the top left dial and bottom right dial, the cardinality of the misclassified data related to the 7 output classes representing the hand gestures are reported.

In details, Fig.3.7 A reports the normalized confusion matrix for the NLR "hand/wrist gestures classifier", while Fig.3.7 B is related to the LDA "hand/wrist gestures classifier".

Fig. 3.8 shows the average confusion matrices when testing the NLR "Spherical

Tesi di dottorato in Scienze e Ingegneria per l'Uomo e l'Ambiente/Science and Engineering for Humans and the Environment,
di Francesca Leone, discussa presso l'Università Campus Bio-Medico di Roma in data 26/07/2021.
La disseminazione e la riproduzione di questo documento sono consentite per scopi di didattica e ricerca,
a condizione che ne venga citata la fonte.

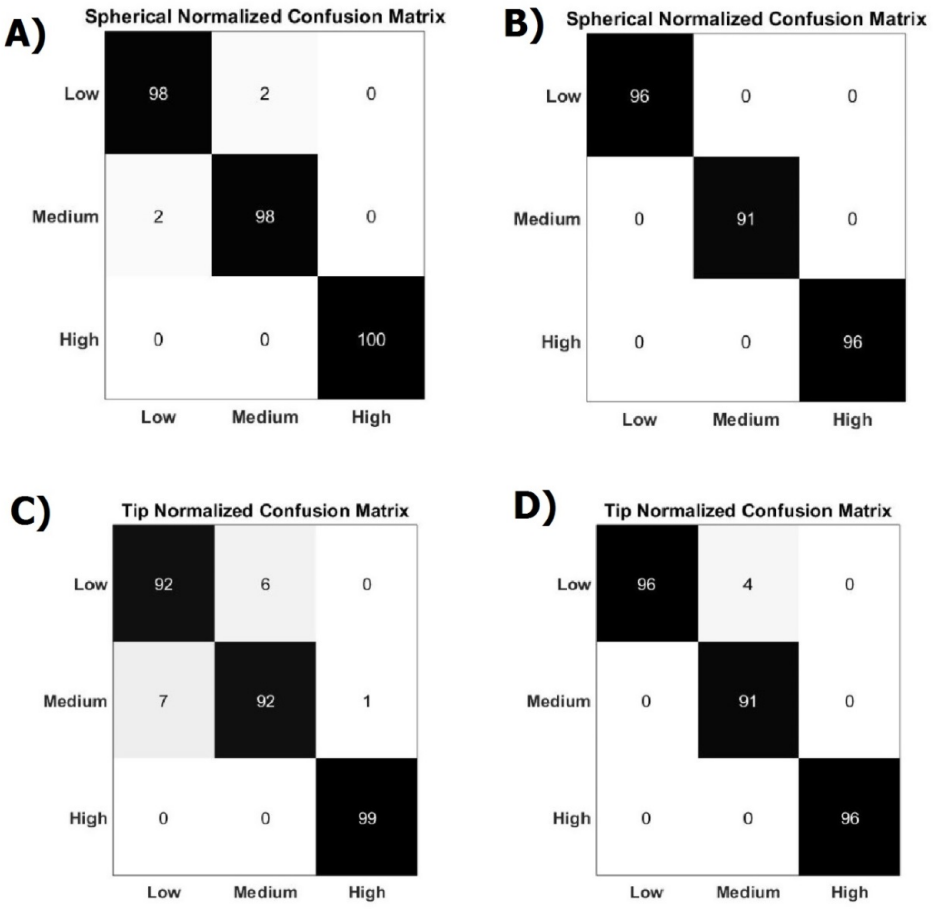

Figure 3.8: Normalized confusion matrix of the "Spherical force classifier" obtained with NLR algorithm (A) and LDA algorithm (B). Normalized confusion matrix of the "Tip force classifier" obtained with NLR algorithm (C) and LDA algorithm (D). The cardinality of the correct classifications is reported on the main diagonal; in the top left dial and bottom right dial, the cardinality of the misclassified data related to the 3 output classes that represented the force levels are reported.

force and Tip force classifiers" on the "GS" (Fig. 3.8 A and C) and the LDA "Spherical force and Tip force classifiers" on "TS" (Fig. 3.8 B and D). As shown in Fig.3.9 the NLR and LDA "hand/wrist gestures classifier" were able to identify 7 hand gestures with an average F1Score of 96.01% and 95.41% respectively (Fig.3.9

Tesi di dottorato in Scienze e Ingegneria per l'Uomo e l'Ambiente/Science and Engineering for Humans and the Environment,
di Francesca Leone, discussa presso l'Università Campus Bio-Medico di Roma in data 26/07/2021.
La disseminazione e la riproduzione di questo documento sono consentite per scopi di didattica e ricerca,
a condizione che ne venga citata la fonte.

A). The "Spherical force classifier" identified the force level reaching an average F1 score of 98.75% and 98.79% with NLR and LDA classifiers, respectively (Fig.3.9 B). The "Tip force classifier" was able to define the force level with an average F1 score of 94.04% and 97.53% with NLR and LDA classifiers, respectively (Fig.3.9 C). The Wilcoxon Signed-Rank test applied to the F1Score values points out no statistically significant difference ("ns") between NLR and LDA algorithms ($p > 0.05$).

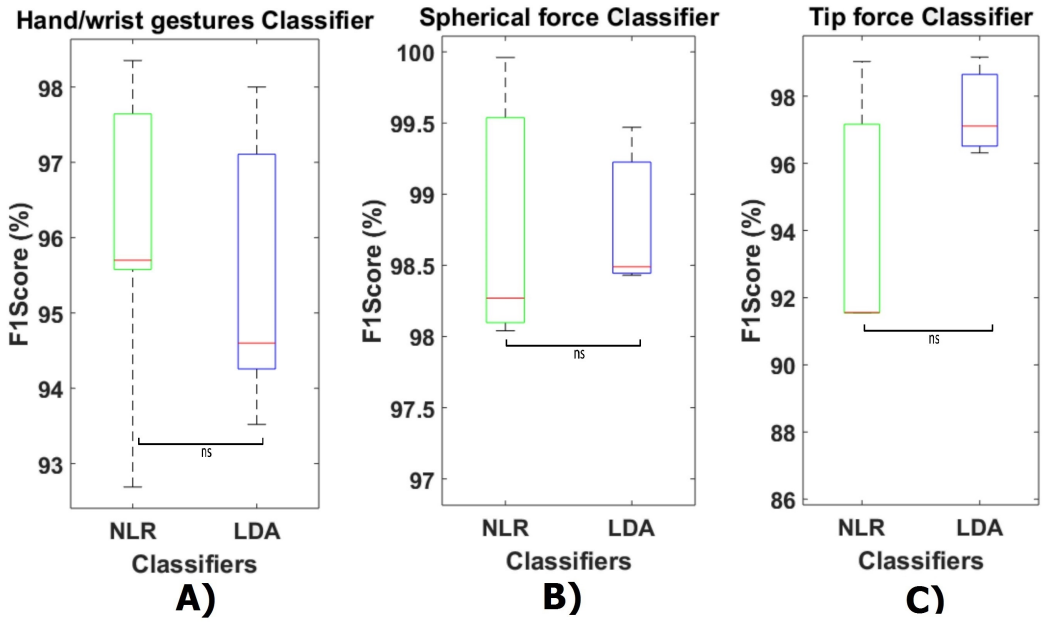

Figure 3.9: A) Average F1Score values calculated on 30 healthy subjects using NLR "hand/wrist gestures classifier" algorithm, tested on "GS", and LDA "hand/wrist gestures classifier" with 5 time domain features, tested on "TS". B) Average F1Score values calculated on 30 healthy subjects using NLR "Spherical force classifier" algorithm, tested on "GS", and LDA "Spherical force classifier" with 5 time domain features, tested on "TS". C) Average F1Score values calculated on 30 healthy subjects using NLR "Tip force classifier" algorithm, tested on "GS", and LDA "Tip force classifier" with 5 time domain features, tested on "TS". Statistical non-significance is indicated by "ns".

Tesi di dottorato in Scienze e Ingegneria per l'Uomo e l'Ambiente/Science and Engineering for Humans and the Environment,
di Francesca Leone, discussa presso l'Università Campus Bio-Medico di Roma in data 26/07/2021.
La disseminazione e la riproduzione di questo documento sono consentite per scopi di didattica e ricerca,
a condizione che ne venga citata la fonte.

To assess the ability of discriminating well the force levels also when considering the FSR sensors, the Fig.3.10 has been introduced: the forces applied to the object from the 31 healthy subjects are showed as the average values of the sum of all the FSR measurements.

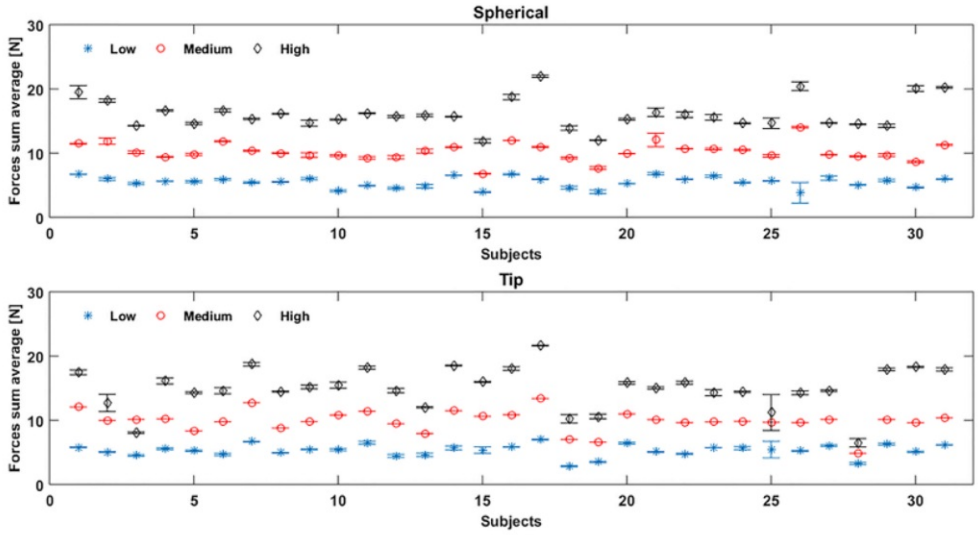

Figure 3.10: Force sum average values are obtained, by FSR measurements, for 31 healthy subjects during, respectively, the "Spherical" and "Tip" gestures, performed six times: the blue, red and black values represent the mean value and standard deviation of respectively low, medium and high force values performed by each subject.

The misclassification error rates, defined as the percent of incorrect classifications, are presented in Tab.3.5 and Tab.3.6 for both the NLR and LDA "hand/wrist gestures classifier".

The NLR "hand/wrist gestures classifier" performed the highest misclassification errors (i.e. 9%) with "Point" class, while the LDA "hand/wrist gestures classifier" performed misclassification errors greater than 10% (i.e. 11%, 12, 7% and 11, 3%) for the "Spherical, Tip and Point" classes, respectively. The NLR and

Tesi di dottorato in Scienze e Ingegneria per l'Uomo e l'Ambiente/Science and Engineering for Humans and the Environment, di Francesca Leone, discussa presso l'Università Campus Bio-Medico di Roma in data 26/07/2021.
La disseminazione e la riproduzione di questo documento sono consentite per scopi di didattica e ricerca, a condizione che ne venga citata la fonte.

Table 3.5: Misclassification error rates of the "hand/wrist gestures classifier" calculated with NLR and LDA algorithms

Misclassification error rates (%)		
	Hand/Wrist gestures Classifier	
Classes	NLR Classifier	LDA Classifier
Rest	1	1
Spherical	6	11
Tip	5	12,7
Platform	5	7
Point	9	11,3
Wrist Supination	5	7
Wrist Pronation	2	4

Table 3.6: Misclassification error rates of Spherical and Tip Force Classifier calculated with NLR and LDA algorithms

Misclassification error rates (%)				
	NLR Classifier		LDA Classifier	
Classes	Spherical Force Classifier	Tip Force Classifier	Spherical Force Classifier	Tip Force Classifier
Low	2	8	4	4
Medium	3	8,5	8	8,5
High	1	2	4	4

LDA "Spherical force classifier" reached the maximum misclassification error (i.e. 3% and 8%, respectively) for the "Medium" force level. The "Tip NLR and LDA force classifier" presented the same maximum misclassification error (i.e. 8.5%) for the "Medium" force level.

3.4.1 Discussion

As shown in Tab.3.2 the NLR and LDA "hand/wrist gestures classifier" were able to identify 7 hand gestures with an average F1Score about equals the 95%. Also the "Spherical force classifier" and "Tip force classifier" obtained average F1 score above 96%. These results seem to be very promising if we consider that similar

Tesi di dottorato in Scienze e Ingegneria per l'Uomo e l'Ambiente/Science and Engineering for Humans and the Environment, di Francesca Leone, discussa presso l'Università Campus Bio-Medico di Roma in data 26/07/2021.
La disseminazione e la riproduzione di questo documento sono consentite per scopi di didattica e ricerca, a condizione che ne venga citata la fonte.

values of average F1Score have been achieved only from six healthy subjects and for gesture classification[76], without considering the force levels. The comparative analysis between NLR and LDA classifier, applied to F1Score values, reported no statistically significant difference between them.

Confusion matrices, reported in Fig.3.7, Fig.3.8, confirmed the positive results of the accuracy parameter. The cardinality of the correct classifications on the main diagonal underlined the high classification accuracy even if some misclassified data out of the main diagonal suggested lower performance of "Tip force classifier" respect to "Spherical force classifier". This is due to the major difficulty encountered by few subjects in modulating between low and medium force levels during a Tip grasp. The high force levels were always well discriminated at 99% of average accuracy for both the NLR and LDA force classifiers. In Tab. 3.5, the LDA "hand/wrist gestures classifier" obtained a greater misclassification error rates than NLR "hand/wrist gestures classifier" ranging from 1% to maximum 12,7% for discriminating 7 hand/wrist gestures classes by using data including different muscular activations related to desired force levels. This may due to the fact that linear classifiers, with straight line or plane decision boundary, could not be the most appropriate method for a 7 multi-class problem with features not linearly separable at all. In comparison to the results presented in Scheme et al.[7], the misclassification error values, obtained for the "Spherical" and "Tip" classes with the LDA "hand/wrist gestures classifier", were lower than 17% and, thus, it can be considered an effective result. Moreover, the misclassification error values, obtained for the "Spherical" and "Tip" classes with the NLR "hand/wrist

Tesi di dottorato in Scienze e Ingegneria per l'Uomo e l'Ambiente/Science and Engineering for Humans and the Environment, di Francesca Leone, discussa presso l'Università Campus Bio-Medico di Roma in data 26/07/2021.
La disseminazione e la riproduzione di questo documento sono consentite per scopi di didattica e ricerca, a condizione che ne venga citata la fonte.

gestures classifier" were, respectively, equals to 6% and 5% and these results can be considered positive for an usable system ($< 10\%$)[7]. Finally, the misclassification error rates for the "Spherical and Tip force classifiers" are similar (Tab. 3.6), ranging from 1% to maximum $8,5\%$ for both the NLR and LDA classifiers.

Almost all healthy subjects were able to modulate the force levels and fall into the range displayed by the visual feedback, without generating high variance values, as shown in Fig.3.10. Fewer subjects difficulty reproduced the force values within the force intervals, despite the visual feedback as reference. For instance, in Fig.3.10, the subjects 25 and 3 were not able to well differentiate between medium and high force levels during Tip grasp (represented as red and black points), while subject 28 performed the three force levels too closed during Tip grasp. This depended on the subject's difficulty to maintain the applied force within the force intervals.

These results are also more appreciable if we take into account that NLR, used for the classification of both hand/wrist gestures and force levels, was trained and tested using only raw scaled sEMG signals as input features. On the other hand, the LDA algorithm employed the minimum number of classification parameters and computational burden. However, the use of time domain features extraction based on time windowing, make the class evaluation time equals to the window shift and the system delay approximates to the time window length[17]. Furthermore, the same number of sensors were adopted to classify 7 gesture classes with respect to the previous 5[17] and to identify 3 levels of force during the execution of "Spherical" and "Tip" grasps. The proposed hierarchical classification archi-

Tesi di dottorato in Scienze e Ingegneria per l'Uomo e l'Ambiente/Science and Engineering for Humans and the Environment,
di Francesca Leone, discussa presso l'Università Campus Bio-Medico di Roma in data 26/07/2021.
La disseminazione e la riproduzione di questo documento sono consentite per scopi di didattica e ricerca,
a condizione che ne venga citata la fonte.

tecture permitted to decode the user's motion intention and desired force levels with high reliability. The proposed hierarchical pattern recognition approach has obtained effective results with both NLR and LDA algorithms that have been demonstrated to be suitable for discriminating both hand/wrist gestures and force levels applied during grasping tasks.

3.5 Experimental validation on upper limb amputees

3.5.1 Experimental setup and protocol

Fifteen trans-radial amputees were enrolled, 12 male and 3 female (aged 45 ± 13.44) at the INAIL prosthesis center in Vigorso di Budrio. The study protocol complied with the Declaration of Helsinki and was approved by the local ethics committee (Comitato Etico di Area Vasta Emilia Centro (CE-AVEC), reference number: CP-PPRAS1/1-01). All patients signed informed consent for voluntary participation in the study. The experimental setup was composed of twelve commercial sEMG sensors (Ottobock 13E200 = 50, 27 mm × 18 mm × 9.5 mm) and two hand dynamometers (Vernier HD BTA, 46 mm x 28 mm x 170 mm) that were used for the EMG and force signals acquisition, respectively. A custom electronic interface (Fig.3.11.A) was developed to connect properly the sensors to the NI-DAQ 6218 (National Instruments). The described experimental setup was connected via USB to the PC (MSI prestige 15, Intel (R) Core (TM) i7-1185G7 CPU @ 1.80 GHz), to allow data acquisition by using a LabView software. For each arm, six sEMG sensors were located equidistantly from each other on an elastic bracelet, located 4 cm below the patient's elbow Fig.3.11. The number of

Tesi di dottorato in Scienze e Ingegneria per l'Uomo e l'Ambiente/Science and Engineering for Humans and the Environment,
di Francesca Leone, discussa presso l'Università Campus Bio-Medico di Roma in data 26/07/2021.
La disseminazione e la riproduzione di questo documento sono consentite per scopi di didattica e ricerca,
a condizione che ne venga citata la fonte.

Table 3.7: Summary of the trans-radial patients information

Patient	Age	Sex	Amp.side	Dom.limb	Years from amp.	Expert	Stump length (cm)
P1	25	M	DX	DX	11	yes	12
P2	37	M	SX	DX	13	yes	9
P3	52	F	DX	DX	37	no	6
P4	57	M	DX	DX	25	yes	15
P5	40	F	SX	DX	26	yes	8
P6	54	M	DX	DX	24	yes	14
P7	26	F	SX	DX	25	no	7
P8	61	M	DX	DX	13	yes	22
P9	32	M	DX	DX	6	yes	7
P10	43	M	DX	DX	18	yes	21
P11	64	M	SX	DX	20	yes	7
P12	31	M	DX	DX	7	yes	5
P13	41	M	DX	DX	5	yes	23
P14	47	M	SX	DX	25	yes	26
P15	65	M	DX	DX	50	yes	14.5

sEMG sensors was described in section 3.2.

In order to evaluate the real time robustness of the proposed PR strategy, a prosthetic system, composed of hand device (RoboLimb, by Touch Bionics) and wrist module (Wrist Rotator, by Ottobock) was employed. A custom electronic board and relative firmware was developed in order to control the prosthesis via Bluetooth.

The tasks were performed in a single experimental session. The electrodes placement was the same over the repetition of each task. Demonstrations of each movement were displayed following a predefined list on a computer screen (Fig.3.11.C and Fig.3.11.D). During the offline training, for each movement, the clinical operator instructed all participants to follow the demonstration of his motion and to perform it with a comfortable and consistent level of effort. Then, in the real-time phase, the participants were asked to reproduce the same tasks in the most similar way to the offline training. The performance of the proposed

Tesi di dottorato in Scienze e Ingegneria per l'Uomo e l'Ambiente/Science and Engineering for Humans and the Environment, di Francesca Leone, discussa presso l'Università Campus Bio-Medico di Roma in data 26/07/2021.
La disseminazione e la riproduzione di questo documento sono consentite per scopi di didattica e ricerca, a condizione che ne venga citata la fonte.

approach[69] was evaluated during an experimental session, that was organized as follows:

- Step 1 - Force thresholds settings. To define the three threshold values for the low, medium, and high force level, the mean values obtained from three acquisitions were considered for each level. This procedure was employed for both Spherical and Tip grasps, for a total of 18 acquisitions. The average values will be used, for each level, as a reference during step 2.

- Step 2- Training step. In a initial phase before the training, the patient was asked to perform bi-manually the following 7 hand and wrist gestures for six times, and to hold each for 3 seconds: Rest, Spherical, Tip , Platform,Point, Wrist supination and Wrist pronation. For the grasping tasks, the amputees were asked to modulate also the force, according to three force levels, established as following: the low level was fixed between the $\pm$ 10 % of the mean value for the low threshold, the medium level was fixed as $\pm$ 10 % of the mean value for the medium threshold, while the high level starts from -10 % of the highest threshold and continued until the maximum value. These force bands are needed to reduce the difficult for amputees to repeatably perform a punctual value of force. Then, each of the three classifiers was trained by using the recorded data by including all the 3 force levels.

- Step 3- Online Validation. Before starting the real-time evaluation, the prosthetic system was connected to the PC via Bluetooth. The outputs of the proposed PR algorithms, i.e. the hand/wrist gestures and the desired force

Tesi di dottorato in Scienze e Ingegneria per l'Uomo e l'Ambiente/Science and Engineering for Humans and the Environment, di Francesca Leone, discussa presso l'Università Campus Bio-Medico di Roma in data 26/07/2021.
La disseminazione e la riproduzione di questo documento sono consentite per scopi di didattica e ricerca, a condizione che ne venga citata la fonte.

level, were sent via Bluetooth to the prosthetic system in order to replicate the discriminated motion with the prosthesis, also giving a feedback to the patient. For the "Spherical" and "Tip" grasps, the hand device was controlled at 3 different speeds, based on the level of classified force. The second dynamometer was used to record the force applied by the prosthetic system. The patient was asked to perform each motion task for 3 times, starting from the rest; for the grasping tasks, each level of force was considered as a different tasks, for a total of 33 recordings. All motion tasks were recorded for 5 seconds[133].

In detail, after the step 2, the recorded sEMG data were organized in a DataSet matrix with 6 columns, each coupled with an EMG sensor. The training and test was subdivided by considering the two ways data split approach[128]: the 70% of the data were reserved for the "TrainingSet" (TR), while the remaining 30% of the data for the "Test Set" (TS). For the LR and NLR algorithm, the first-order iterative optimization algorithm "Gradient descent" was used to set the optimal internal parameters. One vs. all approach was introduced to adapt the LR,LDA and the NLR classification algorithms to the multi-class classification problem.

Firstly, in this study, a statistical analysis based on the Mann-Whitney test with Bonferroni correction was carried out to assess if the performances of the three proposed algorithms increased significantly with or without TD domain features extraction. Indeed, in literature, the use of EMG-PR based strategies with TD features, has used often to improve the robustness of the proposed pros-

Tesi di dottorato in Scienze e Ingegneria per l'Uomo e l'Ambiente/Science and Engineering for Humans and the Environment,
di Francesca Leone, discussa presso l'Università Campus Bio-Medico di Roma in data 26/07/2021.
La disseminazione e la riproduzione di questo documento sono consentite per scopi di didattica e ricerca,
a condizione che ne venga citata la fonte.

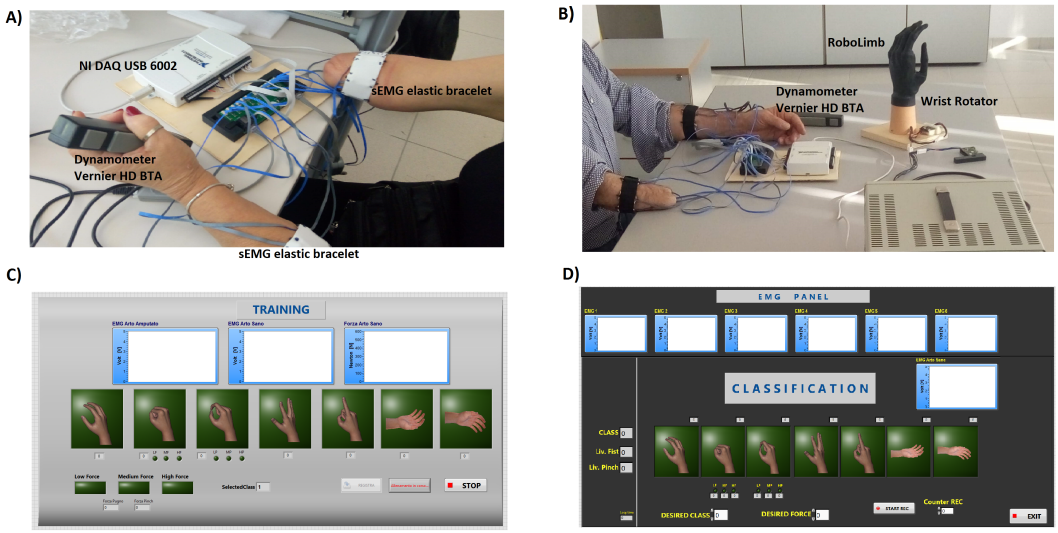

Figure 3.11: The experimental setup was composed of: (A) two sEMG elastic bracelets to record with 12 sEMG sensors Ottobock 13E200 the signals from both the arms; the NI DAQ USB 6002 to allow the acquisition of the sEMG signals and dynamometers data; two hand dynamometers (Vernier HD BTA, 46 mm x 28 mm x 170 mm) to study the force information from both the healthy limb and the bench prosthesis. (B) the prosthetic system was composed of hand device (RoboLimb, by Touch Bionics) and wrist module (Wrist Rotator, by Ottobock). The software interface has been created with the Labview platform to (C) record the sEMG signals and the dynamometer data and to train offline the classifiers and (D) to record in real-time the outputs of the trained classifiers.

thetic systems[134,135]. In particular, the features extraction avoided the generation of large-scale-dataset without performing the downsampling step and the time to complete the training is not too long. In detail, the feature extraction was performed by calculating the following five time domain features[131], reported previously in Section 3.3.2: Enhanced Mean Absolute value (EMAV), Enhanced Wavelength (EWL), Slope Sign Change (SSC), Root Mean Square (RMS), Variance (VAR). Data were segmented by using a window of 150 ms with an overlap of 100 ms[122]. The same algorithms introduced in the Section 3.3.1 and 3.3.2 were

Tesi di dottorato in Scienze e Ingegneria per l'Uomo e l'Ambiente/Science and Engineering for Humans and the Environment,
di Francesca Leone, discussa presso l'Università Campus Bio-Medico di Roma in data 26/07/2021.
La disseminazione e la riproduzione di questo documento sono consentite per scopi di didattica e ricerca,
a condizione che ne venga citata la fonte.

tested on transradial amputees. Their performance were evaluated offline through F1Score and the misclassification errors values, and also in real-time by considering the motion selection time, the motion completion time and motion completion rate.

3.5.2 Experimental Results

3.5.3 Offline performance

A preliminary comparison between the performance of the three algorithms (LR, LDA, and NLR) with or without the features extraction step was carried out to evaluate how to improve the robustness of the proposed classifiers. In this analysis, we had also considered the LR algorithm to evaluate if can be used as well as the NLR algorithm, without affecting the classification performance. The advantage of using LR were to simplify the training step of the model (without the polynomial expansion) and to speed out the real time prediction (within 80 ms) when controlling the prosthetic system. In detail, the results in terms of F1Score (Fig.3.12) from 15 trans-radial amputees (Tab.3.7) with the use or not of the TD features, introduced in Section 3.3.2, were reported for the "Hand/wrist gestures classifier", "Spherical force classifier" and "Tip force classifier" (Fig.3.11).

For the "Hand/wrist gestures classifier", the Mann-Whitney test applied to the F1Score values points out statistically significant difference ("*") between LDA algorithm without and with the features extraction step. Instead, for the "Spherical force classifier", there was a statistically significant difference ("*") between both LR and LDA algorithms without and with the features extraction step

Tesi di dottorato in Scienze e Ingegneria per l'Uomo e l'Ambiente/Science and Engineering for Humans and the Environment, di Francesca Leone, discussa presso l'Università Campus Bio-Medico di Roma in data 26/07/2021.
La disseminazione e la riproduzione di questo documento sono consentite per scopi di didattica e ricerca, a condizione che ne venga citata la fonte.

respectively. Regarding the "Tip force classifier", all the three algorithms (LR, LDA and NLR) had revealed a statistically significant difference ("*") without and with the features extraction step respectively.

In detail, the mean average F1Score (Fig.3.12) for the LR "hand/wrist gestures classifier", the "Spherical force classifiers" and "Tip force classifiers" were equals respectively to 93.05 % ± 9.53, 98.24 % ± 4.57, 98.43 % ± 3.91 with FE, and equals respectively to 90.57 % ± 11.08, 96.91 % ± 4.47, 93.10 % ± 7.18, without FE. The LDA "hand/wrist gestures classifier" reaches an average classification F1Score equals to 93.21 % ± 10.47 with FE and 83.20 % ± 12.19 without FE; while the LDA "Spherical force classifiers" and "Tip force classifiers" showed an average F1Score value of 98.80 % ± 2.87 and 96.24 % ± 6.22 with FE, respectively, and equals to 95.71 % ± 5.06 and 90.30 % ± 8.66, without FE, respectively. Finally, the NLR "hand/wrist gestures classifier", the "Spherical force classifiers" and "Tip force classifiers" obtained the mean average F1Score equals respectively to 92.03 % ± 5.79, 97.34 % ± 5.79, 97.94 % ± 3.11 with FE, and equals respectively to 92.84 % ± 10.28, 97.50 % ± 3.84, 94.78 % ± 6.93, without FE.

All the algorithms showed the best performance with the features extraction step. Thus, in this study, the following results of the hierarchical PR-based strategy were presented by considering the statistical analysis reported in this section. The box plots in Fig.3.13 and Fig.3.14 showed the F1Score and the misclassification errors for each classes, for the "hand/wrist gestures classifier", the "Spherical force classifier" and "Tip force classifier" obtained with the LR, LDA and NLR with FE step.

Tesi di dottorato in Scienze e Ingegneria per l'Uomo e l'Ambiente/Science and Engineering for Humans and the Environment,
di Francesca Leone, discussa presso l'Università Campus Bio-Medico di Roma in data 26/07/2021.
La disseminazione e la riproduzione di questo documento sono consentite per scopi di didattica e ricerca,
a condizione che ne venga citata la fonte.

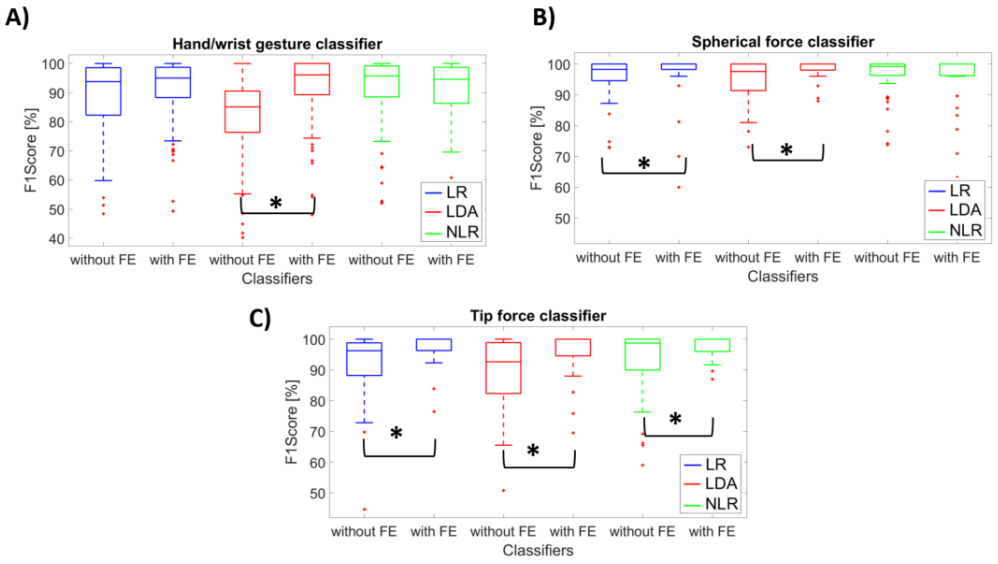

Figure 3.12: Average F1Score values calculated on 15 trans-radial amputees using the LR (in blue), LDA (in red) and NLR (in green) algorithms for (A) the "hand/wrist gestures classifier", (B) the "Spherical force classifier" and (C) the "Tip force classifier" algorithm, tested on "TS" with and without the 5 time domain features extraction (FE) step. The statistical significance is indicated by "*"

The output motion classes of the "hand/wrist gestures classifier" that have the lowest mean F1Score values (equals about 90 %) were the following showed in Fig.3.13: the Tip class (90.59 % ± 7.52) and Point class (91.33 % ± 12.61) with the LR algorithm; the Spherical class (90.03 % ± 16.28) and Tip class (90.11 % ± 9.59) with the LDA algorithm; the Spherical class (91.24 % ± 11.59), the Tip class (89.68 % ± 7.93), Point class (90.81 % ± 9.97) and the Wrist supination class (90.26 % ± 14.20) with the NLR algorithm. Instead, for both the "Spherical force classifier" and the "Tip force classifier", all the output motion classes obtained a mean F1Score values above 95 % for the three algorithms.

Tesi di dottorato in Scienze e Ingegneria per l'Uomo e l'Ambiente/Science and Engineering for Humans and the Environment,
di Francesca Leone, discussa presso l'Università Campus Bio-Medico di Roma in data 26/07/2021.
La disseminazione e la riproduzione di questo documento sono consentite per scopi di didattica e ricerca,
a condizione che ne venga citata la fonte.

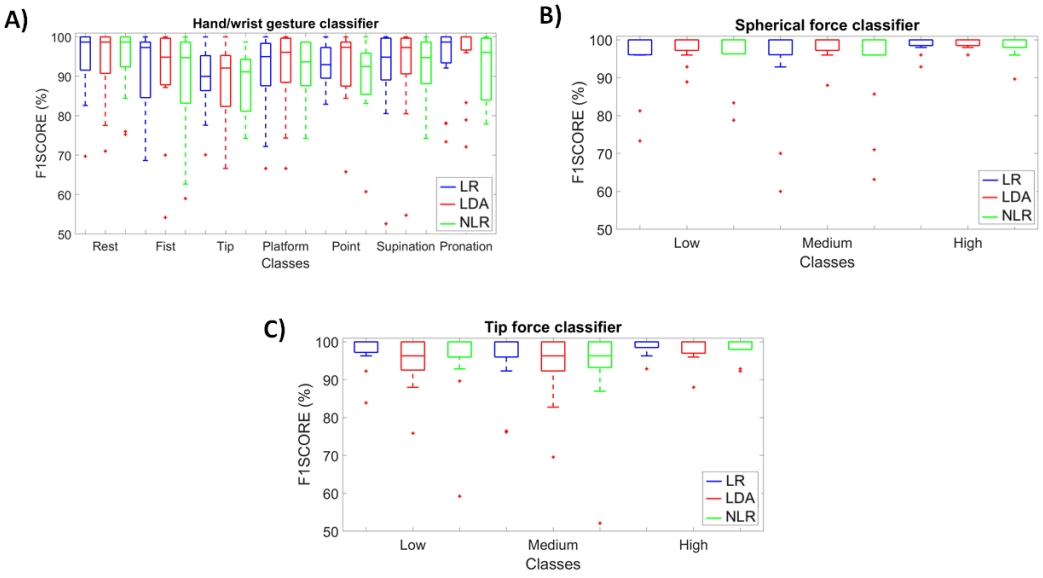

Figure 3.13: Average F1Score values calculated on 15 trans-radial amputees using the LR (in blue), LDA (in red) and NLR (in green) algorithms, tested on "TS" with the 5 time domain features extraction (FE) step: for (A) the "hand/wrist gestures classifier", the F1Score of the 7 hand/wrist gestures classes have been reported; for the (B) the "Spherical force classifier" and (C) the "Tip force classifier" algorithm, the F1Score values of the 3 force levels have been shown.

The mean average misclassification errors in Fig.3.14 for the LR with FE "hand/wrist gestures classifier", "Spherical force classifiers" and "Tip force classifiers" were respectively equals to 6.94 % ± 10.25, 2.05 % ± 5.70, 1.54 % ± 4. The LDA "hand/wrist gestures classifier" with FE reaches an average misclassification errors equals to 6.64 % ± 10.63; while the LDA "Spherical force classifiers" and "Tip force classifiers" show an average misclassification errors values with FE of 1.54 % ± 4.28 and 3.42 % ± 6.45, respectively. Regarding the NLR with FE "hand/wrist gestures classifier", "Spherical force classifier" and "Tip force classi-

Tesi di dottorato in Scienze e Ingegneria per l'Uomo e l'Ambiente/Science and Engineering for Humans and the Environment,
di Francesca Leone, discussa presso l'Università Campus Bio-Medico di Roma in data 26/07/2021.
La disseminazione e la riproduzione di questo documento sono consentite per scopi di didattica e ricerca,
a condizione che ne venga citata la fonte.

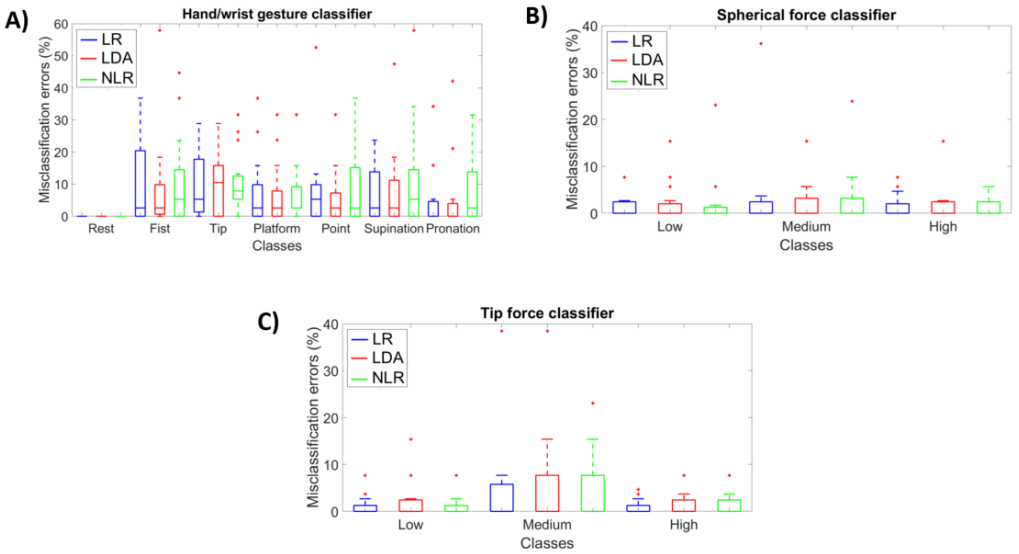

Figure 3.14: Average misclassification errors percentage calculated on 15 trans-radial amputees using the LR (in blue), LDA (in red) and NLR (in green) algorithms, tested on "TS" with the 5 time domain features extraction (FE) step: for (A) the "hand/wrist gestures classifier", the misclassification errors of the 7 hand/wrist gestures classes have been reported; for the (B) the "Spherical force classifier" and (C) the "Tip force classifier" algorithm, the misclassification errors of the 3 force levels have been shown.

fier" obtained the mean average misclassification errors equals to 7.87 % ± 9.88, 2.56 % ± 7.24, 2.05 % ± 4.15, respectively. For all the three algorithms, the "hand/wrist gestures classifier" showed the highest values of misclassification errors for the Spherical and Tip grasping tasks. In detail, for the Spherical motion class the mean misclassification errors were equals to 10.00 ± 12.8, 12.28 ± 21.30, 11.00 ± 14.8 for the LR, LDA and NLR algorithms; while for the Tip motion class, they were equals to 10.00 ± 9.30, 11.28 ± 10.30, 11.00 ± 9.8 for the LR, LDA and NLR algorithms.

Tesi di dottorato in Scienze e Ingegneria per l'Uomo e l'Ambiente/Science and Engineering for Humans and the Environment, di Francesca Leone, discussa presso l'Università Campus Bio-Medico di Roma in data 26/07/2021.
La disseminazione e la riproduzione di questo documento sono consentite per scopi di didattica e ricerca, a condizione che ne venga citata la fonte.

Fig.3.15 shows the average confusion matrix when testing the LR, LDA and NLR "hand/wrist gestures classifier", "Spherical force classifier" and "Tip force classifier" (A, B, C , respectively) on the Test Set (TS), respectively.

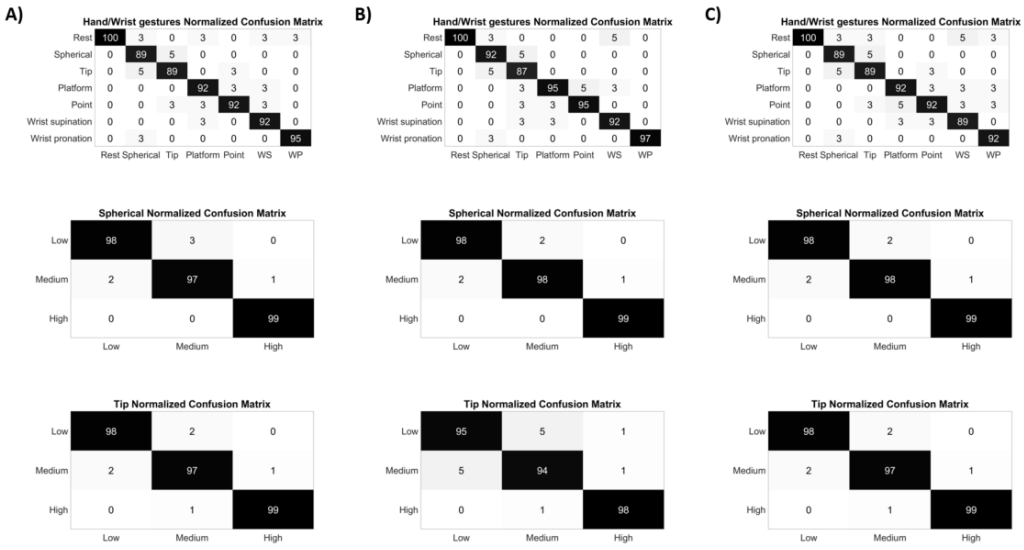

Figure 3.15: Normalized confusion matrix of the "hand/wrist gestures classifier", "Spherical force classifier" and "Tip force classifier" obtained with LR algorithm with FE (A) and LDA algorithm with FE (B) and NLR algorithm with FE (C). The confusion matrices are normalized with respect to the number of data belonging to the "TS".

The comparative analysis, based on the Mann-Whitney test with Bonferroni correction, between LR, LDA and NLR classifiers, applied to F1Score values and misclassification errors, reported no statistically significant difference between them.

The Confusion matrices, reported in Fig. 3.15, confirmed the positive results of the classification accuracy. On the main diagonal the cardinality of the correct

Tesi di dottorato in Scienze e Ingegneria per l'Uomo e l'Ambiente/Science and Engineering for Humans and the Environment, di Francesca Leone, discussa presso l'Università Campus Bio-Medico di Roma in data 26/07/2021.
La disseminazione e la riproduzione di questo documento sono consentite per scopi di didattica e ricerca, a condizione che ne venga citata la fonte.

classifications was reported; for the "hand/wrist gestures classifier", the cardinality of the misclassified data related to the 7 output classes representing the hand gestures were reported; while for the "Spherical force classifier" and "Tip force classifier", the cardinality of the misclassified data related to the 3 output classes that represented the force levels (Low, Medium, High) were considered. For all the three algorithms, the cardinality of the correct classifications on the main diagonal of the "hand/wrist gestures classifier", underlined the high classification accuracy even if some misclassified data out of the main diagonal suggested a bit minus performance of Spherical and Tip motion classes. For the "Spherical force classifier", and "Tip force classifier", the majority of the misclassified data out of the main diagonal are related to the low and medium force levels. Instead, the high force levels were always well discriminated at 99% of average accuracy for the LR and the NLR and at 98% for LDA force classifiers.

3.5.4 Real-time performance

Also a real-time performance evaluation was carried out for each proposed algorithm applied to the hierarchical classification approach. The following performance metrics used in[133] were employed: the motion selection time ("MST"), the motion completion time ("MCT") and the motion completion rate ("MCR"). In detail, the "MST" was defined as the time from the onset to the first correct classification (i.e the time taken to successfully select a target movement); the "MCT" was the time from movement onset to the 10th correct classification (i.e the time from the onset to the completion of the intended movement); finally the

Tesi di dottorato in Scienze e Ingegneria per l'Uomo e l'Ambiente/Science and Engineering for Humans and the Environment, di Francesca Leone, discussa presso l'Università Campus Bio-Medico di Roma in data 26/07/2021.
La disseminazione e la riproduzione di questo documento sono consentite per scopi di didattica e ricerca, a condizione che ne venga citata la fonte.

"MCR" ("success" rate) was the percentage of successfully completed motions out of the total attempted motions.

In our study, all the three classifiers with FE step ("hand/wrist gestures classifier", "Spherical force classifier", and "Tip force classifier"), have been tested in real-time with the LR,LDA and NLR algorithms and have produced a new prediction within 100 ms.

In particular, the "MST", "MCT" and "MCR" have been reported in Fig. 3.16 and Fig. 3.17 and are related to mean value obtained from the 15 trans-radial amputees and calculated over 2 repetitions of all the 11 motion classes.

For the "hand/wrist gestures classifier", the mean "MCT" values among motion classes were equals to 2.34 % ± 1.23, 2.54 % ± 1.44 and 2.41 % ± 1.39 for the LR, LDA and NLR classifiers, respectively.

In detail, for the LR "hand/wrist gestures classifier" classifier, the motion classes with the highest values of "MCT" were the Spherical class with low force (2.97 % ± 1.38), the Tip class with high force (2.95 % ± 1.75) and the Point class (2.60 % ± 1.50); for the LDA "hand/wrist gestures classifier", the Spherical class with low force (2.83 % ± 1.82), the Tip class with low force (2.84 % ± 1.44), the Tip class with high force (2.89 % ± 1.54), the Platform class (3.33 % ± 1.87), and the Point class (2.82 % ± 1.63) show the highest values of "MCT". Finally, regarding the NLR "hand/wrist gestures classifier", the Spherical class with low force (2.72 % ± 1.56), the Tip class with high force (2.96 % ± 1.61), the hand open (2.97 % ± 1.95), and the Point class (2.83 % ± 1.21) reach the "MCT" values almost equals to 3 s.

Tesi di dottorato in Scienze e Ingegneria per l'Uomo e l'Ambiente/Science and Engineering for Humans and the Environment, di Francesca Leone, discussa presso l'Università Campus Bio-Medico di Roma in data 26/07/2021.
La disseminazione e la riproduzione di questo documento sono consentite per scopi di didattica e ricerca, a condizione che ne venga citata la fonte.

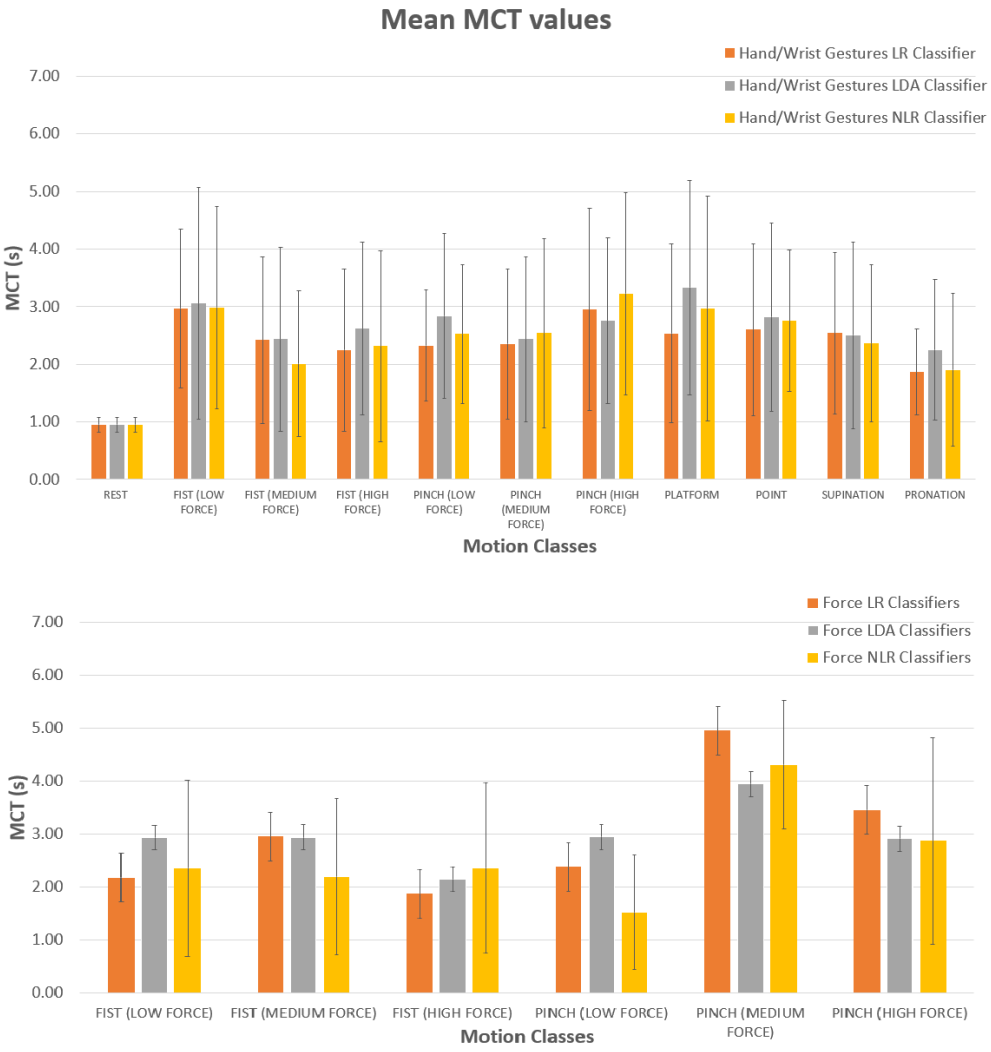

Figure 3.16: Average "MCT" values calculated on 15 trans-radial amputees using: at the top, the LR (in orange), LDA (in grey) and NLR (in yellow) "hand/wrist gestures classifier"; at the bottom, the LR (in orange), LDA (in grey) and NLR (in yellow) force classifiers: the "Spherical force classifier" and the "Tip force classifier" for the Spherical and Tip grasp, respectively; the mean "MCT" values were calculated over 2 repetitions of the reported motion classes.

Tesi di dottorato in Scienze e Ingegneria per l'Uomo e l'Ambiente/Science and Engineering for Humans and the Environment, di Francesca Leone, discussa presso l'Università Campus Bio-Medico di Roma in data 26/07/2021.
La disseminazione e la riproduzione di questo documento sono consentite per scopi di didattica e ricerca, a condizione che ne venga citata la fonte.

For the LR "Spherical force classifier", the Spherical classes with low and medium force obtained the highest "MCT" values (2.48 % ± 1.55 and 2.87 % ± 1.54, respectively). Also the LDA and NLR "Spherical force classifier" show the highest "MCT" values for the low and medium force classes: 3.10 % ± 1.82 (LDA classifier, low force class) and 2.72 % ± 1.26 (LDA classifier, medium force class); 2.55 % ± 1.79 (NLR classifier, low force class) and 2.30 % ± 1.62 (NLR classifier, medium force class). Finally, for the LR "Tip force classifier", the low and high force levels have the "MCT" settled down 2.72 % ± 1.93 and 3.45 % ± 2.07 values, respectively; while the medium force level obtained the "MCT" value over 4 s but within the 5 s (4.95 % ± 1.20). Also for the LDA, the "MCT" values for the medium force level was over 4 s (4.48 % ± 1.49); while for the low force level, it last less than 3 s (2.94 % ± 1.77); for the high force level, it was barely above 3 s (3.05 % ± 1.55). Finally, for the NLR "Tip force classifier", all the three output force levels have the "MCT" values within the 5 s: the low force level show the lowest value (1.52 % ± 1.08); instead, the medium force level reached the highest value, though contained within 5 s (4.37 % ± 1.28); for the high force level, it was barely low 3s (2.65 % ± 1.74).

The mean "MCR" obtained from the three algorithms revealed what are the motion classes more difficult to perform that have also the highest values of "MCT", as described above: for the LR, LDA and NLR "hand/wrist gestures classifier", the mean "MCR" reached an average values of 89.39 % ± 25.34, 83.64 % ± 29.09 and 86.67 % ± 30.14, respectively. About the force classifiers, the mean "MCR" were equals to 77.33 % ± 28.80 for the LR algorithm, 78.11 % ±

Tesi di dottorato in Scienze e Ingegneria per l'Uomo e l'Ambiente/Science and Engineering for Humans and the Environment, di Francesca Leone, discussa presso l'Università Campus Bio-Medico di Roma in data 26/07/2021.
La disseminazione e la riproduzione di questo documento sono consentite per scopi di didattica e ricerca, a condizione che ne venga citata la fonte.

31.96 for the LDA algorithm, and 80.56 % ± 31.71 for the NLR algorithm.

The Mann-Whitney test with Bonferroni correction ($P < 0.016$) applied to the "MST", "MCT" and "MCR" values points out no statistically significant difference ("*") between the three algorithms.

Finally, Fig. 3.18 shows the force signals obtained from the dynamometer when the amputee performed a grasping tasks (Spherical or Tip grasp) with the prosthesis. The two output classes of the "hand/wrist gestures classifier" and "Spherical force classifier" or "Tip force classifier" were sent simultaneously to the prosthesis. In detail, the output of the "hand/wrist gestures classifier" discriminated the desired motion class (among the 7 hand/wrist gestures) to perform with the prosthesis: if the motion class was the "Spherical" or "Tip", the classification approach become hierarchical and also the force levels information was added to the classification strategy by activating a second classifier (force classifier). In this case, the hand device was controlled at 3 different speeds associated to each classified force level. Thus, the dynamometer data, at the top of the Fig. 3.18 A and B, showed the force signals obtained when the prosthesis applied the three force levels (low, medium, and high) on the dynamometer during the Spherical and Tip class, respectively. At the bottom of the Fig. 3.18 A and B, the boxplot represented the force values extracted from the plateau of the dynamometer curve.

Tesi di dottorato in Scienze e Ingegneria per l'Uomo e l'Ambiente/Science and Engineering for Humans and the Environment,
di Francesca Leone, discussa presso l'Università Campus Bio-Medico di Roma in data 26/07/2021.
La disseminazione e la riproduzione di questo documento sono consentite per scopi di didattica e ricerca,
a condizione che ne venga citata la fonte.

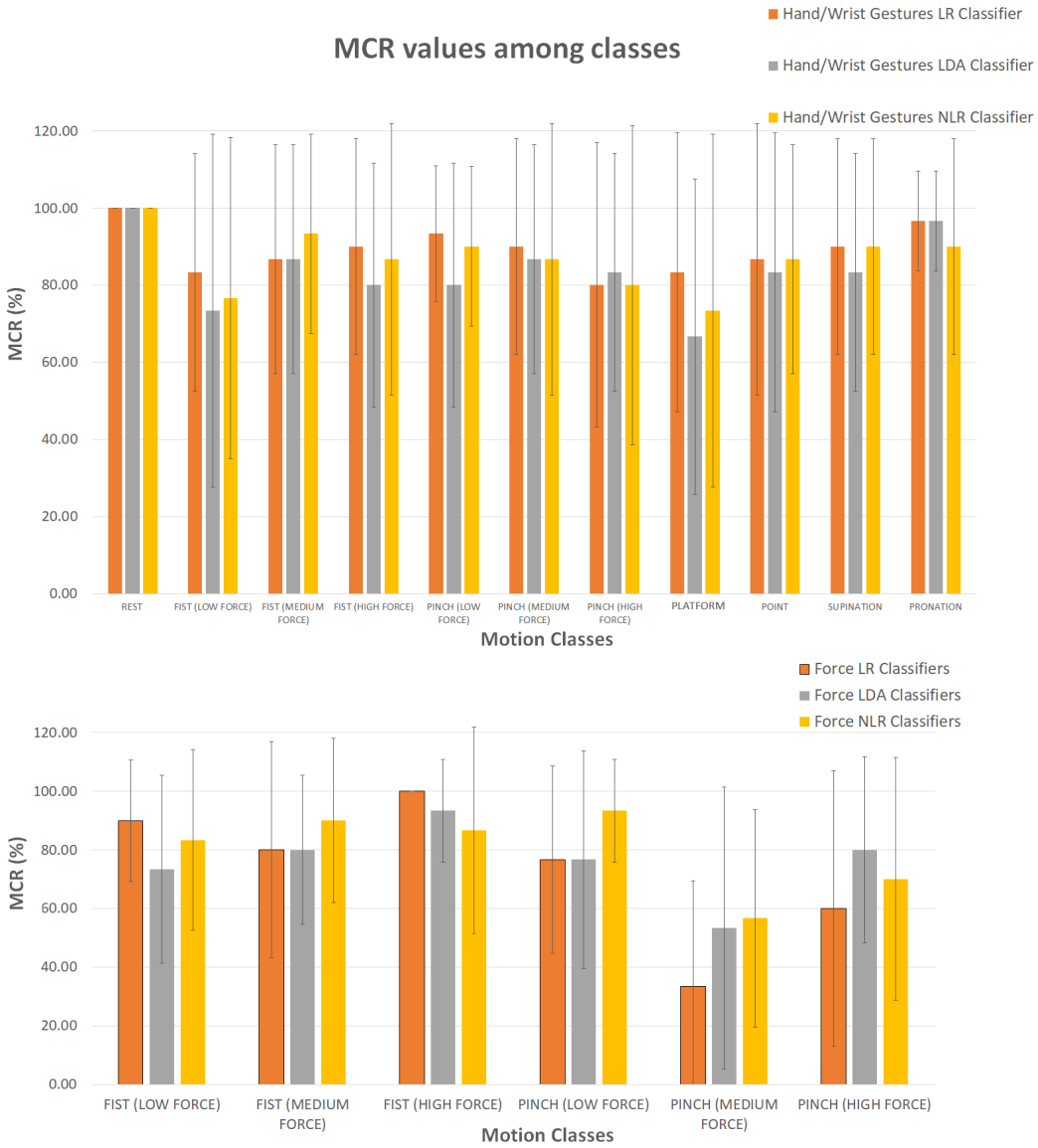

Figure 3.17: Average "MCR" percentages calculated on 15 trans-radial amputees using: at the top, the LR (in orange), LDA (in grey) and NLR (in yellow) "hand/wrist gestures classifier"; at the bottom, the LR (in orange), LDA (in grey) and NLR (in yellow) force classifiers: the "Spherical force classifier" and the "Tip force classifier" for the Spherical and Tip grasp, respectively; the mean "MCR" percentage were calculated over 2 repetitions of the reported motion classes.

Tesi di dottorato in Scienze e Ingegneria per l'Uomo e l'Ambiente/Science and Engineering for Humans and the Environment,
di Francesca Leone, discussa presso l'Università Campus Bio-Medico di Roma in data 26/07/2021.
La disseminazione e la riproduzione di questo documento sono consentite per scopi di didattica e ricerca,
a condizione che ne venga citata la fonte.

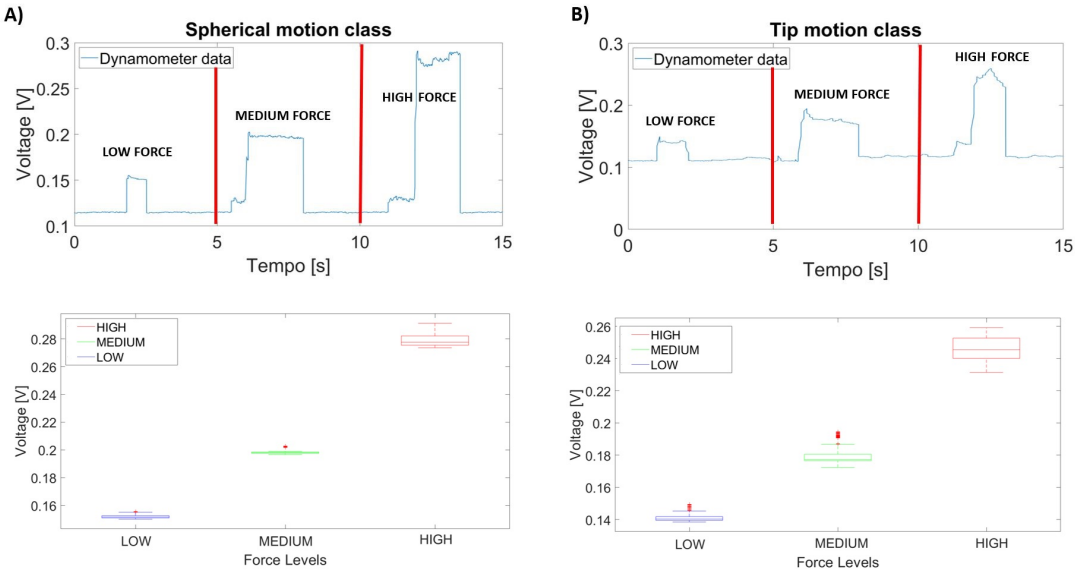

Figure 3.18: At the top, the dynamometer data showed the force signals obtained when the prosthesis apply the three force levels (low, medium, and high) during (A) the Spherical and (B) Tip class. At the bottom, the boxplot represented the force values extracted from the plateau of the dynamometer curve.

Tesi di dottorato in Scienze e Ingegneria per l'Uomo e l'Ambiente/Science and Engineering for Humans and the Environment, di Francesca Leone, discussa presso l'Università Campus Bio-Medico di Roma in data 26/07/2021.
La disseminazione e la riproduzione di questo documento sono consentite per scopi di didattica e ricerca, a condizione che ne venga citata la fonte.

3.6 Discussion

An offline and real-time performance evaluation of the hierarchical PR-based strategy was carried out in this study, by employing the sEMG data of 15 trans-radial amputees. For the offline performance, the F1Score and misclassification error values were reported for each classifier (hand/wrist gestures and force classifiers). The real-time analysis was performed by considering the motion completion time and motion completion rate metrics. Three algorithms based on LR, LDA and NLR were tested both offline and in real-time to assess which of them can guarantee the best performance of the hierarchical PR strategy that was employed to contemporary identify desired hand/wrist gestures and force levels. To this aim, a statistical analysis based on the Mann-Whitney test with Bonferroni correction was carried out for evaluating, firstly, if an increase of the performances occurred with or without TD domain features extraction. Then, it was also applied to understand deeply the difference in terms of the offline and real-time performance of the three proposed algorithms.

3.6.1 Offline performance

A preliminary analysis was carried out to assess a statistical significant difference between the F1Score with or without the FE step, for each classifier and for each proposed algorithm. The results showed that there was a statistically significant difference ("*") between the LDA "Hand/wrist gestures classifier" without and with the features extraction step. In detail, there was an increase of the mean F1Score values of 10.42 % and a reduction of 4.84 % of the misclassification error

Tesi di dottorato in Scienze e Ingegneria per l'Uomo e l'Ambiente/Science and Engineering for Humans and the Environment, di Francesca Leone, discussa presso l'Università Campus Bio-Medico di Roma in data 26/07/2021.
La disseminazione e la riproduzione di questo documento sono consentite per scopi di didattica e ricerca, a condizione che ne venga citata la fonte.

values.

For the "Spherical force classifier", there was a statistically significant increase of the performance for both LR and LDA algorithms, when the FE was applied. For the LR and LDA "Spherical force classifier", the mean F1Score values increase of 1.61 % and 3.09 %, respectively. Also for the "Tip force classifier", the F1Score for the LR and LDA classifiers increased significantly with the FE step (5.94 % and 3.16 %, respectively).

Thus, by applying the FE step, the mean F1Score values, were equals to 93.05 % $\pm$ 9.53, 98.24 % $\pm$ 4.57, 98.43 % $\pm$ 3.91 for the LR, LDA and NLR "hand/wrist gestures classifier", respectively. The "Spherical force classifier" identified the three force levels with an average F1Score of 98.24 % $\pm$ 2.05, 98.80 % $\pm$ 1.54, and the 97.34 % $\pm$ 2.56, for the LR, LDA and NLR classifiers, respectively. The "Tip force classifier" was able to discriminate the three force classes by obtaining an average F1Score values of 98.43 % $\pm$ 1.54, 96.24 % $\pm$ 3.42, and the 97.94 % $\pm$ 2.05 with the LR, LDA and NLR algorithms, respectively. These results seem to be very promising due to the simultaneously classification of hand/wrist gestures and force levels by trans-radial amputees with F1Score over 90 % for the "hand/wrist gestures classifier" and force classifiers, implemented with all the three algorithms. Also, the offline misclassification errors rates, were used to evaluate the classifiers performances: they remained within 10 % and this can be considered a positive result for an usable system[7]. The statistical analysis between the LR, LDA and NLR classifiers, applied to F1Score values and misclassification errors, reported no statistically significant difference among them.

Tesi di dottorato in Scienze e Ingegneria per l'Uomo e l'Ambiente/Science and Engineering for Humans and the Environment,
di Francesca Leone, discussa presso l'Università Campus Bio-Medico di Roma in data 26/07/2021.
La disseminazione e la riproduzione di questo documento sono consentite per scopi di didattica e ricerca,
a condizione che ne venga citata la fonte.

Also the confusion matrices, reported in Fig. 3.15, confirmed the positive result in terms of accuracy and underlined for the "Spherical force classifier" and "Tip force classifier", the majority of the misclassified data out of the main diagonal were related to the low and medium force levels. This is due to the major difficulty encountered by some amputees (as the subjects P1,P2,P3,P5,P7, and P12, described in Tab. 3.7) to modulate between low and medium force levels, especially during a Tip grasp. The difficulty may be due to the shorter length of the stump. In addition, the dynamometer data, in Fig. 3.18, confirmed that the force levels are well differentiable, when the prosthesis hold the dynamometer. Thus, the proposed hierarchical classification architecture had been made more robust to obtain valid results also on trans-radial amputees, and it was tested also in real-time to control simultaneously, trough the introduced prosthetic device, both the motion intentions and desired force levels.

3.6.2 Real-time performance

The real-time results were reported to validate the hierarchical classification approach also to control a prosthetic device. The desired hand/wrist gestures and force levels were discriminated simultaneously, by testing the performance of three different algorithms (i.e LR, LDA and the NLR). For each algorithm, the motion completion time and motion completion rate were reported to identify the robustness of the proposed PR system to discriminate simultaneously hand/wrist gestures and force levels.

For the hand/wrist classifier, the lower mean value of the motion completion

Tesi di dottorato in Scienze e Ingegneria per l'Uomo e l'Ambiente/Science and Engineering for Humans and the Environment, di Francesca Leone, discussa presso l'Università Campus Bio-Medico di Roma in data 26/07/2021.
La disseminazione e la riproduzione di questo documento sono consentite per scopi di didattica e ricerca, a condizione che ne venga citata la fonte.

time, among the 7 motion classes, was obtained with LR algorithm (2.34 % ± 1.22), followed by the NLR (2.41 % ± 1.39) and the LDA (2.54 % ± 1.44) algorithms. For the Spherical and Tip force classifiers, the lowest value of the mean motion completion time was obtained with the NLR algorithm (2.60 % ± 1.50); the LR and LDA force classifiers reached fairly similar mean motion completion time values (2.96 % ± 1.44 and 2.97 % ± 1.51, respectively). Regarding the mean motion completion rate values, the highest percentage was reached with LR "hand/wrist gestures classifier" with FE and was equal to 89.09 % ± 25.76; instead, the lowest percentage was obtained by LDA with FE "hand/wrist gestures classifier" (83.64 % ± 29.09); the NLR with FE "hand/wrist gestures classifier" showed a mean motion completion rate value equal to 86.67 % ± 30.14). For the Spherical and Tip force classifiers, the best performance in terms of mean motion completion rate values was reached with the NLR algorithm (80.56 % ± 31.22), followed by the LR and LDA algorithms (73.33 % ± 28.80 and 76.11 % ± 31.96, respectively). However, if we didn't considered the difficulty encountered from the majority of amputees to reproduce the Tip grasp with the medium force level, the mean motion completion rate values grew to 85.00 % ± 9.01 for the NLR algorithm, and to 81.00 % ± 15.02 and 81.00 % ± 7.60 for the LR and LDA algorithms, respectively.

In detail, for the force classifiers, these lowest values of the motion completion rate should depended also on the lowest values reached by the "hand/wrist gestures classifier" for the Spherical and Tip class. In detail, the LR "hand/wrist gestures classifier" obtained the mean motion completion rate values equals to

Tesi di dottorato in Scienze e Ingegneria per l'Uomo e l'Ambiente/Science and Engineering for Humans and the Environment, di Francesca Leone, discussa presso l'Università Campus Bio-Medico di Roma in data 26/07/2021.
La disseminazione e la riproduzione di questo documento sono consentite per scopi di didattica e ricerca, a condizione che ne venga citata la fonte.

86.67 ± 29.5 and 87.78 ± 27.49 for the Spherical class and Tip motion classes, respectively. Regarding the LDA and NLR "hand/wrist gestures classifier", the mean motion completion rate values were equals to 80.00 ± 35.69 and 85.56 ± 34.23 for the Spherical motion class, respectively; and they were equals to 83.33 ± 30.72 and 85.56 ± 32.43 for the Tip motion class, respectively. This can be due to the difficulty of amputee to keep stable the muscle contraction for both the grasping task and force levels. In particular, the Tip grasping task with the medium level was the most difficult to reproduce and to keep stable in real-time for the majority of amputees.

Thus, the best solution for controlling the prosthetic system in real-time, seems to use simultaneously the LR algorithm with FE for the "hand/wrist gestures classifier" and the NLR with FE for the Spherical and Tip force classifiers. Indeed, these algorithms reached the best compromise between the lowest mean motion completion time values and the highest percentage of the mean motion completion rate values. Both the LR and NLR guaranteed to produce, in real-time, a response every 100 ms. Thus, this can be considered the best solution for the real-time applicability of the hierarchical PR approach.

3.7 Conclusion

In this study, a hierarchical classification approach was developed with the aim to assess the desired hand/wrist gestures, as well as the desired force levels to exert during grasping tasks. A Finite State Machine was introduced to manage and coordinate three classifiers based on the Non-Linear Logistic Regression algorithm.

Tesi di dottorato in Scienze e Ingegneria per l'Uomo e l'Ambiente/Science and Engineering for Humans and the Environment, di Francesca Leone, discussa presso l'Università Campus Bio-Medico di Roma in data 26/07/2021.
La disseminazione e la riproduzione di questo documento sono consentite per scopi di didattica e ricerca, a condizione che ne venga citata la fonte.

Firstly, the classification architecture was evaluated across 31 healthy subjects. A Wilcoxon Signed-Rank test was carried out for the statistical analysis of comparison between NLR and LDA. The comparative analysis reports no statistically significant differences in terms of F1Score performance between NLR and LDA. Thus, this study reveals that the use of non linear classification algorithm, as NLR, is as much suitable as the benchmark LDA classifier for implementing an EMG pattern recognition system, able both to decode hand/wrist gestures and to associate different performed force levels to grasping actions. Then, to investigate also the ability of trans-radial amputees to manage simultaneously desired hand/wrist gestures and three force levels, an extended analysis based on LR, NLR and LDA algorithm had been carried out to assess the robustness, both in offline and in real-time, of the hierarchical PR system. To this purpose, a prosthetic system composed of hand device (RoboLimb) and wrist module (WristRotator) was employed to validate the presented method when trans-radial amputees controlling multi-fingered hand prostheses and exerted force levels. A statistical analysis based on the Mann-Whitney test with Bonferroni correction ($p<0.016$) was carried out to assess the best solution when considering the performance of three different algorithms: the comparative analysis reports not statistically significant differences in terms of F1Score and misclassification errors between the LR, NLR and LDA classifiers. Also in real-time, the Mann-Whitney test with Bonferroni correction ($P < 0.016$) applied to the MST, MCT and MCR values points out no statistically significant difference between the three algorithms. However, considering also the real-time performance, the best solution to decode simultaneously

Tesi di dottorato in Scienze e Ingegneria per l'Uomo e l'Ambiente/Science and Engineering for Humans and the Environment,
di Francesca Leone, discussa presso l'Università Campus Bio-Medico di Roma in data 26/07/2021.
La disseminazione e la riproduzione di questo documento sono consentite per scopi di didattica e ricerca,
a condizione che ne venga citata la fonte.

the hand/wrist gestures and force levels seems to be the simultaneous use of the LR algorithm with FE for the "hand/wrist gestures classifier", and the NLR with FE for the Spherical and Tip force classifiers. Finally, the proposed method allowed to extract from EMG signals all the valuable information regarding not only muscle contractions related to hand/wrist motions but also the changes of muscle activation patterns depending on the influence of different force levels.

Tesi di dottorato in Scienze e Ingegneria per l'Uomo e l'Ambiente/Science and Engineering for Humans and the Environment,
di Francesca Leone, discussa presso l'Università Campus Bio-Medico di Roma in data 26/07/2021.
La disseminazione e la riproduzione di questo documento sono consentite per scopi di didattica e ricerca,
a condizione che ne venga citata la fonte.

4

Tesi di dottorato in Scienze e Ingegneria per l'Uomo e l'Ambiente/Science and Engineering for Humans and the Environment,
di Francesca Leone, discussa presso l'Università Campus Bio-Medico di Roma in data 26/07/2021.
La disseminazione e la riproduzione di questo documento sono consentite per scopi di didattica e ricerca,
a condizione che ne venga citata la fonte.

Parallel PR-based classification strategy to simultaneously control 3-DoFs of elbow, wrist and hand

4.1 Introduction

In the field of myoelectric control systems, pattern recognition (PR) algorithms have become always more interesting to predict complex electromyography patterns involving more than 2 Degrees of Freedom (DoFs) movements.

When considering a poliarticulated prostheses with several DoFs, related to the elbow, wrist, and hand, the simultaneous control of combined movements of different joints (e.g. pouring water into a glass) ensure greater dexterity than the sequential one[136].

From the literature analysis presented in Chapter 1.0.2, the sequential managing of one DoF at a time from the user had been considered a major limitation of the proposed PR strategies, when complex multi-DoFs tasks had to be performed. The majority of the classification strategies are based on single, hierarchical and parallel linear discriminant analysis (LDA) classifiers able to discriminate until 19 wrist/hand gestures (in the 3-DoFs case), considering both combined and discrete

Tesi di dottorato in Scienze e Ingegneria per l'Uomo e l'Ambiente/Science and Engineering for Humans and the Environment, di Francesca Leone, discussa presso l'Università Campus Bio-Medico di Roma in data 26/07/2021.
La disseminazione e la riproduzione di questo documento sono consentite per scopi di didattica e ricerca, a condizione che ne venga citata la fonte.

motions. However, this strategies were introduced to classify simultaneously only 2 DoFs and were limited by the lack of online performance measures. Moreover, the use of sequential control strategies caused a cognitive burden especially during the planning of the intended movement because the user can not perform fluid, lifelike combined movements[43].

In this chapter, a novel parallel classification approach based on the LR algorithm, with the regularization parameter and the FE step, was introduced to provide classification of complex tasks that involved up to 3 DoFs, by keeping the number of electrodes to a bare minimum and the classification error rates under 10 %. Moreover both the offline and real-time performance metrics were evaluated and compared with the LDA parallel classification approach. We extracted the following time-domain features: mean absolute value (MAV), wavelength length (WL), slope sign change (SSC), root mean square (RMS), variance (VAR) from the raw sEMG signals of only 6 channels sensors. In detail, the proposed model discriminated between the following 26 motion classes and no motion class: 6 discrete motions (elbow flexion, elbow extension, hand open, hand close, wrist supination, wrist pronation), the rest state, and other 20 complex motions performed during daily life activities, and derived from the combination of the discrete motions, reported in Tab.4.1.

Also, the analysis of the real-time performance was evaluated with the motion selection time, motion completion time, and the completion rate for all the 27 motion classes[133]. The offline and real-time performances were compared with the LDA benchmark algorithm, by using three LDA classifiers with the same

Tesi di dottorato in Scienze e Ingegneria per l'Uomo e l'Ambiente/Science and Engineering for Humans and the Environment, di Francesca Leone, discussa presso l'Università Campus Bio-Medico di Roma in data 26/07/2021.
La disseminazione e la riproduzione di questo documento sono consentite per scopi di didattica e ricerca, a condizione che ne venga citata la fonte.

Table 4.1: Report of daily activities where the considered 27 motion classes are involved

Motion Classes		Motion Classes	Daily Activity
Discrete	1	F	elbow flexion for bringing something to you
	2	E	elbow flexion for giving something to someone
	3	C	close hand for holding something
	4	O	open hand for giving something
	5	S	wrist supination for rotating an object
	6	P	wrist supination for rotating an object
No Motion	7	NM	
Combined	8	FCS	brings a biscuit to your mouth
	9	EOP	rest your open hand on the table
	10	FCP	bring the back of your closed hand to your forehead
	11	EOS	bring the back of your open hand onto the table
	12	FOS	bring your open hand to your mouth
	13	ECP	beat your fist on the table
	14	FOP	Bring the back of your open hand to your forehead
	15	ECS	Bring the back of your closed hand onto the table
	16	CS	Rotate the back of your closed hand to open the lid of a pot
	17	OP	Rotate your open hand down
	18	OS	Rotate the back of your open hand
	19	CS	Turn your closed hand down to turn the door handle
	20	FC	Flex your elbow with your hand closed (bring your fist to your mouth)
	21	EO	Extend your open hand (karate blow)
	22	FO	Flex your elbow with your hand closed
	23	EC	Extend your elbow with your hand closed
	24	ES	flex your elbow and rotate your wrist upwards
	25	EP	Extend your elbow and rotate your wrist down
	26	FP	Flex your elbow and rotate your wrist down
	27	ES	Extend your elbow and rotate your wrist upward

Acronyms of Tab.4.1: F: elbow flexion; FO: elbow flexion with hand open; FC: elbow flexion with hand close; FS: elbow flexion with wrist supination; FP: elbow flexion with wrist pronation; FOS: elbow flexion with hand open and wrist supination; FOP: elbow flexion with hand open and wrist pronation; FCS: elbow flexion with hand close and wrist supination; FCP:elbow flexion with hand close and wrist pronation; E: elbow extension; EO: elbow extension with hand open; EC: elbow extension with hand close; ES: elbow extension with wrist supination; EP: elbow extension with wrist pronation; EOS: elbow extension with hand open and wrist supination; EOP: elbow extension with hand open and wrist pronation; ECS: elbow extension with hand close and wrist supination; ECP:elbow extension with hand close and wrist pronation; C: hand close; CS: hand close with wrist supination; CP: hand close with wrist pronation; O: hand open; OS: hand open with wrist supination; OP: hand open with wrist pronation; S: wrist supination; P: wrist pronation; NM: no motion class.

features extraction and parallel classification approach.

Tesi di dottorato in Scienze e Ingegneria per l'Uomo e l'Ambiente/Science and Engineering for Humans and the Environment,
di Francesca Leone, discussa presso l'Università Campus Bio-Medico di Roma in data 26/07/2021.
La disseminazione e la riproduzione di questo documento sono consentite per scopi di didattica e ricerca,
a condizione che ne venga citata la fonte.

4.2 Parallel classification approach

The parallel classification approach, introduced in this section, was implemented by using three classifiers one for each DoF: the "Elbow classifier", the "Wrist classifier", and the "Hand classifier" provided the simultaneous control of the elbow, hand, and wrist joints, respectively.

In detail, the proposed parallel classification approach was implemented with the LR algorithm, to recognize both discrete and combined elbow, wrist, and hand motions. Then, the same approach was reproduced using LDA algorithm in order to perform a comparative analysis.

The control scheme provides the final decision that is composed of the independent outputs of the three joint classifiers.

In particular, the "Elbow classifier" was trained with the TrainingSet 1, organized as reported in Fig.4.1: from the DataSet matrix, described above, that contained the recordings of four repetitions of each of the 27 motion classes, the discrete and combined motion classes were labeled into three output classes. In detail, the output of the "Elbow classifier" determines the elbow flexion (labeled as "Class 1"), extension (labeled as "Class 2") and the "other motions" (labeled as "Class 3") not involving the use of the elbow. In particular, the "Class 1" was represented by the examples of nine discrete and combined motion classes that involved the elbow flexion. The "Class 2" was represented by the examples of nine discrete and combined motion classes that involved the elbow extension. While the "Class 3" was represented by the examples of nine discrete and com-

Tesi di dottorato in Scienze e Ingegneria per l'Uomo e l'Ambiente/Science and Engineering for Humans and the Environment, di Francesca Leone, discussa presso l'Università Campus Bio-Medico di Roma in data 26/07/2021.
La disseminazione e la riproduzione di questo documento sono consentite per scopi di didattica e ricerca, a condizione che ne venga citata la fonte.

bined motion classes that involved other joints, as the hand and wrist. The "Wrist classifier" was trained with the TrainingSet 2 and the same considerations made for the "Elbow classifier" can be applied. The unique difference was the output of the "Wrist classifier", that determines wrist supination (labeled as "Class 1"), pronation (labeled as "Class 2") and the "other motions" (labeled as "Class 3") that does not involve the use of the wrist. Finally, the "Hand classifier" was trained with the TrainingSet 3. The output of the "Hand classifier" manages the hand opening (labeled as "Class 1"), closing (labeled as "Class 2") and the "other motions" (labeled as "Class 3") not implying the use of the hand. The final decision of the parallel classification approach depends on the simultaneous outputs of the three classifiers Fig.4.1:if only one joint classifier outputs the "Class 1" or "Class 2" and the others two classifiers output the "Class 3", the final output will be a 1 DoF motion class; if two joint classifiers output the "Class 1" or "Class 2" and the other one output the "Class 3", the final output will be a 2 DoF motion class; finally if all the three classifiers output the the "Class 1" or "Class 2", the final decision will be a 3 DoFs motion classes.

In this study, all the six EMG channels were always used for every classification decisions. The classification scheme is reported in Fig.4.2, through a flowchart: the final output of this architecture was the movement class derived from the output combinations of the three classifiers.

Tesi di dottorato in Scienze e Ingegneria per l'Uomo e l'Ambiente/Science and Engineering for Humans and the Environment,
di Francesca Leone, discussa presso l'Università Campus Bio-Medico di Roma in data 26/07/2021.
La disseminazione e la riproduzione di questo documento sono consentite per scopi di didattica e ricerca,
a condizione che ne venga citata la fonte.

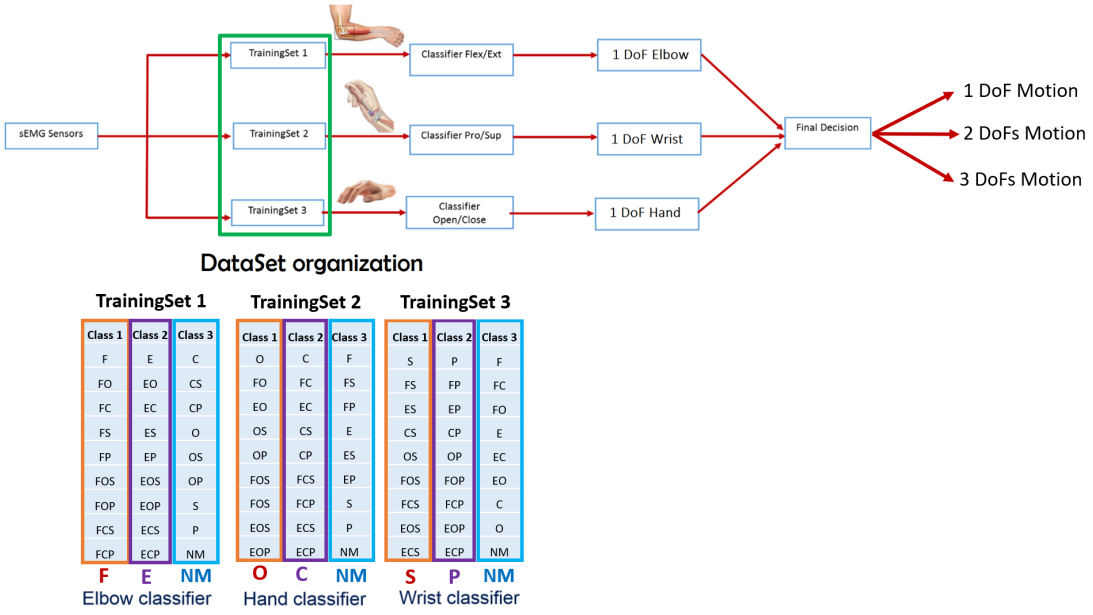

Figure 4.1: Block diagram describing the parallel classification approach composed by three joint classifiers ("Elbow classifier", "Wrist classifier" and "Hand classifier"), each trained with a different TrainingSet.

4.3 Experimental validation on healthy subjects

4.3.1 Experimental Setup and protocol

Fifteen healthy subjects (aged: 36 ± 13), were enrolled in the experiments. The sEMG data were acquired by using a suitable software on Labview platform and DAQ USB 6002 device, with a 1 KHz. The PC (Samsung Intel(R) Core (TM) i7-4500U CPU @ 1.80 GHz) and DAQ communicated by means of an USB port. Six commercial active sEMG sensors (Ottobock 13E200 = 50, 27 mm × 18 mm × 9.5 mm) were placed in this way: four sensors were equidistantly fixed on a elastic bracelet placed about 5 cm below the subject's elbow Fig.A 4.3; instead the

Tesi di dottorato in Scienze e Ingegneria per l'Uomo e l'Ambiente/Science and Engineering for Humans and the Environment,
di Francesca Leone, discussa presso l'Università Campus Bio-Medico di Roma in data 26/07/2021.
La disseminazione e la riproduzione di questo documento sono consentite per scopi di didattica e ricerca,
a condizione che ne venga citata la fonte.

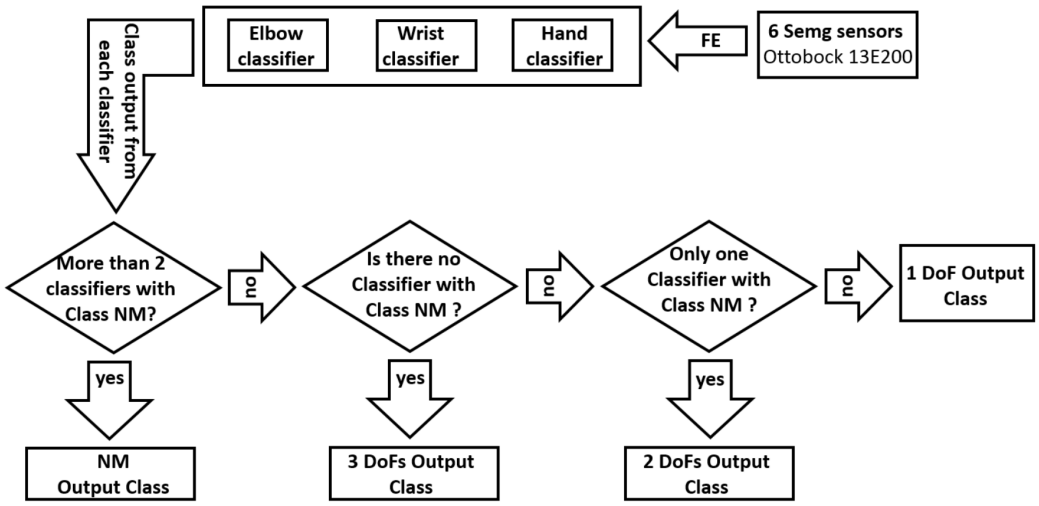

Figure 4.2: Flowchart for the parallel classification approach, used for classifying 27 motion classes related to elbow, wrist and hand joints

remaining two sensors were used to include biceps and triceps activity to record the elbow flexion and extension, respectively. The number of sEMG sensors was chosen equal to six to avoid a high-dimensional feature space and maintain simple the hardware[137].

The subject was sitting in front of a monitor Fig.B 4.3 and was asked to produce each of the 27 gestures reported in REF Table I: the discrete motions were elbow flexion and extension, hand open and close and, wrist supination and pronation; the combined motions were up to two and three elbow, wrist, and hand DoFs combinations. The participants were asked to produce each of these gestures for four times and hold it for 3 s with an interval of rest state about 2 s between each repetition. The sEMG data were organized in a DataSet matrix with 6

Tesi di dottorato in Scienze e Ingegneria per l'Uomo e l'Ambiente/Science and Engineering for Humans and the Environment,
di Francesca Leone, discussa presso l'Università Campus Bio-Medico di Roma in data 26/07/2021.
La disseminazione e la riproduzione di questo documento sono consentite per scopi di didattica e ricerca,
a condizione che ne venga citata la fonte.

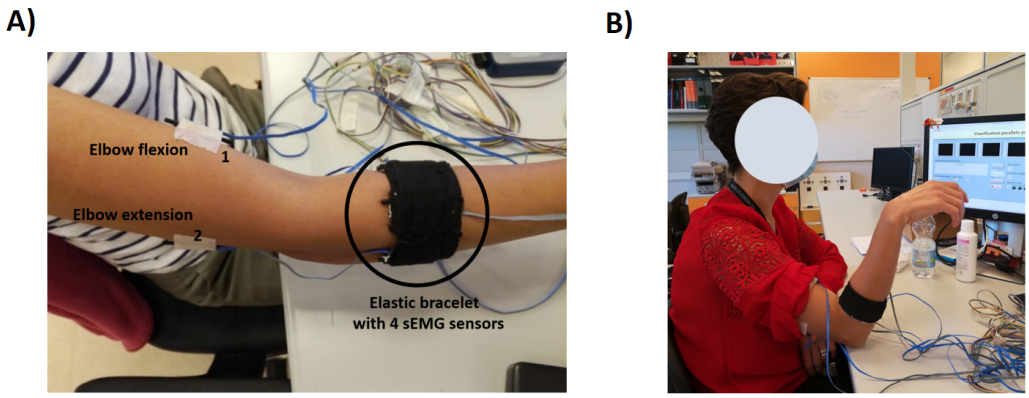

Figure 4.3: The experimental setup was composed by: (i) a sEMG elastic bracelet, (ii) NI DAQ USB 6002, (iii) Labview interface software to acquire the sEMG signals.

column, each coupled with an EMG sensor. The training and test was subdivided by considering the two ways data split approach[128] for both the algorithms: the 70 % of the data were reserved for the "TrainingSet" (TR), while the remaining 30 % of the data for the "Test Set" (TS). One vs. all approach was introduced to adapt the LDA and LR classification algorithms to the multi-class classification problem. For the LR algorithm, the first-order iterative optimization algorithm "Gradient descent" was used to set the optimal internal parameters.

The same algorithms described in Section 3.3.1 and 3.3.2 were employed in the parallel classification approach. The Mann-Whitney test (U-test) applied to the F1Score, points out no statistically significant difference between LR and NLR algorithms for the "Elbow classifier", the "Wrist classifier", and "Hand classifier" (at $p < 0.05$). Thus, the following analysis in the section 4.3 will considered the comparison between the LR and LDA algorithms.

Tesi di dottorato in Scienze e Ingegneria per l'Uomo e l'Ambiente/Science and Engineering for Humans and the Environment,
di Francesca Leone, discussa presso l'Università Campus Bio-Medico di Roma in data 26/07/2021.
La disseminazione e la riproduzione di questo documento sono consentite per scopi di didattica e ricerca,
a condizione che ne venga citata la fonte.

4.3.2 Experimental Results

4.3.3 Offline performance

The offline results of the parallel classification approach are reported for both LR and LDA algorithms in Tab. 4.2, 4.3,4.4 for the three classifiers ("Elbow classifier", "Wrist classifier", and "Hand classifier") in terms of F1Score Fig.4.4.

The reported results were obtained by considering the mean values on 15 healthy subjects and by segmenting data with a windows of 150 ms and an overlap of 100 ms[122] for the features extraction, as described above, for both the algorithms. The mean F1Score values, over the three output classes, reached an average classification F1Score equals to 96.1 % ± 2.9 (Tab. 4.2), 91.7 % ± 4.1 (Tab. 4.3), 91.0 % ± 4.8 (Tab. 4.4), for the LR "Elbow classifier", "Wrist classifier", and "Hand classifier", respectively. The mean misclassification error rates remained under the 10 % value, that can be considered positive for an usable system[53]. For the LDA "Elbow classifier", "Wrist classifier", and "Hand classifier", the mean F1Score values were equals to 94.5 % ± 4.8 (Tab. 4.2), 90.7 % ± 4.1 (Tab. 4.3), 89.3 % ± 4.8 (Tab. 4.4), respectively. Figure 4.5 shows also the average confusion matrix when testing both the LR and LDA classifiers on the "TS", over the three output classes that represent the controllable DoFs of each classifier.

The Mann-Whitney test applied to the F1Score points out no statistically significant difference between LR and LDA algorithms for the "Elbow classifier", the "Wrist classifier", and "Hand classifier" (Fig.4.4).

Tesi di dottorato in Scienze e Ingegneria per l'Uomo e l'Ambiente/Science and Engineering for Humans and the Environment,
di Francesca Leone, discussa presso l'Università Campus Bio-Medico di Roma in data 26/07/2021.
La disseminazione e la riproduzione di questo documento sono consentite per scopi di didattica e ricerca,
a condizione che ne venga citata la fonte.

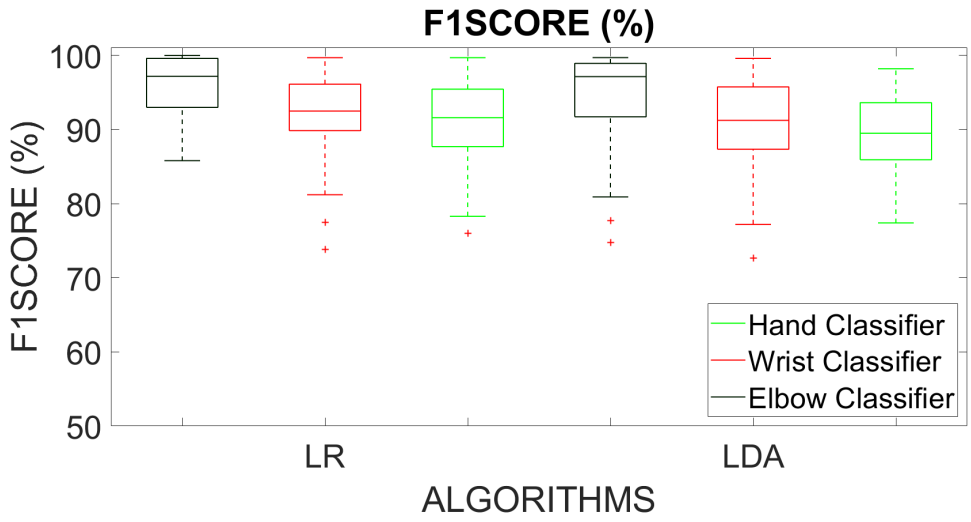

Figure 4.4: Box plots of the average F1Score values calculated on 15 healthy subjects using LR and LDA algorithms with five time domain features, tested on "TS," for the Elbow, Wrist, and Hand classifiers.

Table 4.2: F1Score values for the "Elbow classifier"

	ELBOW CLASSIFIER	
	F1Score	
	LR	LDA
CLASS 1	95,0 ± 4,5	93,1 ± 7,3
CLASS 2	98,6 ± 2,3	97,7 ± 2,9
CLASS 3	94,6 ± 4,1	92,7 ± 6,5
MEAN	96,1 ± 2,9	94,5 ± 4,8

Table 4.3: F1Score values for the "Wrist classifier"

	WRIST CLASSIFIER	
	F1Score	
	LR	LDA
CLASS 1	91,9 ± 4,3	91,0 ± 5,1
CLASS 2	94,9 ± 5,0	94,4 ± 5,2
CLASS 3	88,3 ± 6,3	86,8 ± 6,3
MEAN	91,7 ± 4,1	90,7 ± 4,1

4.3.4 Real-time performance

Both the LR and LDA classifiers were evaluated in real-time by considering the performance metrics introduced in the Section 3.5.4.

Tesi di dottorato in Scienze e Ingegneria per l'Uomo e l'Ambiente/Science and Engineering for Humans and the Environment,
di Francesca Leone, discussa presso l'Università Campus Bio-Medico di Roma in data 26/07/2021.
La disseminazione e la riproduzione di questo documento sono consentite per scopi di didattica e ricerca,
a condizione che ne venga citata la fonte.

Table 4.4: F1Score values for the "Hand classifier"

	HAND CLASSIFIER	
	F1Score	
	LR	LDA
CLASS 1	93,6 ± 5,4	92,3 ± 4,9
CLASS 2	89,7 ± 5,7	87,8 ± 5,8
CLASS 3	89,7 ± 5,3	87,7 ± 5,4
MEAN	91,0 ± 4,8	89,3 ± 4,8

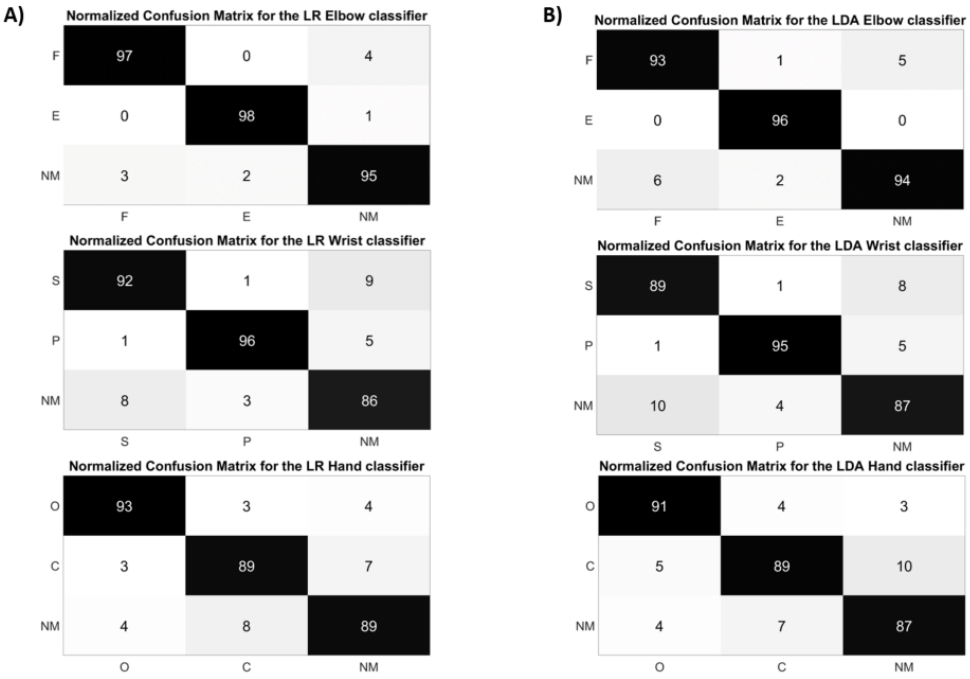

Figure 4.5: Normalized confusion matrix of the Elbow, Wrist, and Hand Classifiers obtained with the LR (A) and LDA (B) algorithms. The confusion matrices are normalized concerning the number of data belonging to the "TS".

In particular, the MST, MCT and MCR had been reported in Tab. 4.5 and were related to the mean values obtained from the 15 healthy subjects and calculated over 2 repetitions of all the 27 motion classes.

Tesi di dottorato in Scienze e Ingegneria per l'Uomo e l'Ambiente/Science and Engineering for Humans and the Environment, di Francesca Leone, discussa presso l'Università Campus Bio-Medico di Roma in data 26/07/2021.
La disseminazione e la riproduzione di questo documento sono consentite per scopi di didattica e ricerca, a condizione che ne venga citata la fonte.

The mean MCT values among the 27 motion classes was equals to 1.84 ± 1.25 s and 2.49 ± 1.87 s for the LR and LDA algorithms, respectively (Fig.4.6).

The mean MCR calculated with both LR and LDA algorithms for the 15 healthy subjects revealed what are the motion classes more difficult to perform (Fig.4.7): if considering the discrete motion classes, the elbow extension had the mean MCR values equals to 79 % ± 40 and 80 % ± 37 for the LR and LDA algorithms, respectively.

Regarding the 2 DoFs motion classes, the LR algorithm had the MCR above the 85 % excepted for the following complex movements that involved the hand or the elbow joint with the wrist rotations: the elbow extension with hand open (76 % ± 44), the hand open with wrist supination (82 % ± 39), and hand open with wrist pronation (82 % ± 38). Instead for the LDA algorithm, a major number of 2 DoFs motion classes that involved elbow with hand and wrist rotations (9 on a total of 12 motion classes) have the mean MCR that ranged from 73 % to 83 % (Tab.4.5).

Also for the 3 DoFs motion classes, the LR algorithm had better performance with respect to the LDA algorithm: for the LR, the mean MCR was above the 85 % excepted for the elbow flexion with hand close and wrist supination (82 % ± 39). Instead for the LDA, the mean MCR values ranged from 73 % to 83 %, excepted for the elbow extension with hand open and wrist pronation (97 % ± 13) and elbow extension with hand close and wrist pronation (87 % ± 30) (Tab.4.5).

The Mann-Whitney test applied to the MST values points out no statistically significant difference ("*") between LR and LDA algorithms, while a significant

Tesi di dottorato in Scienze e Ingegneria per l'Uomo e l'Ambiente/Science and Engineering for Humans and the Environment,
di Francesca Leone, discussa presso l'Università Campus Bio-Medico di Roma in data 26/07/2021.
La disseminazione e la riproduzione di questo documento sono consentite per scopi di didattica e ricerca,
a condizione che ne venga citata la fonte.

difference has been revealed for both the MCT and MCR values (Fig. 4.8).

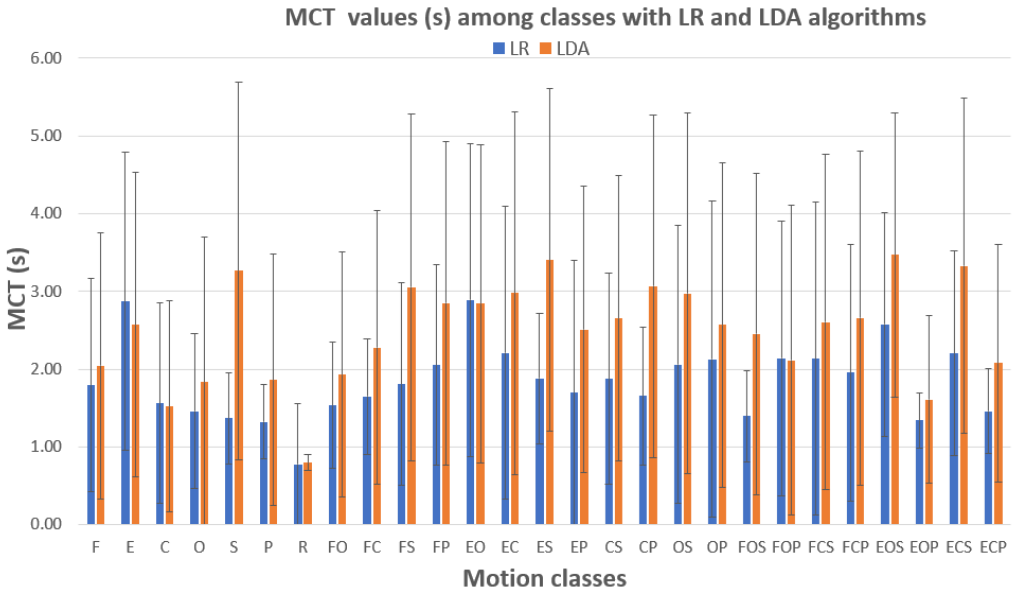

Figure 4.6: Mean and standard deviation values of motion completion time values, performed by subjects, for all the 27 motion classes, with both LR (blue color) and LDA (orange color) algorithms.

Tesi di dottorato in Scienze e Ingegneria per l'Uomo e l'Ambiente/Science and Engineering for Humans and the Environment, di Francesca Leone, discussa presso l'Università Campus Bio-Medico di Roma in data 26/07/2021.
La disseminazione e la riproduzione di questo documento sono consentite per scopi di didattica e ricerca, a condizione che ne venga citata la fonte.

Table 4.5: The mean "MST", "MCT" and "MCR" values related to 1 DoF, 2 DoFs and 3 DoFs, for the LR and LDA algorithms.

Motion Classes		LR			LDA		
MEAN		MST	MCT	MCR	MST	MCT	MCR
1 DoF	F	0.23 ± 0.23	1.80 ± 1.37	94 ± 24	0.13 ± 0.15	2.04 ± 1.72	90 ± 21
	E	0.55 ± 0.66	2.87 ± 1.92	79 ± 40	0.58 ± 0.68	2.57 ± 1.95	80 ± 37
	C	0.67 ± 1.50	1.56 ± 1.29	94 ± 24	0.62 ± 1.58	1.52 ± 1.36	93 ± 26
	O	0.21 ± 0.19	1.46 ± 0.99	97 ± 12	0.27 ± 0.52	1.83 ± 1.87	87 ± 30
	S	0.17 ± 0.15	1.37 ± 0.58	97 ± 12	1.17 ± 2.09	3.27 ± 2.43	83 ± 31
	P	0.26 ± 0.19	1.32 ± 0.48	100 ± 0	0.26 ± 0.35	1.86 ± 1.62	90 ± 28
	R	0.05 ± 0.01	0.78 ± 0.77	100 ± 0	0.05 ± 0.01	0.80 ± 0.11	100 ± 0
	MEAN	0.30 ± 0.42	1.59 ± 1.05	94.42 ± 16	0.44 ± 0.76	1.98 ± 1.58	89 ± 24.71
2 DoFs	FO	0.31 ± 0.20	1.53 ± 0.81	94 ± 24	0.30 ± 0.33	1.93 ± 1.58	90 ± 28
	FC	0.40 ± 0.27	1.65 ± 0.74	94 ± 24	0.36 ± 0.37	2.28 ± 1.76	80 ± 37
	FS	0.64 ± 1.51	1.81 ± 1.30	94 ± 24	0.80 ± 1.61	3.05 ± 2.23	70 ± 41
	FP	0.62 ± 0.61	2.05 ± 1.89	91 ± 26	0.80 ± 1.11	2.85 ± 2.08	73 ± 32
	EO	0.55 ± 0.49	2.89 ± 2.01	76 ± 44	0.44 ± 0.43	2.84 ± 2.05	73 ± 32
	EC	0.60 ± 0.97	2.21 ± 1.89	85 ± 34	1.05 ± 1.81	2.98 ± 2.33	77 ± 45
	ES	0.35 ± 0.27	1.88 ± 0.84	100 ± 0	0.64 ± 0.96	3.40 ± 2.20	87 ± 45
	EP	0.40 ± 0.37	1.70 ± 1.70	91 ± 26	0.37 ± 0.38	2.51 ± 1.84	83 ± 36
	CS	0.33 ± 0.30	1.88 ± 1.36	94 ± 24	0.63 ± 0.85	2.65 ± 1.83	87 ± 42
	CP	0.26 ± 0.16	1.65 ± 0.89	100 ± 0	0.71 ± 1.61	3.07 ± 2.21	77 ± 42
	OS	0.48 ± 0.83	2.06 ± 1.79	82 ± 39	1.01 ± 1.85	2.97 ± 2.32	70 ± 46
	OP	0.68 ± 1.54	2.13 ± 2.03	82 ± 38	0.70 ± 1.64	2.57 ± 2.09	80 ± 32
	MEAN	0.46 ± 0.62	1.95 ± 1.43	90.25 ± 25.25	0.65 ± 1.07	2.76 ± 2.04	79 ± 39
3 DoFs	FOS	0.29 ± 0.16	1.40 ± 0.59	100 ± 0	0.20 ± 0.15	2.45 ± 2.06	80 ± 37
	FOP	0.63 ± 0.91	2.14 ± 1.77	88 ± 33	0.20 ± 0.15	2.11 ± 1.99	77 ± 37
	FCS	0.58 ± 0.80	2.13 ± 2.01	82 ± 39	0.31 ± 0.43	2.61 ± 2.15	73 ± 42
	FCP	0.41 ± 0.39	1.96 ± 1.65	91 ± 26	0.29 ± 0.32	2.66 ± 2.15	73 ± 42
	EOS	0.49 ± 0.40	2.58 ± 1.44	88 ± 33	0.59 ± 0.67	3.47 ± 1.83	73 ± 37
	EOP	0.36 ± 0.21	1.34 ± 0.35	100 ± 0	0.30 ± 0.22	1.61 ± 1.07	97 ± 13
	ECS	0.44 ± 0.38	2.20 ± 1.32	94 ± 24	1.17 ± 1.84	3.33 ± 2.15	83 ± 32
	ECP	0.46 ± 0.28	1.46 ± 0.55	100 ± 0	0.42 ± 0.32	2.08 ± 1.53	87 ± 30
	MEAN	0.45 ± 0.44	1.90 ± 1.21	93 ± 19	0.43 ± 4.1	2.54 ± 1.87	80 ± 34
	MEAN	0.42 ± 0.52	1.84 ± 1.25	92 ± 21	0.54 ± 0.84	2.49 ± 1.87	82 ± 34

Tesi di dottorato in Scienze e Ingegneria per l'Uomo e l'Ambiente/Science and Engineering for Humans and the Environment,
di Francesca Leone, discussa presso l'Università Campus Bio-Medico di Roma in data 26/07/2021.
La disseminazione e la riproduzione di questo documento sono consentite per scopi di didattica e ricerca,
a condizione che ne venga citata la fonte.

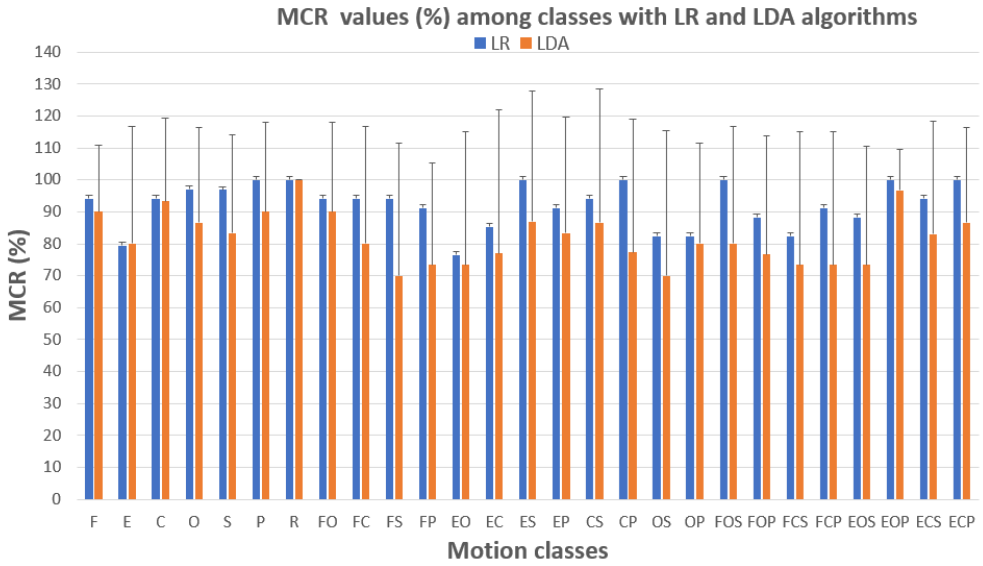

Figure 4.7: Mean and standard deviation values of motion completion rate values, performed by subjects, for all the 27 motion classes, with both LR (blue color) and LDA (orange color) algorithms.

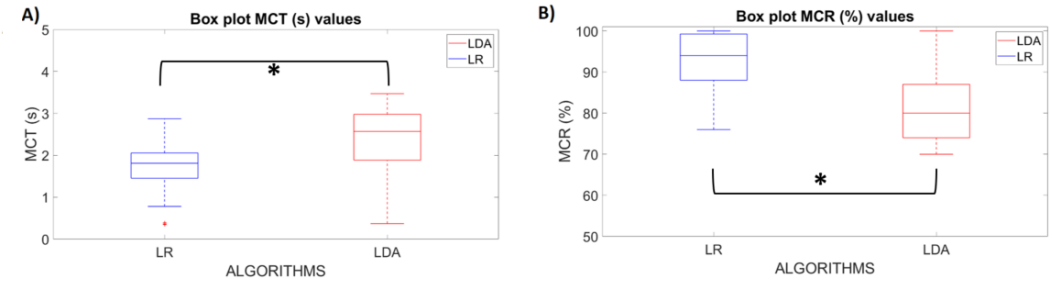

Figure 4.8: A) Box plot of the average MCT values calculated on 15 healthy subjects using LR and LDA algorithms. B) Box plot of the average MCR values calculated on 15 healthy subjects using LR and LDA algorithms. Statistical significance is indicated by "*".

Tesi di dottorato in Scienze e Ingegneria per l'Uomo e l'Ambiente/Science and Engineering for Humans and the Environment,
di Francesca Leone, discussa presso l'Università Campus Bio-Medico di Roma in data 26/07/2021.
La disseminazione e la riproduzione di questo documento sono consentite per scopi di didattica e ricerca,
a condizione che ne venga citata la fonte.

4.4 Discussion

4.4.1 Offline performance

The results, obtained from 15 healthy subjects, for the simultaneous classification of 27 motion classes, were summarized in terms of mean F1Score values (Fig.4.4) in Tab.4.2, Tab.4.3, Tab.4.4. The "Elbow Classifier" reached the highest mean F1Score values (96.1 % ± 2.9 with LR algorithm, 94.5 % ± 4.8 with LDA algorithm); the "Wrist Classifier" obtained the mean F1Score values equals to 91.7 % ± 4.1 with LR algorithm and 90.7 % ± 4.1 with LDA algorithm; the "Hand Classifier" reached the lowest values equals to 91.0 % ± 4.8 with LR algorithm, and 89.3 % ± 4.8 with the LDA algorithms. The discrimination of the hand motions combined with the wrist movements was more difficult also in[88]. These results seem to be very promising if we consider the importance for amputee subjects of controlling simultaneously more than two DoFs during daily living activities.

Confusion matrices, reported in Fig.4.5 confirmed the positive results of the accuracy parameter. The cardinality of the correct classifications on the main diagonal underlined the high classification accuracy even if some misclassified data out of the main diagonal suggested a bit minus performance of both LR and LDA "Wrist classifier" and "Hand classifier" respect to the "Elbow classifier." This can be due to the major difficulty to discriminate between combined wrist and hand motion classes.

It is interesting to note that the parallel classification approach with the three LR classifiers obtained the best offline classification performances both in terms

Tesi di dottorato in Scienze e Ingegneria per l'Uomo e l'Ambiente/Science and Engineering for Humans and the Environment,
di Francesca Leone, discussa presso l'Università Campus Bio-Medico di Roma in data 26/07/2021.
La disseminazione e la riproduzione di questo documento sono consentite per scopi di didattica e ricerca,
a condizione che ne venga citata la fonte.

of F1Score.

The statistical analysis, based on the Mann-Whitney test, confirmed no statistically significant difference ("*") between the F1Score values of the LR and LDA "Elbow classifier", "Wrist classifier", and "Hand classifier".

4.4.2 Real-time performance

The motion completion time values obtained with both LR and LDA algorithms were reported in Fig. 4.6: for the LR algorithm, the mean motion completion time values were equals to 1.73 ± 0.58 s, 1.95 ± 0.36 s, and 1.90 ± 0.45 s for the 1 DoF, 2 DoFs, and 3 DoFs motion classes, respectively.

Conversely, for the LDA algorithm the mean motion completion time values were equals to 2.18 ± 0.63 s, 2.76 ± 0.40 s, and 2.54 ± 0.63 s for the 1 DoF, 2 DoFs, and 3 DoFs motion classes, respectively (Fig. 4.6). The results suggest that the difference in real-time prediction is not marginal: the mean motion completion time values were over 2 s for the LDA with respect to the LR algorithm (less than 2 s) for 2 and 3 DoFs.

In addition, the LDA classifiers presented the motion completion time values one second higher than LR classifiers for the following motion classes (Fig. 4.6): supination (S, 1.90 s), elbow flexion with wrist supination (FS, 1.24 s), elbow extension with wrist supination (ES, 1.52 s), hand closing with wrist pronation (CP, 1.41 s), elbow flexion with hand opening and wrist supination (FOS, 1.05 s), elbow extension with hand closing and wrist supination (ECS, 1.13 s).

Thus, it is worth noting that the LR classifiers reached higher real-time per-

Tesi di dottorato in Scienze e Ingegneria per l'Uomo e l'Ambiente/Science and Engineering for Humans and the Environment, di Francesca Leone, discussa presso l'Università Campus Bio-Medico di Roma in data 26/07/2021.
La disseminazione e la riproduzione di questo documento sono consentite per scopi di didattica e ricerca, a condizione che ne venga citata la fonte.

formance, especially for the combined motions with wrist supination. This can be considered a positive results since previous studies have presented conflicting data regarding the contribution of the muscles involved in pronation and supination that are generally deep muscles[138].

The number of successful motions over the total number of motions attempted (27 motion classes x 2 repetitions= 54 total motion attempted) was reported as the motion completion rate for both LDA and LR algorithms in Fig. 4.7. For the LDA algorithm, the motion completion rate values were significantly lower than that obtained with LR for the following 2 and 3 DoFs motion classes: the motion completion rate of the elbow flexion with wrist supination motion class was 24.12 % lower than that with the LR algorithm; the hand close with wrist pronation motion class (22.67 % lower); the elbow flexion with hand opening and the wrist supination class (20.00 % lower). These results confirm the lower robustness of LDA classifiers to classify in real-time the 2 and 3 DoFs combined motions with wrist supination.

The statistical analysis, based on the Mann-Whitney test, confirmed a statistically significant difference ("*") between the LR and LDA motion completion time values (Fig. 4.8.A) and between the LR and LDA motion completion rate values (Fig. 4.8.B). Thus, in real-time, the parallel classification approach based on the three LR classifiers ensured better performance than the LDA classifiers and seems to be the most robust approach.

Tesi di dottorato in Scienze e Ingegneria per l'Uomo e l'Ambiente/Science and Engineering for Humans and the Environment, di Francesca Leone, discussa presso l'Università Campus Bio-Medico di Roma in data 26/07/2021.
La disseminazione e la riproduzione di questo documento sono consentite per scopi di didattica e ricerca, a condizione che ne venga citata la fonte.

4.5 Experimental validation on TMR patient

4.5.1 Case Study Report

The introduced parallel classification approach was evaluated also on a TMR patient (female, aged: 29) with shoulder disarticulation (SD) after a traumatic event, who underwent TMR procedure at Policlinico Campus Bio-Medico of Rome in date 15/06/2018. The patient had 5 reinnervated control sites and one natively innervated muscle sites used for the direct control of the elbow F/E wrist S/P and hand O/C joints. In detail, the monitoring of muscle activity generated by the muscles reinnervated with TMR were evaluated, in a non-invasive way, through the use of six surface electromyographic sensors (Ottobock). These sensors have been located in the areas where, through palpation, the activation of the muscle signals related to the re-innervated muscle district was found. In particular, the sensors were placed on the following muscle reinnervated sites, used for the control of 3 degrees of freedom (elbow, wrist and hand) Fig. 4.9:

- The musculocutaneous nerve, which innervates the muscles of the anterior arm and in particular of the coracobrachialis muscle, has been reinnervated at the clavicular portion of the pectoralis major muscle. This muscle site is involved for the elbow flexion movement.
- The axillary nerve, which innervates the teres minor and ends as the deltoid branch, has been retained on the native deltoid muscle and is involved for the elbow extension.

Tesi di dottorato in Scienze e Ingegneria per l'Uomo e l'Ambiente/Science and Engineering for Humans and the Environment, di Francesca Leone, discussa presso l'Università Campus Bio-Medico di Roma in data 26/07/2021.
La disseminazione e la riproduzione di questo documento sono consentite per scopi di didattica e ricerca, a condizione che ne venga citata la fonte.

- The median nerve, originating from the brachial plexus and originating from the lateral secondary trunk (cervical spinal nerves C5-C7), has been reinnervated on the dorsal major muscle and is involved in the wrist pronation.
- The radial nerve, which innervates the medial and lateral heads of the brachial triceps muscle, has been reinnervated on the sternal part of the pectoralis major and is involved for the wrist supination.
- The median nerve relating to the medial cords of the brachial plexus has been reinnervated on the abdominal portion of the pectoralis major muscle and is involved in the closing hand.
- The radial nerve, which innervates the posterior portion of the upper limb, has been reinnervated on the great dorsal muscle and is involved in the opening hand.

The success of nerve transpositions was assessed by serial visits and instrumental examinations (every 2-4 weeks). Three months after the surgery (September 2018), the treated subject reported sporadic involuntary contractions of the re-innervated muscles. The first finding of a voluntary activation of re-innervated muscles occurred during the fourth post-surgery month (October 2018); in this same period the presence of the motor evoked potentials was observed in the reinnervated muscles through the transcranial magnetic stimulation (TMS). From this evidence, the subject began to be aware of these preliminary voluntary contractions and to exercise them, even autonomously (1-2 daily sessions, of about 30 minutes each, to be carried out at home).

Tesi di dottorato in Scienze e Ingegneria per l'Uomo e l'Ambiente/Science and Engineering for Humans and the Environment,
di Francesca Leone, discussa presso l'Università Campus Bio-Medico di Roma in data 26/07/2021.
La disseminazione e la riproduzione di questo documento sono consentite per scopi di didattica e ricerca,
a condizione che ne venga citata la fonte.

Francesca Leone

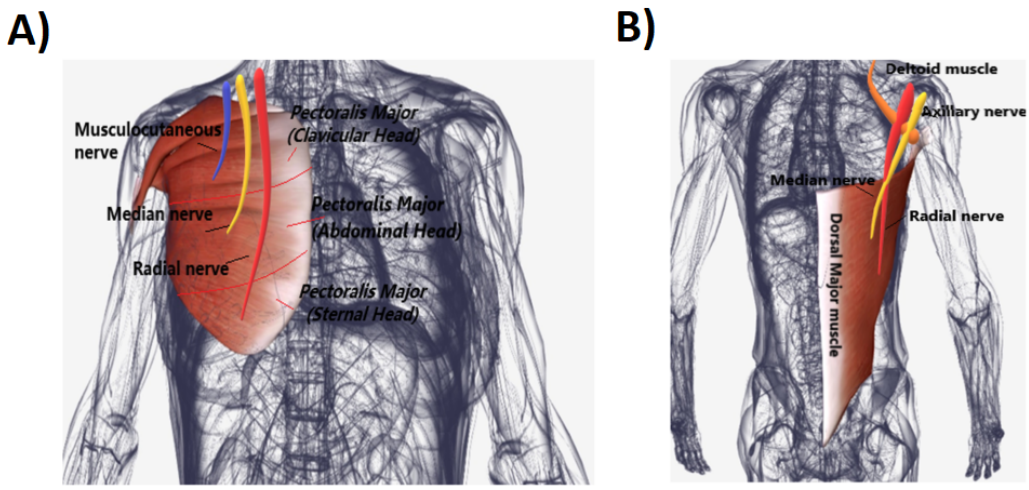

Figure 4.9: Scheme of the reinnervated sites for the TMR patient.A: the musculocutaneous nerve (blue), the median nerve (yellow), and radial (red) nerves transfer on the clavicular head, the abdominal head and the sternal head of the pectoralis major muscle, respectively; B: the axillary nerve (orange) transfer on the deltoid muscle; the median nerve (yellow) and the radial nerve (red) transfer on the dorsal muscle.

The TMR patient had learned to associate the contraction of reinnervated muscles at specific movements of the prosthetic system, with the virtual reality system in Fig. 4.10: this system allow TMR patient to move with the on/off DC control strategy the avatar of an arm that mimic the lost upper limb behavior, replicating the performance of the human arm. Each EMG sensor allowed TMR patient to manage the movement of a single degree of freedom of the virtual arm. The degree of freedom is activated when the corresponding EMG signal exceeds the preset threshold. It is possible to activate several degrees of freedom at the same time.

This system was tested during the training of the TMR subject, starting from June 2018. The training involved the execution of simple gestures (with 1 DoF),

Tesi di dottorato in Scienze e Ingegneria per l'Uomo e l'Ambiente/Science and Engineering for Humans and the Environment,
di Francesca Leone, discussa presso l'Università Campus Bio-Medico di Roma in data 26/07/2021.
La disseminazione e la riproduzione di questo documento sono consentite per scopi di didattica e ricerca,
a condizione che ne venga citata la fonte.

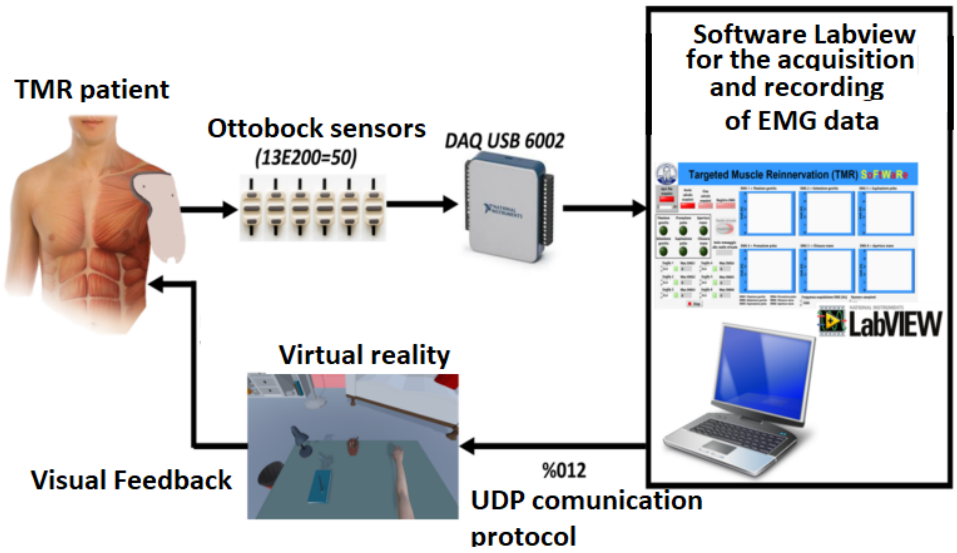

Figure 4.10: Block diagram of the interfacing system with electromyographic signals and the virtual reality for training the TMR patient.

and complex gestures (with 2 DoFs), that are reported in Tab.4.1. After this preliminary training with the virtual reality system, that aimed the patient to learn how controlling the sEMG signals from the reinnervated sites to move the virtual arm, the TMR patient began a second training phase with the experimental prosthesis, presented in Fig. 4.11. The patient was close to the bench prosthetic system, and she was asked to activate the muscles to control the corresponding DoFs of the prosthetic arm. In Fig. 4.11, the patient performed the supination of the wrist and the flexion of the elbow with the prosthetic system.

In order to assess the ability of controlling multiple DoFs simultaneously, in a more natural and intuitive way, the offline and real-time performance of the parallel classification approach has been evaluated on the TMR subject to discriminate

Tesi di dottorato in Scienze e Ingegneria per l'Uomo e l'Ambiente/Science and Engineering for Humans and the Environment,
di Francesca Leone, discussa presso l'Università Campus Bio-Medico di Roma in data 26/07/2021.
La disseminazione e la riproduzione di questo documento sono consentite per scopi di didattica e ricerca,
a condizione che ne venga citata la fonte.

Figure 4.11: The TMR patient control the bench prosthetic system composed of three different modules: the elbow with active flexion/extension (Hosmer); the HANNES hand; the wrist with active pronation/supination (Ottobock).

27 motion classes, reported in Tab.4.1

4.5.2 Experimental Setup and protocol

The sEMG data were acquired at 1 KHz by using a suitable software on Labview platform and DAQ USB 6002 device, to create 3 Datasets, used for both the LR and LDA "Elbow classifier", "Wrist classifier", and "Hand classifier", introduced before in Section 3.4.1. The PC (Samsung Intel(R) Core (TM) i7-4500U CPU @ 1.80 GHz) and DAQ communicated by means of an USB port. Six commercial active sEMG sensors (Ottobock 13E200 = 50, 27 mm × 18 mm × 9.5 mm) were placed on the reinnervated sites (described in Fig. 4.9), after clinical palpation

Tesi di dottorato in Scienze e Ingegneria per l'Uomo e l'Ambiente/Science and Engineering for Humans and the Environment,
di Francesca Leone, discussa presso l'Università Campus Bio-Medico di Roma in data 26/07/2021.
La disseminazione e la riproduzione di questo documento sono consentite per scopi di didattica e ricerca,
a condizione che ne venga citata la fonte.

Fig. 4.12.

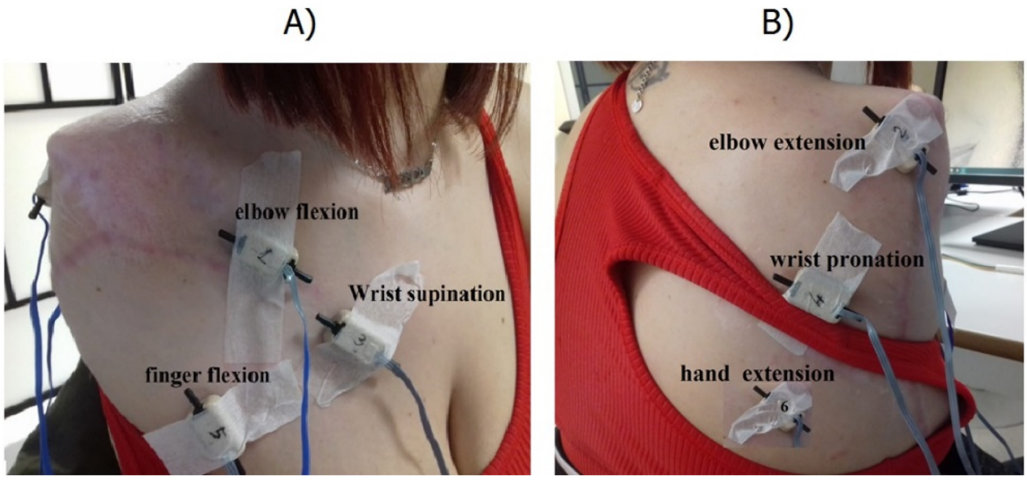

Figure 4.12: A) sEMG electrode placement on the anterior part of the pectoralis major muscle for the elbow flexion movement, wrist supination and hand closing; B) sEMG electrode placement on the posterior part of the dorsal major muscle for the elbow extension, wrist pronation and hand opening movements.

The TMR subject was sitting in front of a monitor (Fig 4.13) and was asked to produce each of the 27 gestures reported in Tab.4.1: the discrete motions were elbow flexion and extension, hand open and close and, wrist supination and pronation; the combined motions were up to two and three elbow, wrist, and hand DoFs combinations. The TMR patient was asked to produce each of these gestures for four times and hold it for 3 s with an interval of rest state about 2 s between each repetition. The sEMG data were collected in eight experimental sessions, from July to September. Depending on the availability and the physical condition of the TMR amputee during the reported day, one or two experimental

Tesi di dottorato in Scienze e Ingegneria per l'Uomo e l'Ambiente/Science and Engineering for Humans and the Environment, di Francesca Leone, discussa presso l'Università Campus Bio-Medico di Roma in data 26/07/2021.
La disseminazione e la riproduzione di questo documento sono consentite per scopi di didattica e ricerca, a condizione che ne venga citata la fonte.

sessions were recorded within the same day. For instance, for both these days (9/07/2020 and 9/09/2020), two experimental sessions were recorded within the same day. The electrodes placement was the same over the repetition of each task, within the same day. Then, at the end of the acquisition day, the physiotherapists marked on the amputee's body with a dermographic pen the muscle sites in order to place the electrodes in the same way over different days. Demonstrations of each movement were displayed following a predefined list on a computer screen (Fig.4.13). During the offline training, for each movement, the clinical operator instructed the TMR amputee to follow the demonstration of his motion and to perform it with a comfortable and consistent level of effort. Then, in the real-time phase, the TMR amputee was asked to reproduce the same tasks in the most similar way to the offline training.

The same algorithms described in Section 3.3.1 and 3.3.2 were employed in the parallel classification approach.

4.5.3 Experimental Results

4.5.4 Offline performance

The offline results of the parallel classification approach are reported for both LR and LDA algorithms in Tab. 4.5, 4.6,4.7 for the three classifiers ("Elbow classifier", "Wrist classifier", and "Hand classifier") in terms of F1Score (Fig.4.14).

In detail, the reported results were obtained by considering the acquisition of 8 days (from July to September, Tab. 4.5, 4.6,4.7), by using the same algorithms described before in the Section 3.3.1 and 3.3.2. In Fig.4.14, the mean F1Score

Tesi di dottorato in Scienze e Ingegneria per l'Uomo e l'Ambiente/Science and Engineering for Humans and the Environment,
di Francesca Leone, discussa presso l'Università Campus Bio-Medico di Roma in data 26/07/2021.
La disseminazione e la riproduzione di questo documento sono consentite per scopi di didattica e ricerca,
a condizione che ne venga citata la fonte.

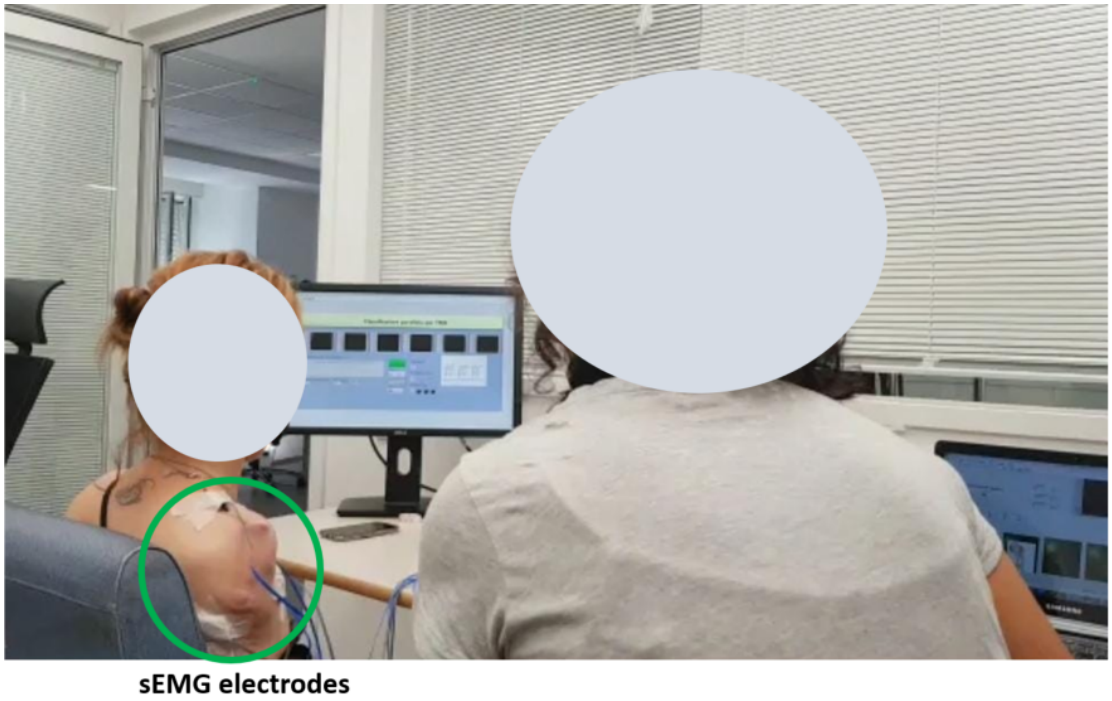

Figure 4.13: Training Session: recording of the DataSet based on sEMG signals for training the "Elbow classifier", "Wrist classifier", and "Hand classifier" through the Labview software interface.

values, over the three output classes, reached an average classification F1Score equals to 86.1 % ± 7.7, 79.3 % ± 8.8, 86.5 % ± 2.6, for the LR "Elbow classifier", "Wrist classifier", and "Hand classifier", respectively. In Fig. 4.15, the average confusion matrix were reported when testing both the LR and LDA classifiers on the "TS", over the three output classes.

A statistical analysis, based on the Mann-Whitney test, applied to the F1Score, was made firstly to assess if there was a statistical significant difference between the results of the LR and LDA algorithms, considering the last acquisition day of

Tesi di dottorato in Scienze e Ingegneria per l'Uomo e l'Ambiente/Science and Engineering for Humans and the Environment, di Francesca Leone, discussa presso l'Università Campus Bio-Medico di Roma in data 26/07/2021.
La disseminazione e la riproduzione di questo documento sono consentite per scopi di didattica e ricerca, a condizione che ne venga citata la fonte.

Table 4.6: F1Score values for the "Elbow classifier"

	Elbow classifier					
	LR			LDA		
TMR patient	F1			F1		
Trial days	Elbow flexion	Elbow extension	NM	Elbow flexion	Elbow extension	NM
6/07/2020 (morning)	62,30	76,0	84,40	66.9	77.7	84.5
7/07/2020 (morning)	95,50	96,90	95,10	94.4	97.1	95.2
8/07/2020 (afternoon)	78,50	93,40	84,30	81.7	93.1	88.1
9/07/2020 (morning)	79,90	93,00	80,80	82.5	92.7	81.7
9/07/2020 (afternoon)	73,60	81,50	82,00	72.9	77.3	82.8
9/09/2020 (morning-first trial)	86,90	89,70	83,50	88.1	89.2	82.9
9/09/2020 (morning-second trial)	87,90	99,00	87,70	88.7	96.4	87.0
10/09/2020 (afternoon)	90,90	94,10	88,60	90.1	95.1	89.1

Table 4.7: F1Score values for the "Wrist classifier"

	Wrist classifier					
	LR			LDA		
TMR patient	F1			F1		
Trial days	Wrist supination	Wrist pronation	NM	Wrist supination	Wrist pronation	NM
6/07/2020 (morning)	83,60	87,70	80,60	81.3	87.4	80.8
7/07/2020 (morning)	65,70	66,00	63,60	73.8	72.1	73.7
8/07/2020 (afternoon)	87,50	87,70	80,90	86.9	90.1	86.1
9/07/2020 (morning)	72,50	71,70	69,30	75.4	77.9	80.2
9/07/2020 (afternoon)	88,50	89,50	86,30	89.1	91.0	85.6
9/09/2020 (morning-first trial)	89,20	83,00	88,90	86.5	82.7	90.1
9/09/2020 (morning-second trial)	77,00	81,50	83,50	76.5	80.3	84.9
10/09/2020 (afternoon)	70,50	73,50	74,80	72.3	78.0	77.9

July and the last acquisition day of September. For both these days (9/07/2020 (afternoon) and 10/09/2020 (afternoon)), the the Mann-Whitney test points out no statistically significant difference between LR and LDA algorithms for the "Elbow classifier", "Wrist classifier", and "Hand classifier" (Fig.4.14). Then, based on these results, to assess if there was a significant improvement of the performance over the time, in terms of the F1Score, between the last day of July and September, the statistical analysis was performed for both the algorithms. The Mann-Whitney test points out no statistically significant difference between these days for both the algorithms.

Tesi di dottorato in Scienze e Ingegneria per l'Uomo e l'Ambiente/Science and Engineering for Humans and the Environment,
di Francesca Leone, discussa presso l'Università Campus Bio-Medico di Roma in data 26/07/2021.
La disseminazione e la riproduzione di questo documento sono consentite per scopi di didattica e ricerca,
a condizione che ne venga citata la fonte.

Table 4.8: F1Score values for the "Hand classifier"

	Hand classifier					
	LR			LDA		
TMR patient	F1			F1		
Trial days	Hand close	Hand open	NM	Hand close	Hand open	NM
6/07/2020 (morning)	98,60	79,40	76,70	98.9	81.7	79.3
7/07/2020 (morning)	94,90	85,30	81,90	97.4	84.7	83.0
8/07/2020 (afternoon)	99,00	79,30	79,20	98.6	81.5	80.5
9/07/2020 (morning)	99,40	83,00	81,80	98.9	83.7	83.4
9/07/2020 (afternoon)	98,60	83,90	83,70	98.4	84.1	83.4
9/09/2020 (morning-first trial	99,90	78,20	76,60	100.0	79.9	80.5
9/09/2020 (morning-second trial	98,60	77,10	75,80	98.5	75.7	73.9
10/09/2020 (afternoon)	99,60	82,20	82,80	99.1	84.3	85.3

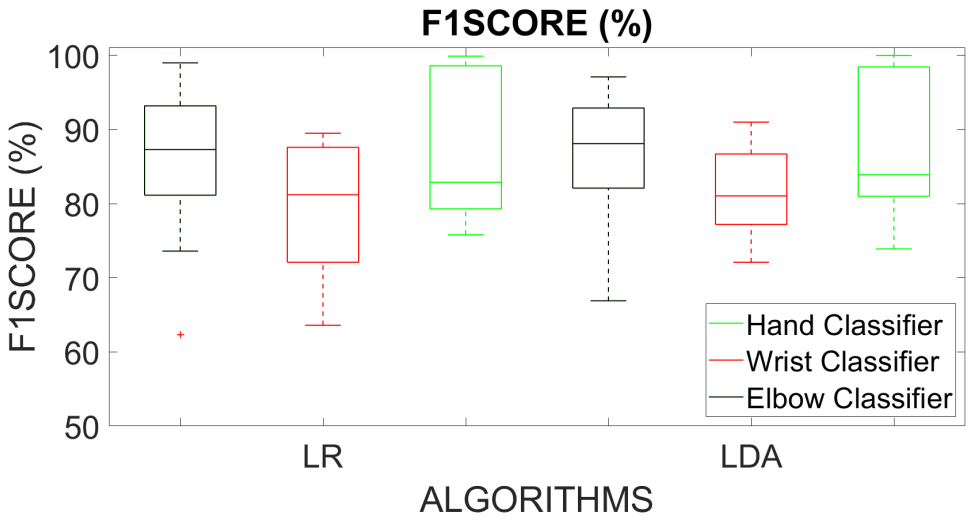

Figure 4.14: Box plots of the average F1Score values calculated on TMR patient using LR and LDA algorithms with five time domain features, tested on "TS," for the Elbow, Wrist, and Hand classifiers.

Tesi di dottorato in Scienze e Ingegneria per l'Uomo e l'Ambiente/Science and Engineering for Humans and the Environment,
di Francesca Leone, discussa presso l'Università Campus Bio-Medico di Roma in data 26/07/2021.
La disseminazione e la riproduzione di questo documento sono consentite per scopi di didattica e ricerca,
a condizione che ne venga citata la fonte.

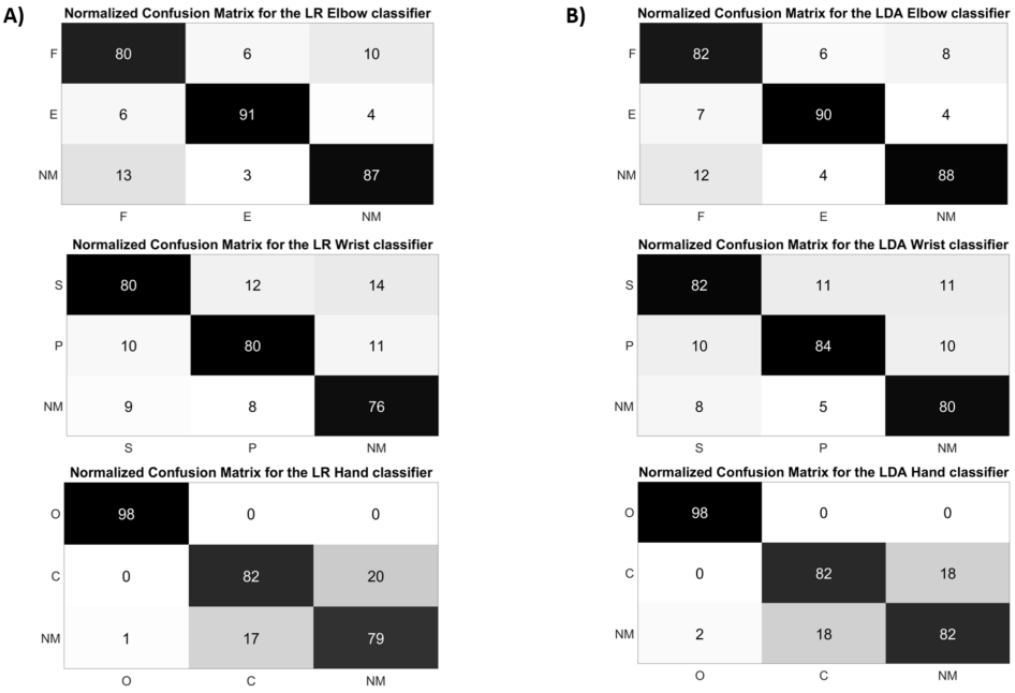

Figure 4.15: Normalized confusion matrix of the Elbow, Wrist, and Hand Classifiers obtained with the LR (A) and LDA (B) algorithms. The confusion matrices are normalized concerning the number of data belonging to the "TS",for the Elbow, Wrist, and Hand classifiers.

Tesi di dottorato in Scienze e Ingegneria per l'Uomo e l'Ambiente/Science and Engineering for Humans and the Environment,
di Francesca Leone, discussa presso l'Università Campus Bio-Medico di Roma in data 26/07/2021.
La disseminazione e la riproduzione di questo documento sono consentite per scopi di didattica e ricerca,
a condizione che ne venga citata la fonte.

4.5.5 Real-time performance

Both the LR and LDA classifiers were evaluated in real-time by considering the performance metrics reported in the Section 3.5.4.

The boxplot (Fig.4.16) reported the mean MCT values (related to the 8 acquisitions) among the 27 motion classes: the mean MCT values were equals to 3.40 ± 1.70 s and 3.70 ± 1.60 s for the LR and LDA algorithms, respectively.

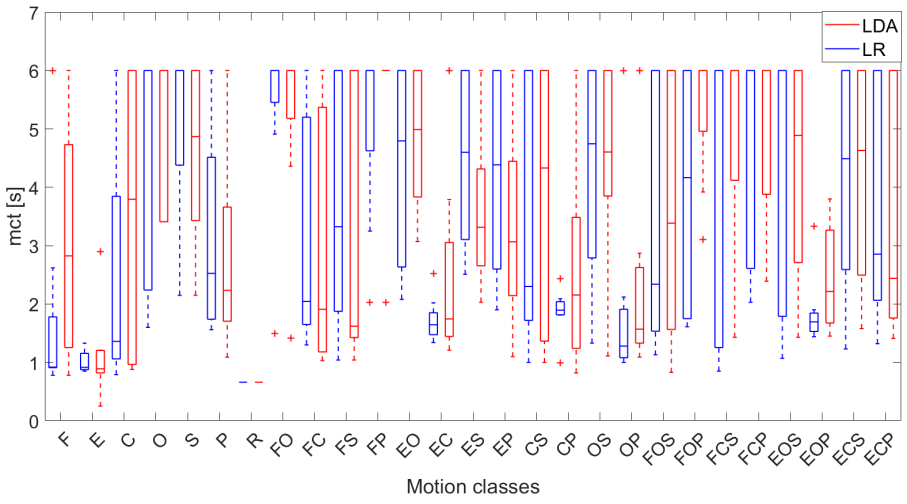

Figure 4.16: Box plot of the average "MCT" values (related to the 8 acquisitions) calculated on TMR patient using the LR and LDA algorithms.

The mean MCT values (related to the 8 acquisition days), showed an increasing trend if we considered the 1, 2 and 3 DoFs motion classes (Fig. 4.17). The increase of the mean MCR values was confirmed also in Fig. 4.18 that showed the percentage of bad classified classes, over time.

In Fig.4.20 the mean and standard deviation values of the MCR, among the 27

Tesi di dottorato in Scienze e Ingegneria per l'Uomo e l'Ambiente/Science and Engineering for Humans and the Environment,
di Francesca Leone, discussa presso l'Università Campus Bio-Medico di Roma in data 26/07/2021.
La disseminazione e la riproduzione di questo documento sono consentite per scopi di didattica e ricerca,
a condizione che ne venga citata la fonte.

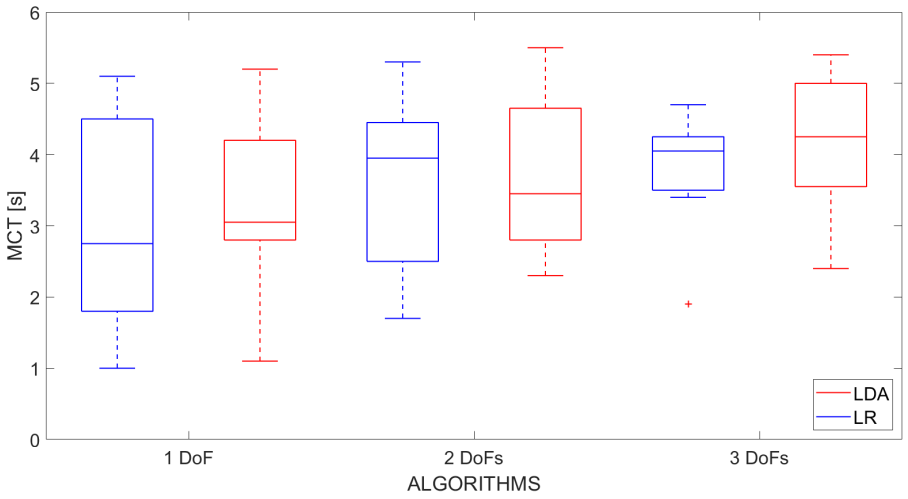

Figure 4.17: Box plots of the mean MCT values (related to the 8 acquisition days), when considering the 1, 2 and 3 DoFs motion classes for both the LR and LDA algorithms.

motion classes, were reported, considering the 8 acquisition days. Considering the mean MCR of the last day of July and the last day of September, an increase of the performance can be observed (Fig.4.19): for the LR algorithm, the mean MCR value increased from 50 (last day of July) % to 100 % (last day of September) for 1 DoF motion classes, from 50 % (last day of July) to 75 % for 2 DoFs classes (last day of September), and from 50 % (last day of July) to 63 % (last day of September) for the 3 DoFs motion classes. Also for the LDA algorithm, there was an improvement: the mean MCR values classes increased from 58 (last day of July) % to 92 % (last day of September) for 1 DoF motion classes, from 62 % (last day of July) to 71 % for 2 DoFs classes (last day of September), and from 45 % (last day of July) to 63 % (last day of September) for the 3 DoFs motion classes.

Tesi di dottorato in Scienze e Ingegneria per l'Uomo e l'Ambiente/Science and Engineering for Humans and the Environment,
di Francesca Leone, discussa presso l'Università Campus Bio-Medico di Roma in data 26/07/2021.
La disseminazione e la riproduzione di questo documento sono consentite per scopi di didattica e ricerca,
a condizione che ne venga citata la fonte.

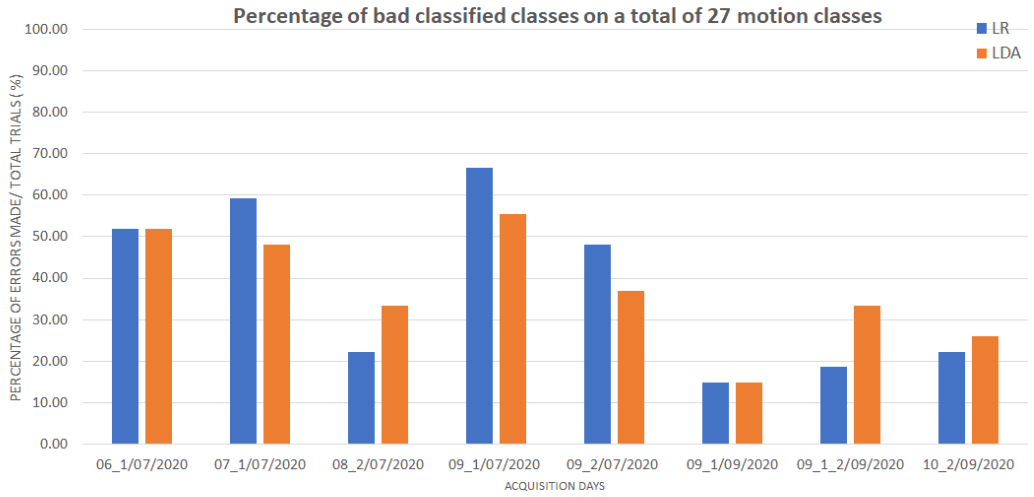

Figure 4.18: Percentage of bad classified classes on a total of 27 motion classes, for both the LR and LDA algorithms, over the 8 acquisition days (from July to September).

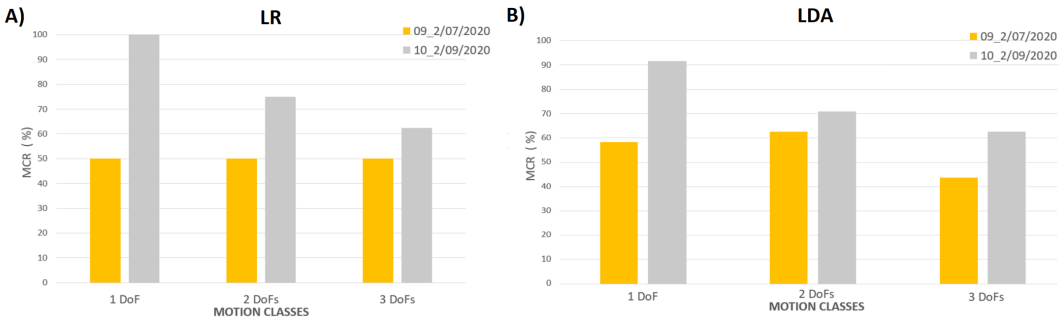

Figure 4.19: The mean MCR of the last day of July and the last day of September related to the LR (A) and LDA (B) algorithms.

The Mann-Whitney test applied to the MCR values points out the statistically significant difference between the last acquisition day of July and September for

Tesi di dottorato in Scienze e Ingegneria per l'Uomo e l'Ambiente/Science and Engineering for Humans and the Environment,
di Francesca Leone, discussa presso l'Università Campus Bio-Medico di Roma in data 26/07/2021.
La disseminazione e la riproduzione di questo documento sono consentite per scopi di didattica e ricerca,
a condizione che ne venga citata la fonte.

both the LR and LDA algorithms.

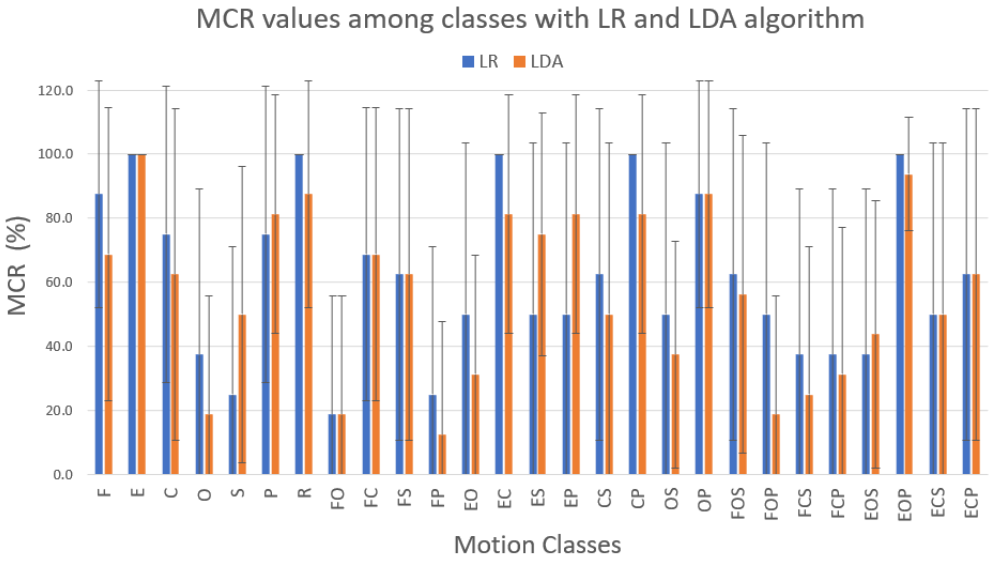

Figure 4.20: Mean and standard deviation values of motion completion rate values (related to the 8 acquisitions), performed by TMR patient, for all the 27 motion classes, with both LR (blue color) and LDA (orange color) algorithms.

Tesi di dottorato in Scienze e Ingegneria per l'Uomo e l'Ambiente/Science and Engineering for Humans and the Environment, di Francesca Leone, discussa presso l'Università Campus Bio-Medico di Roma in data 26/07/2021.
La disseminazione e la riproduzione di questo documento sono consentite per scopi di didattica e ricerca, a condizione che ne venga citata la fonte.

4.5.6 Discussion

4.5.7 Offline performance

The results for the simultaneous movements (27 classes) related to the 8 acquisition days were summarized in Tab. 4.5, 4.6,4.7 for the three classifiers ("Elbow classifier", "Wrist classifier", and "Hand classifier") in terms of F1Score (Fig.4.14). The "Elbow Classifier" and the "Hand Classifier" reached the highest mean F1Score values: they were equals to 86.1 % ± 7.7 and 86.5 % ± 2.6 with the LR "Elbow Classifier" and "Hand Classifier", respectively; 86.5 % ± 7.2 and 87.3 % ± 2.4 with the LDA "Elbow Classifier" and "Hand Classifier", respectively. The "Wrist Classifier" obtained the lowest mean F1Score values equals to 79.3 % ± 8.8 with LR algorithm and 81.7 % ± 6.2 with LDA algorithm. These lower values than that obtained for the elbow and hand joints can be due to the major difficulty to control the wrist motions during 2 and 3 DoFs complex motions[88]. Confusion matrices, reported in Fig. 4.15 confirmed the presence of misclassified data out of the main diagonal for all the three LR and LDA classifiers.

The statistical analysis based on the Mann-Whitney test confirmed no statistically significant difference between the mean F1Score values of LR and LDA "Elbow classifier", "Wrist classifier", and "Hand classifier".

It is interesting to note that the parallel classification approach with both LR and LDA classifiers obtained promising results that can be improved by training the TMR patient over time and thus, by extending the analysis for a major number of months.

Tesi di dottorato in Scienze e Ingegneria per l'Uomo e l'Ambiente/Science and Engineering for Humans and the Environment,
di Francesca Leone, discussa presso l'Università Campus Bio-Medico di Roma in data 26/07/2021.
La disseminazione e la riproduzione di questo documento sono consentite per scopi di didattica e ricerca,
a condizione che ne venga citata la fonte.

4.5.8 Real-time performance

The mean motion completion time values (related to the 8 acquisition days), showed an increasing trend if we considered the 1, 2 and 3 DoFs motion classes (Fig. 4.17): for the LR algorithm, they were equal to 3.00 ± 1.60 s (1 DoF) and 3.60 ± 1.20 (2 DoFs) s and 3.80 ± 0.90 s (3 DoFs). Instead, for the LDA algorithm, they were equal to 3.20 ± 1.40 s (1 DoF), 3.70 ± 1.10 s (2 DoFs) and 4.20 ± 1.00 s (3 DoFs). Thus, the LDA algorithm presented the motion completion time values slightly higher than LR classifiers, especially for the 2 and 3 DoFs motion classes. In particular, in Fig. 4.16 we can observe which are the motion classes with the highest mean motion completion time values, related to the 8 acquisition days, obtained with the LR algorithm: hand open (4.50 ± 2.07), and wrist supination (5.00 ± 1.65) for the 1 DoF motion classes; elbow flexion with hand open (5.30 ± 1.58), elbow flexion with wrist pronation (5.20 ± 1.59), elbow extension with hand open (4.40 ± 1.80), elbow extension with wrist supination (4.50 ± 1.63), for the 2 DoFs motion classes; elbow flexion with hand close and wrist supination (4.40 ± 2.50), elbow flexion with hand close and wrist pronation (4.70 ± 1.86), and elbow extension with hand open and wrist supination (4.45 ± 2.32) for the 3 DoFs motion classes. The statistical analysis, based on the Mann-Whitney test, does not reveal a significant difference between the motion completion time values obtained with the LR and LDA algorithms.

The mean motion completion rate values, shown in Fig. 4.20, confirmed that the motion classes most difficult to be performed were the same that had the highest mean motion completion time values. In addition, it is worth noticing that

Tesi di dottorato in Scienze e Ingegneria per l'Uomo e l'Ambiente/Science and Engineering for Humans and the Environment, di Francesca Leone, discussa presso l'Università Campus Bio-Medico di Roma in data 26/07/2021.
La disseminazione e la riproduzione di questo documento sono consentite per scopi di didattica e ricerca, a condizione che ne venga citata la fonte.

the Mann-Whitney test points out the statistically significant difference between the last acquisition day of July and September for both the LR and LDA algorithms. The increase of the mean motion completion rate values was confirmed also in Fig. 4.18 that showed the percentage of bad classified classes, over time: for both the LR and LDA algorithms a decrease of the percentage of errors made was evident. In detail, for the LR algorithm, this percentage of errors went from the 59.26 % (trial on 7/07/2020) to 14.81 % (trial on 10/09/2020). Regarding the LDA algorithm, this percentage of errors decreased from the 55.56 % (trial on 9/07/2020) to 14.81 % (trial on 9/09/2020).

4.6 Conclusion

In this chapter, a novel parallel PR-based strategy for classifying 27 motion classes (up to 3 DoFs) was proposed. It relies on the use of three parallel LR classifiers to simultaneously control multiple DoFs related to the elbow, wrist and hand joints. To date, the single, hierarchical, and parallel classification approaches, based on the LDA classifiers, were introduced to discriminate until 19 wrist/hand gestures (in the 3-DoFs case), considering both combined and discrete motions[68].

The proposed method was applied to the sEMG signals recorded from 15 healthy subjects (Sect. 4.3) and a TMR patient (Sect. 4.5), by using 6 commercial sEMG sensors. Then, a comparative analysis among the performance of LR and LDA algorithms was done by considering the Mann-Whitney test. A feature set consisting of TD features[131] was used to process the data with a windows of 150 ms with an overlap of 100 ms[122].

Tesi di dottorato in Scienze e Ingegneria per l'Uomo e l'Ambiente/Science and Engineering for Humans and the Environment, di Francesca Leone, discussa presso l'Università Campus Bio-Medico di Roma in data 26/07/2021.
La disseminazione e la riproduzione di questo documento sono consentite per scopi di didattica e ricerca, a condizione che ne venga citata la fonte.

Twenty-seven motion classes (up to 3 DoFs) were tested with both offline (in terms of F1Score) and online (in terms of MCT, MST, MCR) performance measures.

About the offline results obtained from the 15 healthy subjects, the Mann-Whitney test applied to the F1Score, points out no statistically significant difference between LR and LDA algorithms for the "Elbow classifier", the "Wrist classifier", and "Hand classifier". In detail, the mean F1Score values were above the 90 % for all the classifiers, and the mean misclassification error rates remained under the 10 % value, that can be considered positive for an usable system[53]. Instead, the offline analysis performed on TMR patients showed that the classification performance reached lower mean F1Score values than that on healthy subjects: they were equals to 86 % for the "Elbow classifier" and "Hand classifier" and 80 % for the "Wrist classifier".

Moreover, it was verified the real-time robustness of the proposed PR-based parallel strategy. About the real-time results from healthy subjects, despite the LDA was considered the benchmark classifier for real-time employment[139], the performances of the LR algorithm in terms of motion completion time values were statistically better than that obtained with the LDA one. Instead, for the TMR subjects, there wasn't a statistical significance difference between the performance obtained with the LR and LDA algorithms. However, the Mann-Whitney test applied to the motion completion rate values points out the statistically significant difference between the last acquisition day of July and September for both the LR and LDA algorithms and a positive trend of this performance metric was

Tesi di dottorato in Scienze e Ingegneria per l'Uomo e l'Ambiente/Science and Engineering for Humans and the Environment,
di Francesca Leone, discussa presso l'Università Campus Bio-Medico di Roma in data 26/07/2021.
La disseminazione e la riproduzione di questo documento sono consentite per scopi di didattica e ricerca,
a condizione che ne venga citata la fonte.

confirmed over the time. Hence, these results strongly encourage to further investigate the performance of this PR solution for TMR patient, by extending the number of acquisition and of TMR patients. As the proposed system has reached an advanced grade of accuracy also on TMR patients, an embedding solution will be proposed to control simultaneously and in a natural way different joints of a complex multi-DoFs prosthetic device.

Tesi di dottorato in Scienze e Ingegneria per l'Uomo e l'Ambiente/Science and Engineering for Humans and the Environment,
di Francesca Leone, discussa presso l'Università Campus Bio-Medico di Roma in data 26/07/2021.
La disseminazione e la riproduzione di questo documento sono consentite per scopi di didattica e ricerca,
a condizione che ne venga citata la fonte.

5

Conclusion

This thesis aims at providing promising PR-based strategies for (i) controlling simultaneously, with a hierarchical classification strategy, the hand/wrist gestures and exerted forces during grasping tasks; (ii) discriminating up to 27 motion classes (3 DoFs) related to several joints, as the elbow, hand, and wrist. The common purpose is to address the future research towards the development of

Tesi di dottorato in Scienze e Ingegneria per l'Uomo e l'Ambiente/Science and Engineering for Humans and the Environment, di Francesca Leone, discussa presso l'Università Campus Bio-Medico di Roma in data 26/07/2021.
La disseminazione e la riproduzione di questo documento sono consentite per scopi di didattica e ricerca, a condizione che ne venga citata la fonte.

prostheses that are functional and able to mimic the lost upper limb behavior, replicating the performance of the human arm.

To achieve the first purpose, an extended analysis of the performance of the hierarchical PR-based strategy was presented in Chapter 3, by reporting the results on 31 healthy subjects, and then both offline and real-time performance related to sEMG data recorded from 15 transradial amputees. The analysis performed on sEMG data recorded from 31 healthy subjects shows that there were no statistically significant differences in terms of F1Score performance between NLR and LDA. Therefore, this study reveals that the use of non linear classification algorithm, as NLR, is as much suitable as the benchmark LDA classifier for implementing an EMG pattern recognition system, able both to decode hand/wrist gestures and to associate different performed force levels to grasping actions. Then, an extended analysis based on LR, NLR and LDA algorithm had been carried out to assess the robustness, both in offline and in real-time, of the hierarchical PR system. A real scenario, composed of hand device (RoboLimb) and wrist module (WristRotator) was controlled in real-time by using the hierarchical PR-based strategy and both offline and real-time performance metrics were evaluated to investigate the ability of trans-radial amputees to manage simultaneously desired hand/wrist gestures and three force levels. The comparative analysis, based on Mann-Whitney test (U-test) with Bonferroni correction ($p<0.016$), reports not statistically significant differences in terms of F1Score and misclassification errors between the LR, NLR and LDA classifiers. However, considering also the real-time performance, the best solution to decode simultaneously the hand/wrist

Tesi di dottorato in Scienze e Ingegneria per l'Uomo e l'Ambiente/Science and Engineering for Humans and the Environment,
di Francesca Leone, discussa presso l'Università Campus Bio-Medico di Roma in data 26/07/2021.
La disseminazione e la riproduzione di questo documento sono consentite per scopi di didattica e ricerca,
a condizione che ne venga citata la fonte.

gestures and force levels seems to be the simultaneous use of the LR algorithm with FE for the "hand/wrist gestures classifier", and the NLR with FE for the Spherical and Tip force classifiers. Future works will be focused on the validation of the presented method on an embedding solution of this classification system: the final electronic device, composed of a micro-controller unit, will allow amputee to wear the prosthetic device to control simultaneously hand/wrist gestures and force levels.

Regarding the second purpose, the parallel classification approach was presented in Chapter 4 to provide the simultaneous classification of complex motion classes (up to 3 DoFs), by keeping the number of electrodes to a bare minimum and the classification error rates under 10 %. The Mann-Whitney test (U-test) applied to the F1Score and misclassification errors values, points out no statistically significant difference between LR and LDA algorithms for the "Elbow classifier", the "Wrist classifier", and "Hand classifier". However, the LR classifiers reached higher real-time performance, especially for the combined 2 and 3 DoFs motions with wrist supination. This can be considered a positive results since the difficulty to discriminate the contribution of the muscles involved wrist rotations that are generally deep muscles. Also an analysis of the preliminary offline and real-time results, obtained from a TMR subject, were carried out and seem to be promising, despite the few number of acquisition day related to two months (from July to September). The statistical analysis based on the Mann-Whitney test (U-test), confirmed no statistically significant difference between the mean F1Score values and misclassification errors rate of LR and LDA "Elbow classifier", "Wrist

Tesi di dottorato in Scienze e Ingegneria per l'Uomo e l'Ambiente/Science and Engineering for Humans and the Environment, di Francesca Leone, discussa presso l'Università Campus Bio-Medico di Roma in data 26/07/2021.
La disseminazione e la riproduzione di questo documento sono consentite per scopi di didattica e ricerca, a condizione che ne venga citata la fonte.

classifier", and "Hand classifier" (at $p < 0.05$). Regarding the real-time analysis, the mean "MCT" values (related to the 8 acquisition days), showed an increasing trend if we considered the 1, 2 and 3 DoFs motion classes with an significant decrease of the percentage number of the bad classified classes. Thus, this PR-based system obtained promising results also on TMR patient. Future development will regard collect additional sEMG data from TMR patient in order to validate the proposed system for a major number of months, by training over time the TMR patient, until the classification error rates will be under 10 % for each joint. After reaching an advanced grade of real time accuracy by TMR patient, an embedding version of this classification system will be developed to control a multi-DoFs prosthetic device. In this scenario, future works will be focused to integrate the embedding version of the classification system with the multi-DoFs prosthesis and to clinically validate the final system.

In particular, future works will be focused on the validation of the presented method on an embedding solution of this classification system: the final electronic device, composed of a micro-controller unit, will aim to allow amputee to wear the prosthetic device to control simultaneously hand/wrist gestures and force levels. This step forward will be relevant for implementing practical technological solutions to adopt in a real scenario, by taking into account energy save policies to perform long-term test on an increasing number of trans-radial amputees and TMR patients. When positive results will be obtained also with the embedded solutions, for both the introduced hierarchical and parallel classification approaches, the systems will be re-engineered to comply with the normative

Tesi di dottorato in Scienze e Ingegneria per l'Uomo e l'Ambiente/Science and Engineering for Humans and the Environment,
di Francesca Leone, discussa presso l'Università Campus Bio-Medico di Roma in data 26/07/2021.
La disseminazione e la riproduzione di questo documento sono consentite per scopi di didattica e ricerca,
a condizione che ne venga citata la fonte.

concerning medical devices and it will be used by amputees during future trials.

Tesi di dottorato in Scienze e Ingegneria per l'Uomo e l'Ambiente/Science and Engineering for Humans and the Environment, di Francesca Leone, discussa presso l'Università Campus Bio-Medico di Roma in data 26/07/2021.
La disseminazione e la riproduzione di questo documento sono consentite per scopi di didattica e ricerca, a condizione che ne venga citata la fonte.

References

[1] A. L. Ciancio, F. Cordella, R. Barone, R. A. Romeo, A. D. Bellingegni, R. Sacchetti, A. Davalli, G. Di Pino, F. Ranieri, V. Di Lazzaro et al., "Control of prosthetic hands via the peripheral nervous system," Frontiers in neuroscience, vol. 10, p. 116, 2016.

[2] L. A. Jones and S. J. Lederman, Human hand function. Oxford university press, 2006.

[3] F. Cordella, F. Di Corato, G. Loianno, B. Siciliano, and L. Zollo, "Robust pose estimation algorithm for wrist motion tracking," in 2013 IEEE/RSJ International Conference on Intelligent Robots and Systems. IEEE, 2013, pp. 3746–3751.

[4] R. Reiter, "Eine neue elektrokunsthand," Grenzgebiete der Medizin, vol. 1, no. 4, pp. 133–135, 1948.

[5] P. F. Pasquina, B. N. Perry, M. E. Miller, G. S. Ling, and J. W. Tsao, "Recent advances in bioelectric prostheses," Neurology: Clinical Practice, vol. 5, no. 2, pp. 164–170, 2015.

[6] A. L. Ciancio, F. Cordella, K.-P. Hoffmann, A. Schneider, E. Guglielmelli, and L. Zollo, "Current achievements and future directions of hand prostheses controlled via peripheral nervous system," in The Hand. Springer, 2017, pp. 75–95.

[7] E. Scheme and K. Englehart, "Electromyogram pattern recognition for control of powered upper-limb prostheses: state of the art and challenges for clinical use." Journal of Rehabilitation Research & Development, vol. 48, no. 6, 2011.

Tesi di dottorato in Scienze e Ingegneria per l'Uomo e l'Ambiente/Science and Engineering for Humans and the Environment, di Francesca Leone, discussa presso l'Università Campus Bio-Medico di Roma in data 26/07/2021.
La disseminazione e la riproduzione di questo documento sono consentite per scopi di didattica e ricerca, a condizione che ne venga citata la fonte.

[8] A. D. Roche, H. Rehbaum, D. Farina, and O. C. Aszmann, "Prosthetic myoelectric control strategies: a clinical perspective," Current Surgery Reports, vol. 2, no. 3, p. 44, 2014.

[9] C. Li, J. Ren, H. Huang, B. Wang, Y. Zhu, and H. Hu, "Pca and deep learning based myoelectric grasping control of a prosthetic hand," Biomedical engineering online, vol. 17, no. 1, p. 107, 2018.

[10] R. Chowdhury, M. Reaz, M. Ali, A. Bakar, K. Chellappan, and T. Chang, "Surface electromyography signal processing and classification techniques," Sensors, vol. 13, no. 9, pp. 12 431–12 466, 2013.

[11] Y. Geng, P. Zhou, and G. Li, "Toward attenuating the impact of arm positions on electromyography pattern-recognition based motion classification in transradial amputees," Journal of neuroengineering and rehabilitation, vol. 9, no. 1, p. 74, 2012.

[12] A. J. Young, L. J. Hargrove, and T. A. Kuiken, "Improving myoelectric pattern recognition robustness to electrode shift by changing interelectrode distance and electrode configuration," IEEE Transactions on Biomedical Engineering, vol. 59, no. 3, pp. 645–652, 2012.

[13] T. Lorrain, N. Jiang, and D. Farina, "Influence of the training set on the accuracy of surface emg classification in dynamic contractions for the control of multifunction prostheses," Journal of neuroengineering and rehabilitation, vol. 8, no. 1, p. 25, 2011.

[14] D. Farina, O. F. Do Nascimento, M.-F. Lucas, and C. Doncarli, "Optimization of wavelets for classification of movement-related cortical potentials generated by variation of force-related parameters," Journal of neuroscience methods, vol. 162, no. 1-2, pp. 357–363, 2007.

[15] D. Staudenmann, I. Kingma, A. Daffertshofer, D. Stegeman, and J. Van Dieën, "Heterogeneity of muscle activation in relation to force direction: a multi-channel surface electromyography study on the triceps surae muscle," Journal of Electromyography and Kinesiology, vol. 19, no. 5, pp. 882–895, 2009.

[16] C. Disselhorst-Klug, T. Schmitz-Rode, and G. Rau, "Surface electromyography and muscle force: Limits in semg–force relationship and new approaches for applications," Clinical biomechanics, vol. 24, no. 3, pp. 225–235, 2009.

Tesi di dottorato in Scienze e Ingegneria per l'Uomo e l'Ambiente/Science and Engineering for Humans and the Environment, di Francesca Leone, discussa presso l'Università Campus Bio-Medico di Roma in data 26/07/2021.
La disseminazione e la riproduzione di questo documento sono consentite per scopi di didattica e ricerca, a condizione che ne venga citata la fonte.

[17] A. D. Bellingegni, E. Gruppioni, G. Colazzo, A. Davalli, R. Sacchetti, E. Guglielmelli, and L. Zollo, "Nlr, mlp, svm, and lda: a comparative analysis on emg data from people with trans-radial amputation," Journal of neuroengineering and rehabilitation, vol. 14, no. 1, p. 82, 2017.

[18] L. C. Smail, C. Neal, C. Wilkins, and T. L. Packham, "Comfort and function remain key factors in upper limb prosthetic abandonment: findings of a scoping review," Disability and Rehabilitation: Assistive Technology, pp. 1–10, 2020.

[19] C. Cipriani, F. Zaccone, S. Micera, and M. C. Carrozza, "On the shared control of an emg-controlled prosthetic hand: analysis of user–prosthesis interaction," IEEE Transactions on Robotics, vol. 24, no. 1, pp. 170–184, 2008.

[20] T. A. Kuiken, D. S. Childress, and W. Z. Rymer, "The hyper-reinnervation of rat skeletal muscle," Brain research, vol. 676, no. 1, pp. 113–123, 1995.

[21] A. Chi, S. Smith, I. Womack, and R. Armiger, "The evolution of man and machine—a review of current surgical techniques and cutting technologies after upper extremity amputation," Current Trauma Reports, vol. 4, no. 4, pp. 339–347, 2018.

[22] M. LeBlanc, "Give hope-give a hand," The LN-4 prosthetic hand, vol. 2014, 2008.

[23] Tech. Rep.

[24] R. Montague, Amputee and Prosthetic Rehabilitation – Standards and Guidelines (2nd Edition). British Society of Rehabilitation Medicine, Oct. 2003, p. 13, available on line. [Online]. Available: https://www.bsrm.org.uk/downloads/ars-gfinaltext.pdf

[25] G. Pomares, H. Coudane, F. Dap, and G. Dautel, "Epidemiology of traumatic upper limb amputations," Orthopaedics & Traumatology: Surgery & Research, vol. 104, no. 2, pp. 273–276, 2018.

[26] K. Ziegler-Graham, E. J. MacKenzie, P. L. Ephraim, T. G. Travison, and R. Brookmeyer, "Estimating the prevalence of limb loss in the united states: 2005 to 2050," Archives of physical medicine and rehabilitation, vol. 89, no. 3, pp. 422–429, 2008.

Tesi di dottorato in Scienze e Ingegneria per l'Uomo e l'Ambiente/Science and Engineering for Humans and the Environment, di Francesca Leone, discussa presso l'Università Campus Bio-Medico di Roma in data 26/07/2021.
La disseminazione e la riproduzione di questo documento sono consentite per scopi di didattica e ricerca, a condizione che ne venga citata la fonte.

[27] C. Bruce, "Cosmetic prosthesis and methods for making the same," Aug. 3 2006, uS Patent App. 10/539,433.

[28] P. Geethanjali, "Myoelectric control of prosthetic hands: state-of-the-art review," Medical Devices (Auckland, NZ), vol. 9, p. 247, 2016.

[29] H. H. Sears, E. K. Iversen, K. B. Hays, and A. D. Dyck, "Method and apparatus for controlling an externally powered prosthesis," Mar. 30 1999, uS Patent 5,888,213.

[30] R. Scott and P. Parker, "Myoelectric prostheses: state of the art," Journal of medical engineering & technology, vol. 12, no. 4, pp. 143–151, 1988.

[31] B. Popov, "The bio-electrically controlled prosthesis," The Journal of bone and joint surgery. British volume, vol. 47, no. 3, pp. 421–424, 1965.

[32] A. Fougner, Ø. Stavdahl, P. J. Kyberd, Y. G. Losier, and P. A. Parker, "Control of upper limb prostheses: terminology and proportional myoelectric control—a review," IEEE Transactions on neural systems and rehabilitation engineering, vol. 20, no. 5, pp. 663–677, 2012.

[33] F. Cordella, A. L. Ciancio, R. Sacchetti, A. Davalli, A. G. Cutti, E. Guglielmelli, and L. Zollo, "Literature review on needs of upper limb prosthesis users," Frontiers in neuroscience, vol. 10, p. 209, 2016.

[34] C. Potluri, M. Anugolu, M. P. Schoen, D. S. Naidu, A. Urfer, and S. Chiu, "Hybrid fusion of linear, non-linear and spectral models for the dynamic modeling of semg and skeletal muscle force: an application to upper extremity amputation," Computers in biology and medicine, vol. 43, no. 11, pp. 1815–1826, 2013.

[35] T. S. Buchanan, D. G. Lloyd, K. Manal, and T. F. Besier, "Neuromusculoskeletal modeling: estimation of muscle forces and joint moments and movements from measurements of neural command," Journal of applied biomechanics, vol. 20, no. 4, pp. 367–395, 2004.

[36] H. Srinivasan, S. Gupta, W. Sheng, and H. Chen, "Estimation of hand force from surface electromyography signals using artificial neural network," in Intelligent Control and Automation (WCICA), 2012 10th World Congress on. IEEE, 2012, pp. 584–589.

Tesi di dottorato in Scienze e Ingegneria per l'Uomo e l'Ambiente/Science and Engineering for Humans and the Environment, di Francesca Leone, discussa presso l'Università Campus Bio-Medico di Roma in data 26/07/2021.
La disseminazione e la riproduzione di questo documento sono consentite per scopi di didattica e ricerca, a condizione che ne venga citata la fonte.

[37] C. Wu, H. Zeng, A. Song, and B. Xu, "Grip force and 3d push-pull force estimation based on semg and grnn," Frontiers in neuroscience, vol. 11, p. 343, 2017.

[38] J. Ren, C. Li, H. Huang, P. Wang, Y. Zhu, B. Wang, and K. An, "Grasping force control of prosthetic hand based on pca and svm," in Advanced Computational Methods in Life System Modeling and Simulation. Springer, 2017, pp. 222–230.

[39] B. Lv, X. Sheng, W. Guo, X. Zhu, and H. Ding, "Towards finger gestures and force recognition based on wrist electromyography and accelerometers," in International Conference on Intelligent Robotics and Applications. Springer, 2017, pp. 373–380.

[40] E. Scheme and K. Englehart, "Training strategies for mitigating the effect of proportional control on classification in pattern recognition based myoelectric control," Journal of prosthetics and orthotics: JPO, vol. 25, no. 2, p. 76, 2013.

[41] E. Scheme, B. Lock, L. Hargrove, W. Hill, U. Kuruganti, and K. Englehart, "Motion normalized proportional control for improved pattern recognition-based myoelectric control," IEEE Transactions on Neural Systems and Rehabilitation Engineering, vol. 22, no. 1, pp. 149–157, 2014.

[42] A. L. Fougner, Ø. Stavdahl, and P. J. Kyberd, "System training and assessment in simultaneous proportional myoelectric prosthesis control," Journal of neuroengineering and rehabilitation, vol. 11, no. 1, p. 75, 2014.

[43] A. J. Young, L. H. Smith, E. J. Rouse, and L. J. Hargrove, "A new hierarchical approach for simultaneous control of multi-joint powered prostheses," in 2012 4th IEEE RAS & EMBS International Conference on Biomedical Robotics and Biomechatronics (BioRob). IEEE, 2012, pp. 514–520.

[44] J. J. Baker, E. Scheme, K. Englehart, D. T. Hutchinson, and B. Greger, "Continuous detection and decoding of dexterous finger flexions with implantable myoelectric sensors," IEEE Transactions on Neural Systems and Rehabilitation Engineering, vol. 18, no. 4, pp. 424–432, 2010.

[45] A. Boschmann, M. Platzner, M. Robrecht, M. Hahn, and M. Winkler, "Development of a pattern recognition-based myoelectric transhumeral prosthesis with multifunctional simultaneous control using a model-driven

Tesi di dottorato in Scienze e Ingegneria per l'Uomo e l'Ambiente/Science and Engineering for Humans and the Environment, di Francesca Leone, discussa presso l'Università Campus Bio-Medico di Roma in data 26/07/2021.
La disseminazione e la riproduzione di questo documento sono consentite per scopi di didattica e ricerca, a condizione che ne venga citata la fonte.

approach for mechatronic systems," in Proceedings of the MyoElectric Controls/Powered Prosthetics Symposium Fredericton, New Brunswick, Canada, 2011.

[46] X. Li, R. Xu, O. W. Samuel, L. Tian, H. Zou, X. Zhang, S. Chen, P. Fang, and G. Li, "A new approach to mitigate the effect of force variation on pattern recognition for myoelectric control," in 2016 38th Annual International Conference of the IEEE Engineering in Medicine and Biology Society (EMBC). IEEE, 2016, pp. 1684–1687.

[47] C. Castellini, E. Gruppioni, A. Davalli, and G. Sandini, "Fine detection of grasp force and posture by amputees via surface electromyography," Journal of Physiology-Paris, vol. 103, no. 3-5, pp. 255–262, 2009.

[48] K. A. Kaczmarek, J. G. Webster, P. Bach-y Rita, and W. J. Tompkins, "Electrotactile and vibrotactile displays for sensory substitution systems," IEEE transactions on biomedical engineering, vol. 38, no. 1, pp. 1–16, 1991.

[49] R. W. Cholewiak and A. A. Collins, "Vibrotactile localization on the arm: Effects of place, space, and age," Perception & psychophysics, vol. 65, no. 7, pp. 1058–1077, 2003.

[50] A. Chatterjee, P. Chaubey, J. Martin, and N. Thakor, "Testing a prosthetic haptic feedback simulator with an interactive force matching task," JPO: Journal of Prosthetics and Orthotics, vol. 20, no. 2, pp. 27–34, 2008.

[51] S. G. Meek, S. C. Jacobsen, and P. P. Goulding, "Extended physiologic taction: design and evaluation of a proportional force feedback system," J Rehabil Res Dev, vol. 26, no. 3, pp. 53–62, 1989.

[52] L. Zollo, G. Di Pino, A. L. Ciancio, F. Ranieri, F. Cordella, C. Gentile, E. Noce, R. A. Romeo, A. D. Bellingegni, G. Vadalà et al., "Restoring tactile sensations via neural interfaces for real-time force-and-slippage closed-loop control of bionic hands," Science robotics, vol. 4, no. 27, 2019.

[53] E. Scheme and K. Englehart, "Electromyogram pattern recognition for control of powered upper-limb prostheses: state of the art and challenges for clinical use." Journal of Rehabilitation Research & Development, vol. 48, no. 6, 2011.

Tesi di dottorato in Scienze e Ingegneria per l'Uomo e l'Ambiente/Science and Engineering for Humans and the Environment, di Francesca Leone, discussa presso l'Università Campus Bio-Medico di Roma in data 26/07/2021.
La disseminazione e la riproduzione di questo documento sono consentite per scopi di didattica e ricerca, a condizione che ne venga citata la fonte.

[54] O. W. Samuel, M. G. Asogbon, Y. Geng, A. H. Al-Timemy, S. Pirbhulal, N. Ji, S. Chen, P. Fang, and G. Li, "Intelligent emg pattern recognition control method for upper-limb multifunctional prostheses: advances, current challenges, and future prospects," IEEE Access, vol. 7, pp. 10 150–10 165, 2019.

[55] X. Jiang, L.-K. Merhi, and C. Menon, "Force exertion affects grasp classification using force myography," IEEE Transactions on Human-Machine Systems, vol. 48, no. 2, pp. 219–226, 2017.

[56] Y. Geng, P. Zhou, and G. Li, "Toward attenuating the impact of arm positions on electromyography pattern-recognition based motion classification in transradial amputees," Journal of neuroengineering and rehabilitation, vol. 9, no. 1, pp. 1–11, 2012.

[57] A. H. Al-Timemy, G. Bugmann, J. Escudero, and N. Outram, "A preliminary investigation of the effect of force variation for myoelectric control of hand prosthesis," in 2013 35th Annual International Conference of the IEEE Engineering in Medicine and Biology Society (EMBC). IEEE, 2013, pp. 5758–5761.

[58] A. H. Al-Timemy, R. N. Khushaba, G. Bugmann, and J. Escudero, "Improving the performance against force variation of emg controlled multifunctional upper-limb prostheses for transradial amputees," IEEE Trans. Neural Syst. Rehabil. Eng, vol. 24, no. 6, pp. 650–661, 2016.

[59] G. Luppescu, M. Lowney, and R. Shah, "Classification of hand gestures using surface electromyography signals for upper-limb amputees."

[60] D. Xiong, D. Zhang, X. Zhao, and Y. Zhao, "Deep learning for emg-based human-machine interaction: A review," IEEE/CAA Journal of Automatica Sinica, vol. 8, no. 3, pp. 512–533, 2021.

[61] S. Hua, C. Wang, and X. Wu, "A novel semg-based force estimation method using deep-learning algorithm," Complex & Intelligent Systems, pp. 1–13, 2021.

[62] M. Jabbari, R. N. Khushaba, and K. Nazarpour, "Emg-based hand gesture classification with long short-term memory deep recurrent neural networks," in 2020 42nd Annual International Conference of the IEEE Engineering in Medicine & Biology Society (EMBC). IEEE, 2020, pp. 3302–3305.

Tesi di dottorato in Scienze e Ingegneria per l'Uomo e l'Ambiente/Science and Engineering for Humans and the Environment, di Francesca Leone, discussa presso l'Università Campus Bio-Medico di Roma in data 26/07/2021.
La disseminazione e la riproduzione di questo documento sono consentite per scopi di didattica e ricerca, a condizione che ne venga citata la fonte.

[63] G. Li, A. E. Schultz, and T. A. Kuiken, "Quantifying pattern recognition—based myoelectric control of multifunctional transradial prostheses," IEEE Transactions on Neural Systems and Rehabilitation Engineering, vol. 18, no. 2, pp. 185–192, 2010.

[64] C. Piazza, M. Rossi, M. G. Catalano, A. Bicchi, and L. J. Hargrove, "Evaluation of a simultaneous myoelectric control strategy for a multi-dof transradial prosthesis," IEEE Transactions on Neural Systems and Rehabilitation Engineering, vol. 28, no. 10, pp. 2286–2295, 2020.

[65] G. Yang and N. Li, "Design of the human surface electromyogra signal acquisition system and signal analysis," in Proceedings of the Seventh Asia International Symposium on Mechatronics. Springer, 2020, pp. 915–926.

[66] M. Ortiz-Catalan, B. Håkansson, and R. Brånemark, "Real-time and simultaneous control of artificial limbs based on pattern recognition algorithms," IEEE Transactions on Neural Systems and Rehabilitation Engineering, vol. 22, no. 4, pp. 756–764, 2014.

[67] D. Tkach, H. Huang, and T. A. Kuiken, "Study of stability of time-domain features for electromyographic pattern recognition," Journal of neuroengineering and rehabilitation, vol. 7, no. 1, p. 21, 2010.

[68] F. Mereu, F. Leone, C. Gentile, F. Cordella, E. Gruppioni, and L. Zollo, "Control strategies and performance assessment of upper-limb tmr prostheses: A review," Sensors, vol. 21, no. 6, p. 1953, 2021.

[69] F. Leone, C. Gentile, A. L. Ciancio, E. Gruppioni, A. Davalli, R. Sacchetti, E. Guglielmelli, and L. Zollo, "Simultaneous semg classification of hand/wrist gestures and forces," Frontiers in neurorobotics, vol. 13, p. 42, 2019.

[70] M. Zecca, S. Micera, M. C. Carrozza, and P. Dario, "Control of multifunctional prosthetic hands by processing the electromyographic signal," Critical Reviews™ in Biomedical Engineering, vol. 30, no. 4-6, 2002.

[71] J. E. Cheesborough, L. H. Smith, T. A. Kuiken, and G. A. Dumanian, "Targeted muscle reinnervation and advanced prosthetic arms," in Seminars in plastic surgery, vol. 29, no. 01. Thieme Medical Publishers, 2015, pp. 062–072.

Tesi di dottorato in Scienze e Ingegneria per l'Uomo e l'Ambiente/Science and Engineering for Humans and the Environment, di Francesca Leone, discussa presso l'Università Campus Bio-Medico di Roma in data 26/07/2021.
La disseminazione e la riproduzione di questo documento sono consentite per scopi di didattica e ricerca, a condizione che ne venga citata la fonte.

[72] D. Yatsenko, D. McDonnall, and K. S. Guillory, "Simultaneous, proportional, multi-axis prosthesis control using multichannel surface emg," in 2007 29th Annual International Conference of the IEEE Engineering in Medicine and Biology Society. IEEE, 2007, pp. 6133–6136.

[73] R. H. Chowdhury, M. B. Reaz, M. A. B. M. Ali, A. A. Bakar, K. Chellappan, and T. G. Chang, "Surface electromyography signal processing and classification techniques," Sensors, vol. 13, no. 9, pp. 12 431–12 466, 2013.

[74] M. A. Oskoei and H. Hu, "Support vector machine-based classification scheme for myoelectric control applied to upper limb," IEEE transactions on biomedical engineering, vol. 55, no. 8, pp. 1956–1965, 2008.

[75] Z. Zhang, K. Yang, J. Qian, and L. Zhang, "Real-time surface emg pattern recognition for hand gestures based on an artificial neural network," Sensors, vol. 19, no. 14, p. 3170, 2019.

[76] F. Duan, L. Dai, W. Chang, Z. Chen, C. Zhu, and W. Li, "semg-based identification of hand motion commands using wavelet neural network combined with discrete wavelet transform," IEEE Transactions on Industrial Electronics, vol. 63, no. 3, pp. 1923–1934, 2015.

[77] M. Atzori, M. Cognolato, and H. Müller, "Deep learning with convolutional neural networks applied to electromyography data: A resource for the classification of movements for prosthetic hands," Frontiers in neurorobotics, vol. 10, p. 9, 2016.

[78] W. Yang, D. Yang, Y. Liu, and H. Liu, "Decoding simultaneous multi-dof wrist movements from raw emg signals using a convolutional neural network," IEEE Transactions on Human-Machine Systems, vol. 49, no. 5, pp. 411–420, 2019.

[79] M. Zia ur Rehman, A. Waris, S. O. Gilani, M. Jochumsen, I. K. Niazi, M. Jamil, D. Farina, and E. N. Kamavuako, "Multiday emg-based classification of hand motions with deep learning techniques," Sensors, vol. 18, no. 8, p. 2497, 2018.

[80] Y. Du, W. Jin, W. Wei, Y. Hu, and W. Geng, "Surface emg-based inter-session gesture recognition enhanced by deep domain adaptation," Sensors, vol. 17, no. 3, p. 458, 2017.

Tesi di dottorato in Scienze e Ingegneria per l'Uomo e l'Ambiente/Science and Engineering for Humans and the Environment, di Francesca Leone, discussa presso l'Università Campus Bio-Medico di Roma in data 26/07/2021.
La disseminazione e la riproduzione di questo documento sono consentite per scopi di didattica e ricerca, a condizione che ne venga citata la fonte.

[81] A. J. Young, L. H. Smith, E. J. Rouse, and L. J. Hargrove, "A comparison of the real-time controllability of pattern recognition to conventional myoelectric control for discrete and simultaneous movements," Journal of neuroengineering and rehabilitation, vol. 11, no. 1, p. 5, 2014.

[82] P. Herberts, C. Almström, R. Kadefors, and P. D. Lawrence, "Hand prosthesis control via myoelectric patterns," Acta Orthopaedica Scandinavica, vol. 44, no. 4-5, pp. 389–409, 1973.

[83] P. Lawrence, P. Herberts, and R. Kadefors, "Experiences with a multifunctional hand prosthesis controlled by myoelectric patterns," Advances in External Control of Human Extremities, pp. 47–65, 1973.

[84] P. Lawrence, "Computer design and simulation of a myoelectric pattern classifier for controlling a multifunctional prosthetic hand," in Physics In Medicine And Biology, vol. 17, no. 5. IOP PUBLISHING LTD DIRAC HOUSE, TEMPLE BACK, BRISTOL BS1 6BE, ENGLAND, 1972, p. 716.

[85] S. M. Wurth and L. J. Hargrove, "A real-time comparison between direct control, sequential pattern recognition control and simultaneous pattern recognition control using a fitts' law style assessment procedure," Journal of neuroengineering and rehabilitation, vol. 11, no. 1, p. 91, 2014.

[86] D. C. Tkach, A. J. Young, L. H. Smith, E. J. Rouse, and L. J. Hargrove, "Real-time and offline performance of pattern recognition myoelectric control using a generic electrode grid with targeted muscle reinnervation patients," IEEE Transactions on Neural Systems and Rehabilitation Engineering, vol. 22, no. 4, pp. 727–734, 2014.

[87] K. Davidge, Multifunction myoelectric control using a linear electrode array. ProQuest, 2008.

[88] A. J. Young, L. H. Smith, E. J. Rouse, and L. J. Hargrove, "Classification of simultaneous movements using surface emg pattern recognition," IEEE Transactions on Biomedical Engineering, vol. 60, no. 5, pp. 1250–1258, 2012.

[89] L. H. Smith and L. J. Hargrove, "Comparison of surface and intramuscular emg pattern recognition for simultaneous wrist/hand motion classification," in 2013 35th annual international conference of the IEEE engineering in medicine and biology society (EMBC). IEEE, 2013, pp. 4223–4226.

Tesi di dottorato in Scienze e Ingegneria per l'Uomo e l'Ambiente/Science and Engineering for Humans and the Environment, di Francesca Leone, discussa presso l'Università Campus Bio-Medico di Roma in data 26/07/2021.
La disseminazione e la riproduzione di questo documento sono consentite per scopi di didattica e ricerca, a condizione che ne venga citata la fonte.

[90] B. Lock, K. Englehart, and B. Hudgins, "Real-time myoelectric control in a virtual environment to relate usability vs. accuracy," in MyoElectric Controls Symposium. Citeseer, 2005, pp. 122–127.

[91] G. Li, A. E. Schultz, and T. A. Kuiken, "Quantifying pattern recognition—based myoelectric control of multifunctional transradial prostheses," IEEE Transactions on Neural Systems and Rehabilitation Engineering, vol. 18, no. 2, pp. 185–192, 2010.

[92] L. A. Miller, K. A. Stubblefield, R. D. Lipschutz, B. A. Lock, and T. A. Kuiken, "Improved myoelectric prosthesis control using targeted reinnervation surgery: a case series," IEEE Transactions on Neural Systems and Rehabilitation Engineering, vol. 16, no. 1, pp. 46–50, 2008.

[93] J. B. Hijjawi, T. A. Kuiken, R. D. Lipschutz, L. A. Miller, K. A. Stubblefield, and G. A. Dumanian, "Improved myoelectric prosthesis control accomplished using multiple nerve transfers," Plastic and reconstructive surgery, vol. 118, no. 7, pp. 1573–1578, 2006.

[94] T. A. Kuiken, G. Li, B. A. Lock, R. D. Lipschutz, L. A. Miller, K. A. Stubblefield, and K. B. Englehart, "Targeted muscle reinnervation for real-time myoelectric control of multifunction artificial arms," Jama, vol. 301, no. 6, pp. 619–628, 2009.

[95] O. C. Aszmann, A. D. Roche, S. Salminger, T. Paternostro-Sluga, M. Herceg, A. Sturma, C. Hofer, and D. Farina, "Bionic reconstruction to restore hand function after brachial plexus injury: a case series of three patients," The Lancet, vol. 385, no. 9983, pp. 2183–2189, 2015.

[96] J. E. Cheesborough, L. H. Smith, T. A. Kuiken, and G. A. Dumanian, "Targeted muscle reinnervation and advanced prosthetic arms," in Seminars in plastic surgery, vol. 29, no. 01. Thieme Medical Publishers, 2015, pp. 062–072.

[97] E. Mastinu, R. Brånemark, O. Aszmann, and M. Ortiz-Catalan, "Myoelectric signals and pattern recognition from implanted electrodes in two tmr subjects with an osseointegrated communication interface," in 2018 40th annual international conference of the IEEE engineering in medicine and biology society (EMBC). IEEE, 2018, pp. 5174–5177.

Tesi di dottorato in Scienze e Ingegneria per l'Uomo e l'Ambiente/Science and Engineering for Humans and the Environment, di Francesca Leone, discussa presso l'Università Campus Bio-Medico di Roma in data 26/07/2021.
La disseminazione e la riproduzione di questo documento sono consentite per scopi di didattica e ricerca, a condizione che ne venga citata la fonte.

[98] E. Mastinu, "Embedded controller for artificial limbs," Ph.D. dissertation, Department of Signals and Systems, Chalmers University of Technology, 2017.

[99] H. Huang, P. Zhou, G. Li, and T. A. Kuiken, "An analysis of emg electrode configuration for targeted muscle reinnervation based neural machine interface," IEEE Transactions on Neural Systems and Rehabilitation Engineering, vol. 16, no. 1, pp. 37–45, 2008.

[100] L. H. Smith and L. J. Hargrove, "Intramuscular emg after targeted muscle reinnervation for pattern recognition control of myoelectric prostheses," in 2013 6th International IEEE/EMBS Conference on Neural Engineering (NER). IEEE, 2013, pp. 1155–1158.

[101] H. Huang, P. Zhou, G. Li, and T. Kuiken, "Spatial filtering improves emg classification accuracy following targeted muscle reinnervation," Annals of biomedical engineering, vol. 37, no. 9, pp. 1849–1857, 2009.

[102] P. Zhou, M. M. Lowery, K. B. Englehart, H. Huang, G. Li, L. Hargrove, J. P. Dewald, and T. A. Kuiken, "Decoding a new neural–machine interface for control of artificial limbs," Journal of neurophysiology, vol. 98, no. 5, pp. 2974–2982, 2007.

[103] I. Batzianoulis, N. E. Krausz, A. M. Simon, L. Hargrove, and A. Billard, "Decoding the grasping intention from electromyography during reaching motions," Journal of neuroengineering and rehabilitation, vol. 15, no. 1, p. 57, 2018.

[104] I. Batzianoulis, A. Simon, L. Hargrove, and A. Billard, "Reach-to-grasp motions: Towards a dynamic classification approach for upper-limp prosthesis," in 2019 9th International IEEE/EMBS Conference on Neural Engineering (NER). IEEE, 2019, pp. 287–290.

[105] Y. Xu, D. Zhang, Y. Wang, J. Feng, and W. Xu, "Two ways to improve myoelectric control for a transhumeral amputee after targeted muscle reinnervation: a case study," Journal of neuroengineering and rehabilitation, vol. 15, no. 1, p. 37, 2018.

[106] T. A. Kuiken, L. A. Miller, K. Turner, and L. J. Hargrove, "A comparison of pattern recognition control and direct control of a multiple degree-of-freedom transradial prosthesis," IEEE journal of translational engineering in health and medicine, vol. 4, pp. 1–8, 2016.

Tesi di dottorato in Scienze e Ingegneria per l'Uomo e l'Ambiente/Science and Engineering for Humans and the Environment, di Francesca Leone, discussa presso l'Università Campus Bio-Medico di Roma in data 26/07/2021.
La disseminazione e la riproduzione di questo documento sono consentite per scopi di didattica e ricerca, a condizione che ne venga citata la fonte.

[107] L. Hargrove, L. Miller, K. Turner, and T. Kuiken, "Control within a virtual environment is correlated to functional outcomes when using a physical prosthesis," Journal of neuroengineering and rehabilitation, vol. 15, no. 1, p. 60, 2018.

[108] A. M. Simon, L. J. Hargrove, B. A. Lock, and T. A. Kuiken, "The target achievement control test: Evaluating real-time myoelectric pattern recognition control of a multifunctional upper-limb prosthesis," Journal of rehabilitation research and development, vol. 48, no. 6, p. 619, 2011.

[109] K. Englehart and B. Hudgins, "A robust, real-time control scheme for multifunction myoelectric control," IEEE transactions on biomedical engineering, vol. 50, no. 7, pp. 848–854, 2003.

[110] L. J. Hargrove, B. A. Lock, and A. M. Simon, "Pattern recognition control outperforms conventional myoelectric control in upper limb patients with targeted muscle reinnervation," in 2013 35th Annual International Conference of the IEEE Engineering in Medicine and Biology Society (EMBC). IEEE, 2013, pp. 1599–1602.

[111] S. M. Wurth and L. J. Hargrove, "A real-time comparison between direct control, sequential pattern recognition control and simultaneous pattern recognition control using a fitts' law style assessment procedure," Journal of neuroengineering and rehabilitation, vol. 11, no. 1, p. 91, 2014.

[112] L. J. Hargrove, L. A. Miller, K. Turner, and T. A. Kuiken, "Myoelectric pattern recognition outperforms direct control for transhumeral amputees with targeted muscle reinnervation: a randomized clinical trial," Scientific reports, vol. 7, no. 1, pp. 1–9, 2017.

[113] A. J. Young, L. H. Smith, E. J. Rouse, and L. J. Hargrove, "A comparison of the real-time controllability of pattern recognition to conventional myoelectric control for discrete and simultaneous movements," Journal of neuroengineering and rehabilitation, vol. 11, no. 1, p. 5, 2014.

[114] N. Parajuli, N. Sreenivasan, P. Bifulco, M. Cesarelli, S. Savino, V. Niola, D. Esposito, T. J. Hamilton, G. R. Naik, U. Gunawardana et al., "Real-time emg based pattern recognition control for hand prostheses: a review on existing methods, challenges and future implementation," Sensors, vol. 19, no. 20, p. 4596, 2019.

Tesi di dottorato in Scienze e Ingegneria per l'Uomo e l'Ambiente/Science and Engineering for Humans and the Environment, di Francesca Leone, discussa presso l'Università Campus Bio-Medico di Roma in data 26/07/2021.
La disseminazione e la riproduzione di questo documento sono consentite per scopi di didattica e ricerca, a condizione che ne venga citata la fonte.

[115] F. Riillo, L. R. Quitadamo, F. Cavrini, E. Gruppioni, C. A. Pinto, N. C. Pastò, L. Sbernini, L. Albero, and G. Saggio, "Optimization of emg-based hand gesture recognition: Supervised vs. unsupervised data preprocessing on healthy subjects and transradial amputees," Biomedical Signal Processing and Control, vol. 14, pp. 117–125, 2014.

[116] R. A. Romeo, F. Cordella, L. Zollo, D. Formica, P. Saccomandi, E. Schena, G. Carpino, A. Davalli, R. Sacchetti, and E. Guglielmelli, "Development and preliminary testing of an instrumented object for force analysis during grasping," in Engineering in Medicine and Biology Society (EMBC), 2015 37th Annual International Conference of the IEEE. IEEE, 2015, pp. 6720–6723.

[117] K. F. Anderson, "Nasa's anderson loop," IEEE Instrumentation & Measurement Magazine, vol. 1, no. 1, pp. 5–15, 1998.

[118] D. M. Powers, "Evaluation: from precision, recall and f-measure to roc, informedness, markedness and correlation," 2011.

[119] S. Benatti, E. Farella, E. Gruppioni, and L. Benini, "Analysis of robust implementation of an emg pattern recognition based control." in BIOSIGNALS, 2014, pp. 45–54.

[120] K. Nazarpour, "Surface emg signals pattern recognition utilizing an adaptive crosstalk suppression preprocessor," in Computational Intelligence Methods and Applications, 2005 ICSC Congress on. IEEE, 2005, pp. 3–pp.

[121] P. Dohnalek, P. Gajdos, and T. Peterek, "Human activity recognition on raw sensor data via sparse approximation," in Telecommunications and Signal Processing (TSP), 2013 36th International Conference on. IEEE, 2013, pp. 700–703.

[122] L. H. Smith, L. J. Hargrove, B. A. Lock, and T. A. Kuiken, "Determining the optimal window length for pattern recognition-based myoelectric control: balancing the competing effects of classification error and controller delay," IEEE Transactions on Neural Systems and Rehabilitation Engineering, vol. 19, no. 2, pp. 186–192, 2011.

[123] A. M. Simon, L. J. Hargrove, B. A. Lock, and T. A. Kuiken, "The target achievement control test: Evaluating real-time myoelectric pattern recognition control of a multifunctional upper-limb prosthesis," Journal of rehabilitation research and development, vol. 48, no. 6, p. 619, 2011.

Tesi di dottorato in Scienze e Ingegneria per l'Uomo e l'Ambiente/Science and Engineering for Humans and the Environment, di Francesca Leone, discussa presso l'Università Campus Bio-Medico di Roma in data 26/07/2021.
La disseminazione e la riproduzione di questo documento sono consentite per scopi di didattica e ricerca, a condizione che ne venga citata la fonte.

[124] L. Resnik, J. Cancio, C. Fantini, A. Ikeda, and N. Sasson, "Pattern recognition control of the deka arm in two transhumeral amputees with targeted muscle reinnervation," in Proc. of MEC'17: Myoelectric Controls Symposium, Fredericton, 2017.

[125] N. Baykal and A. M. Erkmen, "Resilient backpropagation for rbf networks," in KES'2000. Fourth International Conference on Knowledge-Based Intelligent Engineering Systems and Allied Technologies. Proceedings (Cat. No. 00TH8516), vol. 2. IEEE, 2000, pp. 624–627.

[126] A. B. Cheikh, M. Ayari, R. Langar, and L. A. Saidane, "Ohdp: Optimized handover with direction prediction scheme using linear regression for femtocell networks," in 2016 International Conference on Performance Evaluation and Modeling in Wired and Wireless Networks (PEMWN). IEEE, 2016, pp. 1–6.

[127] A. Borgul, A. Margun, K. Zimenko, A. Kremlev, and A. Krasnov, "Intuitive control for robotic rehabilitation devices by human-machine interface with emg and eeg signals," in 2012 17th International Conference on Methods & Models in Automation & Robotics (MMAR). IEEE, 2012, pp. 308–311.

[128] B. D. Ripley, Pattern recognition and neural networks. Cambridge university press, 2007.

[129] L. J. Hargrove, K. Englehart, and B. Hudgins, "A comparison of surface and intramuscular myoelectric signal classification," IEEE transactions on biomedical engineering, vol. 54, no. 5, pp. 847–853, 2007.

[130] M. Welling, "Fisher linear discriminant analysis, vol. 3. department of computer science, university of toronto," 2005.

[131] J. Too, A. R. Abdullah, and N. M. Saad, "Classification of hand movements based on discrete wavelet transform and enhanced feature extraction," Int. J. Adv. Comput. Sci. Appl, vol. 10, no. 6, pp. 83–89, 2019.

[132] G. Purushothaman and R. Vikas, "Identification of a feature selection based pattern recognition scheme for finger movement recognition from multichannel emg signals," Australasian physical & engineering sciences in medicine, vol. 41, no. 2, pp. 549–559, 2018.

Tesi di dottorato in Scienze e Ingegneria per l'Uomo e l'Ambiente/Science and Engineering for Humans and the Environment, di Francesca Leone, discussa presso l'Università Campus Bio-Medico di Roma in data 26/07/2021.
La disseminazione e la riproduzione di questo documento sono consentite per scopi di didattica e ricerca, a condizione che ne venga citata la fonte.

[133] T. A. Kuiken, G. Li, B. A. Lock, R. D. Lipschutz, L. A. Miller, K. A. Stubblefield, and K. B. Englehart, "Targeted muscle reinnervation for real-time myoelectric control of multifunction artificial arms," Jama, vol. 301, no. 6, pp. 619–628, 2009.

[134] P. Geethanjali and K. Ray, "A low-cost real-time research platform for emg pattern recognition-based prosthetic hand," IEEE/ASME Transactions on mechatronics, vol. 20, no. 4, pp. 1948–1955, 2014.

[135] A. Phinyomark, F. Quaine, S. Charbonnier, C. Serviere, F. Tarpin-Bernard, and Y. Laurillau, "Emg feature evaluation for improving myoelectric pattern recognition robustness," Expert Systems with applications, vol. 40, no. 12, pp. 4832–4840, 2013.

[136] Y. Xu, D. Zhang, Y. Wang, J. Feng, and W. Xu, "Two ways to improve myoelectric control for a transhumeral amputee after targeted muscle reinnervation: a case study," Journal of neuroengineering and rehabilitation, vol. 15, no. 1, p. 37, 2018.

[137] M. Tavakoli, C. Benussi, and J. L. Lourenco, "Single channel surface emg control of advanced prosthetic hands: A simple, low cost and efficient approach," Expert Systems with Applications, vol. 79, pp. 322–332, 2017.

[138] K. D. Gordon, R. D. Pardo, J. A. Johnson, G. J. King, and T. A. Miller, "Electromyographic activity and strength during maximum isometric pronation and supination efforts in healthy adults," Journal of orthopaedic research, vol. 22, no. 1, pp. 208–213, 2004.

[139] K. Englehart and B. Hudgins, "A robust, real-time control scheme for multifunction myoelectric control," IEEE transactions on biomedical engineering, vol. 50, no. 7, pp. 848–854, 2003.